

From soil to water: the detachment and transport of microplastics from agricultural soil

Emilee Lyn Severe

Lancaster Environment Centre

Lancaster University

Submitted for the degree of Doctor of Philosophy

October 2024



Dedicated to the memory of N.H.

Declaration

I declare that the work produced for this thesis is my own and has not been submitted for another degree or qualification at any other institution. Collaborations with other researchers are properly acknowledged.

Emilee Lyn Severe

Lancaster University

October 2024

Statement of Authorship

This thesis is prepared in the alternative format as a collection of three papers, one of which has been submitted for publication in a peer-reviewed journal. Chapters 2, 3 and 4 are intended for publication and are presented here in alternative format. All papers have multiple authors and include co-authors outside of my supervisory team. Their contributions are set out below.

Chapter 2 is an adapted version of a manuscript in-review at Environmental Science & Technology as:

Severe E., Surridge B.W.J., Fiener P., Coogan M.P., Platel R.H., James M.R., Quinton J. (2024). *The transport of microplastics from soil in response to surface runoff and splash erosion*.

ES carried out the experiment, lab analysis and prepared the original manuscript. PF gave advice on the experimental design and assisted with manuscript editing. MPC and RHP developed and manufactured the fluorescent linear-low density polyethylene plastic and assisted with the manuscript editing. MRJ gave advice which led to the development of the image analysis procedure and assisted with manuscript editing. BWJS and JQ gave advice on the experimental design, sample collection, data analysis and contributed to the revisions of the manuscript.

Chapter 3 is intended for publication as:

Severe E., Ray S.S., Li W., Zumr D., Dostál T., Krasa J., Wilken F., Fiener P., Maqbool A., Stumpp C., Surridge B.J.W., Gómez J.A., Zafui C., Quinton J. (2024). *Rainfall-induced lateral and vertical microplastics transport of varying sizes in agricultural fields*.

This manuscript is the culmination of a joint experiment designed by 3 PhD students ES, SSR and WL. ES led the data collection and analysis for the MP surface movement and conducted the laboratory splash erosion experiment located in the supplementary text (Appendix 2). SSR led the data collection for MPs in surface runoff. WL led the data collection and analysis for MPs in soil samples. ES, SSR, and WL each wrote the original drafts of the methodologies and results stemming from their datasets. ES led the writing and finalized the

manuscript including the production of all figures within the manuscript text. DZ, TD, JK, FW, assisted with the sample collection, fieldwork, data analysis. AM, CS, JAG, CZ gave advice on the experimental design and analysis. DZ, AM and CZ also assisted with manuscript editing. PF, BWJS and JQ gave advice on the experimental design, data analysis, and contributed to the revisions of the manuscript.

Chapter 4 is intended for submission as:

Severe E., Phan Le Q.N., Maqbool A., SurrIDGE B.J.W., Halsall C., Gómez J.A., Quinton J. (2024). *Microplastics detachment and transport from soil as influenced by polymer age and aggregation within the soil.*

ES carried out the experiment, lab and data analysis and prepared the original manuscript. QNPL gave advice on the experimental design, assisted with laboratory work, and assisted the manuscript editing. AM gave advice on the experimental design and assisted with laboratory work. CH and JAG gave advice on the experimental design and provided laboratory equipment to carry out the experiment. BWJS and JQ gave advice on the experimental design, sample collection, data analysis and contributed to the revisions of the manuscript.

I hereby agree with the above statements:

Professor John N. Quinton
Lancaster Environment Centre
Lancaster University

Dr. Ben W.J. SurrIDGE
Lancaster Environment Centre
Lancaster University

Acknowledgments

I gratefully acknowledge the funding for this research which was received from the European Union's Horizon 2020 research and innovation programme under the Marie Skłodowska-Curie grant agreement No 955334.

I am deeply grateful for the many people who have made this research possible as well as living in Lancaster these past few years so enjoyable. First and foremost, I would like to thank my supervisors, John Quinton and Ben Surridge. I sincerely appreciate all the time you have unselfishly and generously given to me these past few years. Thank you for your constant encouragement, guidance and patience. This work would not have been possible without your support.

I would like to thank all of the supervisors in SOPLAS project for their helpful suggestions to improve my research during our project meetings. I especially would like to thank David, Tomáš, Josef, Florian, Peter, Christine, and José for your valuable insights in our work package meetings and for so graciously hosting me at your institutions during my secondments. I also would like to thank my fellow SOPLAS ESRs: Manuel, Ale, Stoy, Olivia, Ana, Flora, Davi, Gi, Elise, Ahsan, Wang and Saunak. Your friendships have buoyed me up countless times and I have enjoyed spending so much time with you. I especially would like to thank Nhu who has become one of my dearest friends. Thank you for always being willing to act as a sounding board and for your constant and unwavering friendship.

I cannot say enough thanks to my friends in the Lancaster Sustainable Soils group: Jess, Carmen, Csilla, Hongmei, Mengyi, Angeliki, Johanna, Malika, Laura, Cristina, Jenny, Emma, Roisin, Hannah, Helena, Louise, Rosanne, Mary, Holly, Fiona and Anna. Your friendships have made living in Lancaster so enjoyable and thank you for all the help you have given me. I would like to thank my office friends, especially the adopted soils group members, Joseph and Katrina for their advice and enjoyable work break conversations. I would also like to thank everyone in LEC who helped along the way, especially Vassil who has been a huge help in the lab and an invaluable source of advice.

A heartfelt thanks goes to Doris and Sue for taking me in as their "adopted" American granddaughter and treating me like family over the past 3 years. Finally, I would like to thank my family: Mom, Dad, Jeremy, Allie and Geremy. Your love felt so close even though you have been so physically far away. I love you and thank you for always being my #1 fans.

Abstract

Microplastics (MPs) are a contaminant of emerging concern found extensively in various ecosystems across the globe. Many questions remain unanswered regarding the impact MPs will have on earth's biotic and abiotic systems, however, MPs have been shown to be particularly harmful for aquatic organisms. Rainfall-induced erosion from agricultural soils, is thought to be a significant source of MPs to aquatic ecosystems, though little research exists which quantifies the magnitude and rate of MP transported in these processes. There are several transport pathways MPs potentially follow during rainfall-induced erosion including: surface runoff, splash erosion and vertically into the soil with infiltrating rainwater. However, the majority of research investigating the movement of MPs have investigated either the transport of MPs in surface runoff or infiltration into the soil profile, but not both in tandem. Additionally, no research has yet explored MP transport in splash erosion processes. Along with investigating the transport pathways MPs follow, this thesis also explores properties which influence MP transport focusing on properties which distinguish MPs from natural soil particles specifically, density and aging processes. We also investigate how MP size influences transport as this is thought to be a significant property controlling MP transportation processes. This thesis uses innovative methodologies to investigate MP transport during rainfall-induced erosion events, focusing on the pathways MPs follow and how their properties influence their transport behaviour. It presents three rainfall simulation experiments, the first of which explores the differences in transport between MPs and sand, a proxy for natural soil particles. This experiment found that MPs had more rapid transport from the soil surface and distinct transport patterns in surface runoff and splash erosion compared to the sand particle. The second experiment was conducted in an agricultural field without vegetation and explored what transport pathways MPs of various size follow during a rainfall simulation. This research found that the influence of size on transport varied between transport pathways. The final experiment employed methodologies in an attempt to recreate environmentally relevant conditions in laboratory rainfall simulations by comparing the transport of aged and pristine MPs alongside the influence of MP-soil aggregation on transport. The result from this experiment found variable rates of artificial aging between polymers and that low levels of MP-soil aggregation do not reduce MP transport in surface runoff. Together the results from the research presented in this thesis are among the first to investigate the rate as well as the magnitude of MP transport in several transport pathways during rainfall-induced erosion. The knowledge gained in this research gives a holistic

understanding of MP transport processes during rainfall-induced erosion and shows that soils have a high capacity to retain MPs but that MPs are also readily transported from soil in surface runoff and splash erosion processes. To mitigate the transfer of MPs from soil to aquatic ecosystems, policymakers should promote programs and initiatives that reduce soil erosion, which would not only limit MP emissions but also enhance soil health for farmers. Additionally, establishing monitoring programs in agricultural soils near riparian areas would greatly enhance our understanding of the MP retention in soil or transport into water bodies, providing critical data to inform future environmental policies and regulatory decisions. Efforts should be made at individual, community and government levels to reduce plastic consumption, remediate environments plastic-polluted and develop sustainable alternatives to conventional plastics.

Table of Contents

Declaration.....	3
Statement of Authorship	4
Acknowledgements.....	6
Abstract.....	7
List of Tables	12
List of Figures.....	13
List of Abbreviations.....	18
1. General Introduction	19
1.1 Plastics pollution a global issue	19
1.2 Microplastic contamination in agricultural soils	20
1.2.1 Pathways and polymers.....	20
1.2.2 Abundance and distribution of plastics in the soil	22
1.3 Transport processes	23
1.3.1 The role of erosion in the plastic cycle	23
1.3.2 Wind erosion.....	25
1.3.3 Rainfall-induced erosion.....	25
1.3.3.1 Splash erosion.....	26
1.3.3.2 Vertical movement into the soil	27
1.3.3.3 Surface runoff.....	28
1.4 Methods for detecting microplastics in soil.....	30
1.5 Summary and research gaps	32
1.6 Thesis aims and objectives	33
1.7 Thesis structure.....	33
2. The transport of microplastics from soil in response to surface runoff and splash erosion..	35
2.1 Introduction	36
2.2 Methods.....	37
2.2.1 Experimental set-up	37
2.2.2 Particle tracers.....	39
2.2.3 Preparation of fluorescent linear low-density polyethylene particles	41
2.2.4 LLDPEs recovery.....	42
2.2.5 Image collection.....	42
2.2.6 Surface runoff and soil samples	44
2.2.7 Image processing and analysis.....	45
2.2.8 Color thresholding	45
2.2.9 Performance evaluation	46
2.2.10 Effectiveness of the image-based detection method	47

2.2.11 Statistical Analysis.....	49
2.3 Results and Discussion	49
2.3.1 Using photography to track the real-time movement of fluorescent particles	49
2.3.2 Microplastic transport in surface runoff.....	54
2.3.3 Retention and transport into the soil profile.....	56
2.3.4 Microplastic transport via splash erosion.....	57
2.3.5 Mass balance.....	58
2.3.6 Comparing transport pathways between different microplastics	59
2.3.7 Erosion as a mechanism for microplastic transport to terrestrial and freshwater ecosystems	60
2.4 Conclusion.....	62
2.5 Acknowledgements	63
3. Rainfall-induced lateral and vertical microplastics transport of varying sizes in agricultural fields.....	64
3.1 Introduction.....	65
3.2 Methods.....	67
3.2.1 Site description and experimental set-up	67
3.2.2 Observations during the simulation and sample collection.....	69
3.2.3 Sample analysis and microplastic extraction	70
3.2.3.1 Microplastic soil surface movement image processing and analysis.....	70
3.2.3.2 Runoff and sediment analysis	72
3.2.3.3 Soil sample microplastic extraction and analysis.....	73
3.2.4 Data analysis	74
3.3 Results.....	74
3.3.1 Patterns of microplastic movement on the surface of the soil	74
3.3.2 Microplastic delivery in surface runoff.....	76
3.3.3 Vertical tracer movement and retention profile of microplastics.....	79
3.4 Discussion.....	80
3.4.1 Pathways and rates of microplastic transport.....	80
3.4.2 The relationship between microplastic size and transport	81
3.4.3 Transport of microplastics to groundwater and surface waters	83
3.5 Conclusion	83
3.6 Acknowledgements	84
4. Microplastics detachment and transport from soil as influenced by polymer age and aggregation within the soil.....	85
4.1 Introduction.....	86
4.2 Methods.....	88

4.2.1 Microplastics and accelerated aging process	88
4.2.2 Evaluating microplastic aging.....	88
4.2.3 Experimental set-up	89
4.2.4 Wet-dry cycles	90
4.2.5 Image collection and processing.....	91
4.2.6 Microplastics in surface runoff	92
4.2.7 Statistical analysis.....	92
4.3 Results.....	93
4.3.1 Evaluation of microplastic aging and wet-dry cycle methodologies	93
4.3.2 Patterns of movement on the soil surface	96
4.3.3 Microplastic transport in surface runoff.....	97
4.4 Discussion.....	99
4.4.1 Accelerating environmental conditions for lab-based microplastic studies.....	99
4.4.2 Microplastic transport in surface runoff processes	100
4.5 Conclusion	102
4.6 Acknowledgements	102
5. General Discussion	103
5.1 Summary of aims and objectives	103
5.2 Microplastic properties and their influence on transport	105
5.3 Dynamic understanding of microplastic transport during rainfall events.....	108
5.4 Reducing microplastic transport from agricultural soils.....	109
5.5 Future Research	110
6. References	112
7. Appendix 1: UV photography and image analysis to detect fluorescent particles during rainfall simulations	127
8. Appendix 2: Chapter 3- Supplemental Information	132

List of Tables

Table 1.1. Synthesis of research results on the influence of size on the vertical transport of microplastics from the soil surface with the impact of raindrops. Coloured cells indicate the size fraction which were transported furthest into the soil	27
Table 1.2. Synthesis of research results on the influence of size on the transport of microplastics in surface runoff. Coloured cells indicate the size fraction which were transported in the greatest numbers in surface runoff	28
Table 2.1. Threshold ranges for particle detection as used in image J. LLDPE _L ; LLDPE _S ; PMMA; PS; and SAND represents linear low-density polyethylene size large, linear low-density polyethylene size small, polymethyl methacrylate, polystyrene and sand particles, respectively	45
Table 2.2. Table showing the correct and incorrect identification of fluorescent particles in images. LLDPE _L ; PMMA; PS; and SAND represents linear low-density polyethylene size large, polymethyl methacrylate, polystyrene and sand particles, respectively	47
Table 4.1. Microplastics (MPs) found in soil aggregate fractions. Soil mass refers to the mass of soil in grams for each sieved aggregate size fraction. # MPs indicates the number of MPs found in each aggregate size fraction. % MPs indicates the proportion of MPs in each aggregate size fraction in relation to the total number of MPs recovered for all sizes. As the MPs were sieved to 0.25-0.355 mm prior to the experiment any MPs found below 0.355 mm were considered loose in the soil and MPs found in the larger aggregate size fraction were assumed to be bound to soil aggregates	96
Table 5.1. Synthesis of research along with results from this thesis showing influence of size on the transport of microplastics (MPs) in surface runoff. Coloured cells indicate the size fraction which were transported in the greatest numbers in surface runoff.....	107
Table 5.2. Synthesis of research along with results from this thesis showing influence of size on the vertical transport of microplastics (MPs) from the soil surface with the impact of raindrops. Coloured cells indicate the size fraction which were transported furthest into the soil.	108

List of Figures

Figure 1.1. Images showing examples of plastic products used in agriculture. A selection of benefits of using plastic products are highlighted.....	21
Figure 1.2. Images showing examples of primary plastic input through residue of plastic products (left) and secondary plastics input through biosolids (right).....	22
Figure 1.3. Venn diagram illustrating the similarities and differences in a selection of properties of microplastics, mineral soil particles and organic soil particles.....	24
Figure 1.4. Conceptual diagram outlining key research gaps for microplastic (MP) transport in rainfall-induced soil erosion. Green particles represent MPs	32
Figure 2.1. Laboratory set-up for simulation experiment	38
Figure 2.2. Images of the particles used in this experiment. Where image A represents linear low-density polyethylene large particle (LLDPE _L), B represents polymethyl methacrylate particle (PMMA), C represents linear low-density polyethylene small particle (LLDPE _S), D represents polystyrene particle (PS), and E represents the sand particle. Diagram showing the experimental set-up, sample collection and sample processing.....	40
Figure 2.3. Camera and light set-up to photograph the 1 m ² splash mat at the conclusion of a rainfall simulation	43
Figure 2.4. Diagram showing the experimental set-up, sample collection and sample processing. LLDPE _L ; PMMA; PS; and SAND represents linear low-density polyethylene, polymethyl methacrylate, polystyrene and sand particles, respectively.	44
Figure 2.5. Graphs showing the number of particles detected in the image analysis process on blank soil throughout the rainfall simulation (n=4). Panel A shows particles on the surface of the soil box and panel B shows the particles on the splash mat. Each line represents a different replicate. LLDPE _L ; PMMA; PS; SAND; and LLDPE _S represents linear low-density polyethylene large size, polymethyl methacrylate, polystyrene, sand particles, and linear low-density polyethylene small size respectively.....	48

Figure 2.6. Number of particles on the soil surface through time (n=4). Vertical lines indicate the start of surface runoff delivery for each replicate. LLDPE_L; PMMA; PS; and SAND represents linear low-density polyethylene, polymethyl methacrylate, polystyrene and sand particles, respectively.....50

Figure 2.7. Log transformed data showing the rate of decline in number of particles from the soil surface. Panel A shows the decline in number of particles on the surface prior to surface runoff. Panel B shows the decline in numbers of particle from the surface after the onset of surface runoff. Data from four replicates are shown for each particle type in each panel. Comparisons between the linear models in panel A and panel B should not be made due to the difference in x-axis. LLDPE_L; PMMA; PS; and SAND represents linear low-density polyethylene, polymethyl methacrylate, polystyrene and sand particles, respectively (n=4)..52

Figure 2.8. Number of particles on the 50 cm² section of the splash mat through the full rainfall simulation. Each panel shows results from four replicates with each line representing a single replicate (n=4). For the MPs there is an increased rate of accumulation on splash mat when surface runoff begins; this pattern is absent for the sand particle. LLDPE_L; PMMA; PS; and SAND represents linear low-density polyethylene, polymethyl methacrylate, polystyrene and sand particles, respectively53

Figure 2.9. Surface runoff (A) and sediment flux (B) during the rainfall simulations. Data is LLDPE_L; PMMA; PS; and SAND represents linear low-density polyethylene, polymethyl methacrylate, polystyrene and sand particles, respectively (n=4)55

Figure 2.10. Number of particles per litre of surface runoff through time. Time 0 marks time since surface runoff commencement. Lines represent the mean number of particles while the shaded regions mark ± one standard deviation. LLDPE_L; PMMA; PS; and SAND represents linear low-density polyethylene, polymethyl methacrylate, polystyrene and sand particles, respectively (n=4).....56

Figure 2.11. Vertical movement of MPs through the soil profile to a 4 cm depth. Dark lines represent the mean while the shaded regions mark ± one standard deviation. Surface particles were counted once sampling core was in the soil then ultimately subtracted from particles found in the 0-1 cm depth class. Rarely were any particles found in the soil below a 1 cm depth. LLDPE_L; PMMA; PS; and SAND represents linear low-density polyethylene, polymethyl methacrylate, polystyrene and sand particles, respectively (n=4)57

Figure 2.12. Particles found in each transportation compartment measured. Error bars represent ± 1 standard deviation. LLDPE_L; PMMA; PS; and SAND represents linear low-density polyethylene, polymethyl methacrylate, polystyrene and sand particles, respectively (n=4).....59

Figure 3.1. Image showing the preparation for rainfall simulation on the 1 m x 1 m plot. Camera at the base of the plot used for detecting microplastics on the surface of the plots. ..68

Figure 3.2. Images demonstrating the particle detection from the images of the soil surface. Image of the soil surface after perspective correction and cropping (left). Thresholded image detecting the 425-500 μm (red) MPs, black dots are detected microplastics (right). 71

Figure 3.3. Microplastics (MPs) visible on the surface of the plots throughout the duration of rainfall simulations. MP concentration is shown as percentage of particles with respect to the initial number of MPs detected on the soil surface for each plot and particle size. Black lines represent the mean particle number from all the plots and the shaded areas represent one standard deviation from the mean for each MP size (n=4). Red vertical lines indicate changepoints for the 425-500 μm MP and blue vertical lines indicate changepoints for the 125-150 μm MP..... 75

Figure 3.4. Surface runoff and sediment flux during the rainfall simulations across the five plots (n=5). The x-axis shows the time scale of the rainfall simulation (0-30 minutes dry run, 15 minutes of break, and 45-75 minutes wet run). Missing data points in plot 4 are visible, these values were outliers and were excluded from the analysis as the values were twice that of the mean sediment concentration and did not relate to other measured parameters suggesting there may have been an error 77

Figure 3.5. Microplastic (MP) sizes 425-500 μm and 125-150 μm transported in surface runoff across the five plots. The x-axis shows the time scale of the rainfall simulation (0-30 minutes dry run, 15 minutes of break, and 45-75 minutes wet run 78

Figure 3.6. Enrichment ratio of 425-500 μm and 125-150 μm microplastic (MP) in delivered sediments across rainfall simulations on all five plots for dry and wet runs (n=5). Boxes show the median, 1st, and 3rd quartiles; whiskers represent the minimum and maximum values An enrichment factor greater than 1 in all simulations indicates preferential erosion of MP. The dashed line marks the initial concentration in the topsoil (<1 cm) as a factor 1 78

Figure 3.7. The number of detected microplastics (MPs) by the mass of soil. Boxes show the median, 1st and 3rd quartiles; whiskers represent the minimum and maximum values (n=2). **79**

Figure 4.1. Diagram of the experimental set-up showing the microplastic (MP) aging treatment, the determination of how many MPs were bound to soil aggregates, and the rainfall simulations. PE and PS represents polyethylene and polystyrene, respectively**91**

Figure 4.2. Thermogravimetric analysis and differential scanning calorimetry (TGA-DSC) analysis showing the derivative thermogravimetric (DTG) curve (A) and Fourier transform infrared spectroscopy (FTIR) spectra of both the polyethylene (PE) and polystyrene (PS) microplastics (MPs) (B). The DTG curve represents the rate change of mass (% min⁻¹) with respect to temperature in Celsius. The FTIR spectra showing the absorbance by wavelength. Red lines representing aged MPs and black lines represent pristine MPs.**94**

Figure 4.3. SEM images of pristine PS (A), aged PS (B), pristine PE (C), and aged PE (D). Working distance (WD), magnification, and 10 µm scale bar indicated on the bottom of each respective images. PE signifies polyethylene and PS signifies polystyrene**95**

Figure 4.4. The number of microplastics (MPs) on the surface of the soil throughout the rainfall simulations (n=5). Dark lines represent the mean number of particles and the shaded regions represent ± one standard deviation. Vertical lines indicate the changepoint for each treatment**97**

Figure 4.5. Surface runoff transported from the soil boxes in litres per min (A). Gravimetric water content (GWC) of the soil boxes before being placed under the rainfall simulator (B). Letter on the boxplots indicate significance (p < 0.05). For all data n=5.**98**

Figure 4.6. The number of microplastics (MPs) per litre of runoff throughout the rainfall simulation (A) and total number of MPs transported during the rainfall simulations (B). In panel A, lines represent the mean number of particles while the shaded regions mark ± one standard deviation. In panel B, boxplots show the median, 1st, and 3rd quartiles; whiskers represent the minimum and maximum values (n=5). Letter on the boxplots indicate significance (p < 0.05)**99**

Figure 5.1. Conceptual model summarizing the key findings of this thesis. MP represents microplastic**105**

Figure 5.2. Conceptual diagram showing microplastic (green particles) the complexity of transport during a rainfall-induced erosion event. The three transport pathways are shown in detail: surface runoff, vertical transport into the soil and splash erosion.**109**

List of Abbreviations

AMOC – At Most One Changepoint	LZW – Lempel–Ziv–Welch compression
ANOVA – Analysis of variance	m – metre
ATR – Attenuated Total Reflection	mL – millilitre
CI – Confidence Interval	mm – millimetre
cm – centimetre	MP – Microplastic
CO ₂ – Carbon dioxide	NaCl – Sodium Chloride
DSC – Differential Scanning Calorimetry	OH – Hydroxyl
DTG – Derivative thermogravimetric	PA – Polyamide
ER – Enrichment Ratio	PBAT – Polybutylene adipate terephthalate
f/ – F-stop	PE – Polyethylene
FTIR – Fourier Transform Infrared Spectroscopy	PET – Polyethylene terephthalate
g – gram	PELT – Pruned Exact Linear Time
GWC – Gravimetric Water Content	PLA – Polylactic acid
H ₂ O ₂ – Hydrogen peroxide	PMMA – Polymethyl methacrylate
HDPE – High Density Polyethylene	PP – Polypropylene
HSB – Hue Saturation Brightness	PS – Polystyrene
J – Joule	PVC – Polyvinyl chloride
JPEG – Joint Photographic Experts Group	RGB – Red Green Blue
K ₂ S ₂ O ₈ – Potassium persulfate	rpm – revolutions per minute
kg – kilogram	SEM – Scanning Electron Microscope
kHz – Kilohertz	TGA – Thermogravimetric analysis
L – Litre	TIFF – Tagged Image File Format
LDPE – Low-density polyethylene	UV – Ultraviolet
LLDPE – Linear low-density polyethylene	VWC – Volumetric Water Content
LLDPE _L – Linear low-density polyethylene large size	µm – micrometre
LLDPE _S – Linear low-density polyethylene small size	χ ² – Chi-squared
	δ ² H – Deuterium
	°C – Degree Celsius

Chapter 1. General Introduction

1.1 Plastics pollution a global issue

It is estimated that between 1950 and 2015 over 8.3 billion metric tons of plastics were produced, 21% of which was recycled or incinerated and the remaining 79% disposed of in landfills or the natural environment (Geyer *et al.*, 2017). Plastics are comprised of chemical additives and organic polymers derived from both fossil fuels and bio-based carbon sources. The first synthetic plastics were produced in the late 19th century and early 20th century (McCord, 1964). In the 1950s, plastic products became widely used due to their versatility and unique properties including resilience to chemical, photo and microbial deterioration, water resistance, and low-density (Andrady and Neal, 2009; Thompson *et al.*, 2009).

The increase in plastic use has raised significant concerns about the end-of-life disposal of these materials. Plastics degrade at different rates dependent on the environment they are deposited in and the characteristics of the plastic itself (Chamas *et al.*, 2020; Sander *et al.*, 2024). Unlike other organic materials such as wood, plastics rarely fully decompose into CO₂, rather plastics fragment into smaller macro-, micro- and nano-sized pieces. However, this is dependent on the parent material of the plastics, as plastics such as polylactic acid (PLA) and polybutylene adipate terephthalate (PBAT) are synthesized from both plant-derived and fossil fuel-based carbon sources and can be mineralized into CO₂ in varying proportions dependent on environmental conditions (Sander *et al.*, 2024; Zumstein *et al.*, 2018). Plastics primarily derived from fossil fuel sources often show slow rates of decomposition and thus are apt to fragmentation. For example, Chamas *et al.* (2020) estimated that when high density polyethylene (HDPE) plastic bags are within the marine environment they could take as little as 1.8 years to fully degrade, whereas a HDPE fibre or a HDPE resin bead with the same volume as the plastic bag can take up to 465 years and 2000 years to degrade, respectively.

Microplastics (MPs), defined as plastic pieces smaller than 5 mm but larger than 1 µm in length (Thompson *et al.*, 2024), are regarded by some as a persistent pollutant with a capacity to significantly disrupt the ecological function of Earth's systems. Specifically, MPs have been shown to have a negative impact on aquatic (Cole *et al.*, 2015; Palmer and Herat, 2021) and terrestrial (Edwards *et al.*, 2023; Quigley *et al.*, 2024) organisms, and preliminary research indicates that MPs may pose a risk to human health (Bastyans *et al.*, 2022; Jenner *et*

al., 2022; Prata *et al.*, 2020; Yan *et al.*, 2022). Research has found that the physical MP particle itself, as well as the chemical additives found within the polymer, are more toxic to organisms compared to naturally occurring particles of similar sizes (Scherer *et al.*, 2020; Zimmermann *et al.*, 2020). In addition to the risks to biota, MPs have been shown to influence biogeochemical cycles (Chen *et al.*, 2023; Shi *et al.*, 2022; Wang *et al.*, 2022b), as well as soil properties (Cramer *et al.*, 2022; de Souza Machado *et al.*, 2018; Ingraffia *et al.*, 2022; Maqbool *et al.*, 2023), although many of these studies use high concentrations of MPs whereas environmentally-relevant concentrations often show little influence (Schöpfer *et al.*, 2022; Yu *et al.*, 2023). While further research is required to fully understand the impacts of MPs on individual species and ecosystems, it is clear that MP pollution represents a significant global environmental challenge.

1.2 Microplastic contamination in agricultural soils

1.2.1 Pathways and polymers

Agricultural soils receive MPs from both primary and secondary sources. Plastic products, such as mulching films, polytunnels, polymer coated fertilizers, and drip irrigation tape have been widely used in agriculture, beginning in the 1960s (Orzolek, 2017). In 2022, over 2.5 million tonnes of plastic were used for agriculture and gardening in the European Union, Switzerland, Norway and the United Kingdom (Plastics Europe, 2024). Agricultural plastic products provide many economic benefits by increasing crop production and decreasing the need for farmer-facilitated inputs (i.e. irrigation water and agrochemicals) into the soil (Figure 1.1) (Cusworth *et al.*, 2022; FAO, 2021; Hochmuth, 2017; Kasirajan and Ngouajio, 2012; Lamont, 2017).

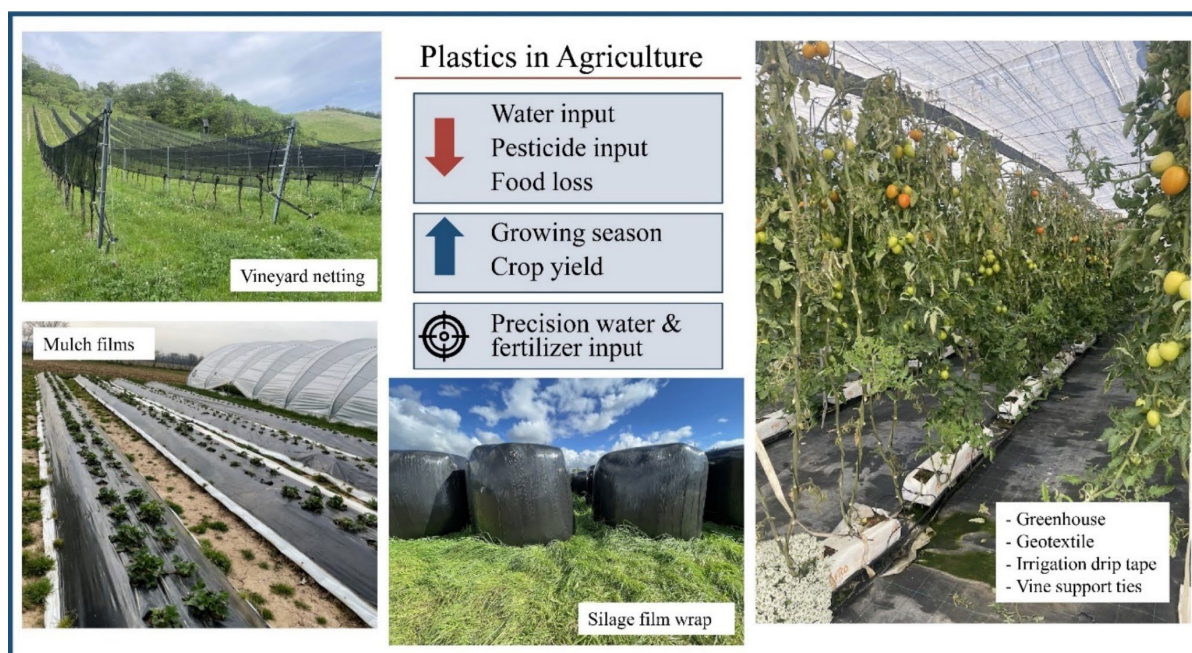


Figure 1.1. Images showing examples of plastic products used in agriculture. A selection of benefits of using plastic products are highlighted.

Once in the environment these plastic products can fragment into MPs, through biotic (Hadad *et al.*, 2005; Munhoz *et al.*, 2024; Yoshida *et al.*, 2016), and abiotic processes, such as photo-oxidation through UV radiation, tillage, heat, water availability (Andrady *et al.*, 2022; Beltrán-Sanahuja *et al.*, 2021; Chamas *et al.*, 2020; Maqbool *et al.*, 2024; Rodriguez *et al.*, 2020). In addition, agricultural plastic products often become contaminated with soil and plant residue which increases the difficulty and cost associated with plastic removal and recycling (FAO, 2021). As a result of both these factors, farms using plastic products are often contaminated with MPs of various polymer types associated with these materials including polyethylene (PE) in its various forms (linear low-density polyethylene [LLDPE], low-density polyethylene [LDPE] and high-density polyethylene [HDPE]), Polyvinyl Chloride (PVC), Polypropylene (PP), PLA and PBAT (FAO, 2021; Pereira *et al.*, 2021). In addition to direct and intentional plastic inputs, agricultural soils are unintentionally receiving macro- and microplastics from numerous sources including, but not limited to, biosolid input, runoff from roads, atmospheric deposition, and litter (Bläsing and Amelung, 2018; Brahney *et al.*, 2020; Cao *et al.*, 2021; Hurley and Nizzetto, 2018; Rillig *et al.*, 2017). As a result, MPs of several polymer types not directly related to agricultural plastic products have been detected in agricultural soils including polystyrene (PS), polymethyl methacrylate (PMMA), polyethylene terephthalate (PET), nylon or polyamide (PA), and tire and brake wear particles (Chen *et al.*, 2020; Corradini *et al.*, 2021; Piehl *et al.*, 2018). As a result of both these

primary and secondary sources of MPs, agricultural soils are thought to be a significant reservoir of MPs in the environment (Figure 1.2) (Kedzierski *et al.*, 2023; Nizzetto *et al.*, 2016b; Rillig, 2012).



Figure 1.2. Images showing examples of primary plastic input through residue of plastic products (left) and secondary plastics input through biosolids (right).

1.2.2 Abundance and distribution of plastics in the soil

Microplastics have been detected in agricultural soils in concentrations ranging from a few MPs kg⁻¹ of soil to thousands of MPs kg⁻¹ of soil (Kedzierski *et al.*, 2023; Piehl *et al.*, 2018). National and global estimates of MP concentrations in agricultural soils have been reported in Büks and Kaupenjohann (2020) and Kedzierski *et al.* (2023), though assessing MP stocks in agricultural soils on the national and global scale is challenging due to various means of MP extraction and MP characterization protocols for soils between research studies (Möller *et al.*, 2020).

Agricultural soils which have no history of using sewage sludge or compost amendments nor using plastic products such as mulching films typically have substantially fewer MPs than soils which have had these amendments and products (Cusworth *et al.*, 2022; Lwanga *et al.*, 2022a; van den Berg *et al.*, 2020; Zhou *et al.*, 2020). Additionally, long-term use of plastic products in agricultural fields has been shown to lead to extensive accumulation of MPs within soils (Huang *et al.*, 2020; Li *et al.*, 2022a; Xu *et al.*, 2022; Zhang *et al.*, 2023).

Microplastics are heterogeneously spatially distributed in agricultural soils, due to the various means of entry into the soil (Brandes *et al.*, 2021; Weber and Opp, 2020). For example, recent research in agricultural fields amended with compost found the perimeter of the agricultural

fields had up to 18 times more MPs due to litter from the roadside as compared to the middle of the fields (Braun *et al.*, 2023).

Within agricultural soils themselves, research is mixed regarding how MP concentrations vary with soil depth due to redistribution of MPs by soil biota, tillage and transportation vertically by infiltrating water (Huerta Lwanga *et al.*, 2017; Kedzierski *et al.*, 2023; Rillig *et al.*, 2017). Generally, MPs are most abundant in plough layers of the soil though MPs have been found in soils up to 1 meter deep (Heerey *et al.*, 2023; Heinze *et al.*, 2024; Weber *et al.*, 2022; Weber and Opp, 2020). There is substantial evidence that with time MPs of all shapes and sizes are incorporated into soil aggregates (Rehm *et al.*, 2021; Zubris and Richards, 2005), although the factors governing MP-soil aggregation processes are not well studied. One research study reported that up to 72% of MPs detected in agricultural soils were bound to soil aggregates (Zhang and Liu, 2018). Overall, the abundance and distribution of MPs in agricultural soils, whether incorporated in soil aggregates or loose within the soil, varies with soil depth, land management practices and geographical location.

1.3 Transport processes

1.3.1 The role of erosion in the plastic cycle

Plastic products are produced and primarily used in the terrestrial environment, with few exceptions, such as the fishing industry. Nevertheless, MPs have been abundantly detected in a variety of ecosystems, including terrestrial (Álvarez-Lopezello *et al.*, 2021; Bergmann *et al.*, 2019; Scheurer and Bigalke, 2018), aquatic (Horton *et al.*, 2017; Koelmans *et al.*, 2019), polar (Bergmann *et al.*, 2017; Obbard *et al.*, 2014; Tekman *et al.*, 2017) and anthropogenic ecosystems (Corradini *et al.*, 2021; Piehl *et al.*, 2018; Treilles *et al.*, 2021) across the globe including locations with no obvious source of MPs. The “plastic cycle” is a recent paradigm which aims to understand not only transportation processes of MPs but also seeks to understand the residence times and transformation of MPs as they cycle through various ecosystems across the globe (Bank and Hansson, 2019; Horton and Dixon, 2018). MP transport throughout the globe is thought to be driven in part by wind and water erosion processes which results in MPs being transferred from the terrestrial to both aquatic and atmospheric environments.

The movement of mineral soil particles in wind and water erosion processes have been long studied though microplastics have a number of unique properties compared to organic and mineral soil particles which could facilitate distinct mobilization and transport behaviours

(Figure 1.3). Firstly, MPs are approximately 30-60% less dense than mineral soil particles, with densities around that of water and SOM (1 g cm^{-3}), whereas mineral soil particles have a generally accepted average density of 2.65 g cm^{-3} (Yang *et al.*, 2022). This difference in density is believed to be a significant factor driving differences in MP transport compared to mineral soil particles (Nizzetto *et al.*, 2016a; Rehm *et al.*, 2021; Waldschläger and Schüttrumpf, 2019). Secondly, the physico-chemical properties of MPs such as hydrophobicity, plasticity and surface charge are likely to influence MP mobilization and transport processes in distinct ways compared to soil particles. Further these properties could influence how MPs interact with the surrounding soil, thereby reducing or accelerating MP transport. Lastly, MPs currently represents an all-encompassing term which includes plastics of all polymer types, morphology and sizes from $1 \mu\text{m}$ to 5 mm (Kooi and Koelmans, 2019; Thompson *et al.*, 2024). This diversity within the definition of MPs themselves adds complexity to making robust comparisons between the transport of MPs to natural soil particles.

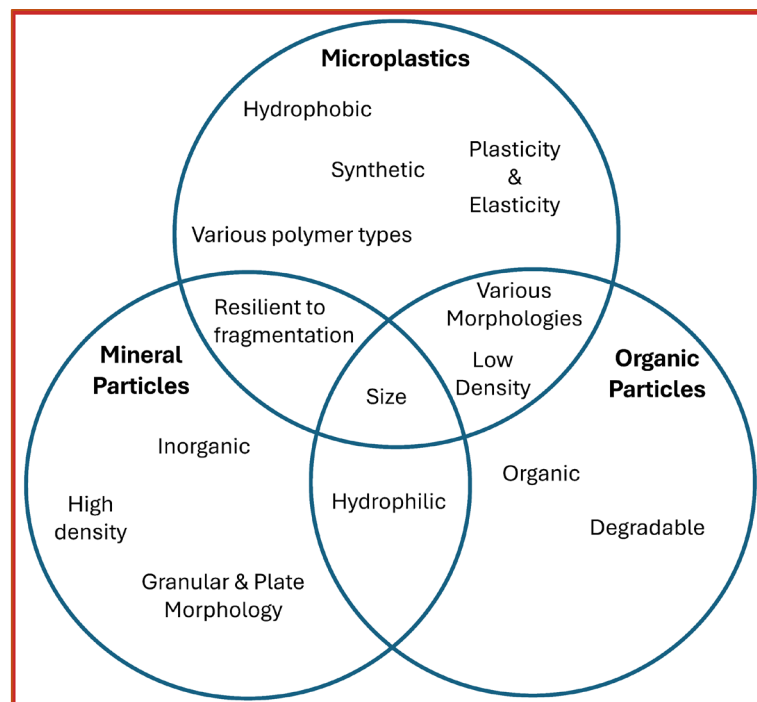


Figure 1.3. Venn diagram illustrating the similarities and differences in a selection of properties of microplastics, mineral soil particles and organic soil particles.

1.3.2 Wind erosion

Wind erosion is thought to be a major driver of MP transport from the terrestrial environment to the atmosphere resulting in MP long-distance transportation and deposition throughout the globe including remote regions (Allen *et al.*, 2019; Bergmann *et al.*, 2019; Brahney *et al.*, 2020, 2021). In an agricultural context, MPs have been shown to be quite mobile in wind erosion processes (Bullard *et al.*, 2021; Esders *et al.*, 2023; Rezaei *et al.*, 2019, 2022; Tian *et al.*, 2022; Yang *et al.*, 2022). In recent research, MPs have been shown to be highly enriched in eroded sediments in agricultural soils ranging from enrichment ratios as low as 2 but up to 200 (Bullard *et al.*, 2021; Rezaei *et al.*, 2019, 2022). However, specific mechanisms of wind erosion as well as characteristics of MPs which lead to mobilization are not well researched.

The density and hydrophobic properties of MPs have been shown to significantly influence the transport of MPs in wind erosion as compared to surrogates for soil particles which were more dense and hydrophilic (Esders *et al.*, 2023). Some research has shown that morphology or shape has an influential role in MP mobilization and transport in wind erosion processes with fibres being transported in higher amounts than beads, fragments or films (Bullard *et al.*, 2021; Tian *et al.*, 2022). The size of the MP particle also likely has a dominate role in MP transport and mobilization. One research study found MPs smaller than 1 mm were more mobile as compared to MPs sized 1-3 mm and 3-5 mm (Tian *et al.*, 2022). Similarly, observational research tracking atmospheric deposition of MPs have found that the majority of MPs found in their samples were smaller than 100 μm (Allen *et al.*, 2019; Bergmann *et al.*, 2019). It is likely that wind erosion is the dominate transportation mechanism of the smaller size fraction ($\geq 100 \mu\text{m}$) of MPs especially in soils with low soil moisture contents (Rezaei *et al.*, 2019).

1.3.3 Rainfall-induced erosion

Erosion driven by rainfall is believed to be a significant transport process moving MPs from soils into freshwater bodies and then ultimately to the marine environment (Nizzetto *et al.*, 2016a; Rehm *et al.*, 2021). Recent models have estimated that in some European catchments a greater mass of MPs are transported from the soil into freshwater ecosystems by surface runoff processes than by effluent input from wastewater treatment plants (Norling *et al.*, 2024; Rehm and Fiener, 2024). These estimates highlight that, whilst agricultural soils are thought to be a significant sink for MPs, they can also act as a source of MPs through erosion processes. Some research has highlighted the considerable influence rainfall-induced erosion

has on terrestrial MP fluxes, but little is known about the processes governing this movement (Horton and Dixon, 2018; Lwanga *et al.*, 2022b). Gaining a deeper understanding of these processes is vital, not only to improve estimates of MP export from terrestrial to aquatic ecosystems, but also to develop appropriate mitigation strategies to reduce MP transport from terrestrial to aquatic ecosystems.

In rainfall-induced erosion events, the processes of splash erosion and surface runoff act as the primary detaching and transport processes, though infiltrating water can also transport particles vertically into deeper soil layers. Whilst there is a critical lack of research reporting how MPs are detached and transported in splash erosion, infiltrating water and surface runoff, we draw on the existing MP transport research as well as the research from the broader related field of soil erosion to shed light on the mechanisms that may govern MP mobilization and transport.

1.3.3.1 Splash erosion

Splash erosion, the impact of raindrops on the soil surface, initiates the first phase in the erosion process, detachment (Ellison, 1948; Morgan, 2009). For soil particles, splash erosion is the primary process detaching soil particles from the soil matrix during soil erosion (Kinnell, 2005; Morgan, 1977). The initial impact of a raindrop can destroy soil aggregates and compact the soil (Ellison, 1948). After a raindrop strikes the soil surface, water constituting the raindrop spreads over the soil surface and ejects small water droplets (Allen, 1988; Zhao *et al.*, 2015), which can result in the transport of soil particles several centimetres away from the raindrop impact site (Legout *et al.*, 2005; Legu dois *et al.*, 2005).

Similar to soil particles, it is likely individual MPs are detached and transported from the soil due to splash erosion. However, no research currently exists which investigates MP detachment nor transport in soil as a result of splash erosion. The detachment of 6 µm spherical polystyrene (PS) MPs from saline water due to raindrop impact has been investigated in one research study. It found that MPs were transported in droplets from the raindrop impact site in varying quantities, with larger droplets transporting a larger number of MPs shorter distances, while smaller droplets transported fewer MPs but over a greater distance from the impact site (Lehmann *et al.*, 2021b). This research demonstrates that MPs can be effectively detached and transported from an environmental matrix due to the impact of raindrops. Other research investigating soil erosion has found hydrophobic soil particles to be more mobile than hydrophilic soil particles in splash erosion (Ahn *et al.*, 2013; Terry and

Shakesby, 1993). As MPs are generally hydrophobic, this could mean that MPs are preferentially influenced by splash erosion compared to soil particles which are typically hydrophilic. Additionally, as particle density is a key characteristic which determines the detachment and transport of soil particles due to splash erosion (Kinnell, 2005), MPs, due to their relatively low density, could be transported further than soil particles and be more readily detached as a function of splash erosion.

1.3.3.2 Vertical movement into the soil

The vertical transport of MPs through the soil profile has been researched to a somewhat greater extent than splash erosion and surface runoff, although much of this research has been conducted in controlled laboratory conditions in columns of soil, sediment or glass beads which are relatively homogeneous in size and shape and not reflective of environmental conditions. Further, these studies rarely use simulated rainfall but instead investigate MP transport in saturated soils with water added continuously with peristaltic pumps.

Research investigating the vertical transport of MPs under simulated rainfall or irrigation has found that the size of MPs is a major factor controlling the number and distance that MPs are transported vertically (Table 1.1). Rehm *et al.* (2021) found MPs sized 53-100 μm were more mobile vertically in the soil as compared to MPs sized 250-300 μm . Other research found MPs < 0.3 mm were the most mobile vertically in the soil, followed by MPs 0.3-1 mm, with MPs 1-5 mm being the least mobile (Zhang *et al.*, 2022). Research conducted by Du *et al.* (2024) compared the vertical migration ability of MPs in 3 size ranges and found that 25-147 μm were the most mobile followed by 0-25 μm and then 147-250 μm MPs. This finding contrasts with research using soil columns without raindrop impact, which generally shows that as MP size decreases, both the number of MPs transported and the distance they travel increase (Li *et al.*, 2024a; O'Connor *et al.*, 2019). The deviation from this pattern that Du *et al.* found in their research may be due to the effect of using soils in their experiments as opposed to sediments, sand particles or glass beads of homogenous sizes.

Table 1.1. Synthesis of research results on the influence of size on the vertical transport of microplastics from the soil surface with the impact of raindrops. Coloured cells indicate the size fraction which were transported furthest into the soil.

Author	Microplastic Size 1	Microplastic Size 2	Microplastic Size 3	Notes
Du <i>et al.</i> (2024)	0-25 μm	25-147 μm	147-250 μm	Column experiments with soils. Irrigation with raindrops was used.
Rehm <i>et al.</i> (2021)	53-100 μm	250-300 μm	-	Field-scale experiment. The depth the microplastics migrated were from natural rainfall over 1.5 years.
Zhang <i>et al.</i> (2022)	< 0.3 mm	0.3-1 mm	1-5 mm	Laboratory rainfall simulations experiments.

Soil texture, organic matter content, and soil chemical properties have been shown to influence the vertical transport of MPs in both column experiments and field-scale studies (Dong *et al.*, 2021; Du *et al.*, 2024; Rehm *et al.*, 2021; Wu *et al.*, 2020). As MPs are transported vertically in soils, they interact physically (i.e. physical straining by pore size) and chemically (i.e. sorption processes) with soil particles which can restrict their downward transport (Liu *et al.*, 2021; Yan *et al.*, 2020). The amount of rainfall a soil receives also can govern the amount and distance MPs are transported vertically (Du *et al.*, 2024; Zhang *et al.*, 2022; Zhao *et al.*, 2022). Current research on vertical MP transport in soil has provided valuable insight into factors influencing MP transport. However, understanding of the vertical transport of MP during rainfall events remains limited, especially in the context of real-world soil conditions and the influence of raindrop impact.

1.3.3.3 Surface runoff

Microplastic characteristics, alongside soil properties, rainfall intensity and MP residence time in the soil, influence how and when MP particles are transported in surface runoff (Han *et al.*, 2022; Rehm *et al.*, 2021; Schell *et al.*, 2022; Zhang *et al.*, 2022). Microplastics having densities around that of water are likely to be buoyant when surface runoff is present on the soil surface, whereas mineral soil particles in surface runoff, “hop” and roll down the slope of the soil (Hardy *et al.*, 2017; Kinnell, 2009). Recent research indicates that the transport of MPs in flows of water is akin to particulate organic carbon, which have similar densities to MPs (Hoellein *et al.*, 2019; Rehm *et al.*, 2021).

Between MPs themselves, size may influence the likelihood of mobilization and transport (Table 1.2.). When comparing the transport of plastics sized 250 μm , 1 mm, 4 mm, 15 mm and 50 mm, the 250 μm MP fraction was transported in the largest numbers (Han *et al.*, 2022). Similarly, Zhang *et al.* (2022), found MPs sized < 0.3 mm were transported in greater

numbers than MPs sized 0.3-1 mm and 1-5 mm. In contrast, other research found no significant difference in the number of MPs sized 53-63 μm and 250-300 μm transported from the soil in surface runoff, however slightly more of the 250-300 μm MPs were transported in the surface runoff (Rehm *et al.*, 2021). In order to gain a comprehensive understanding of which MP sizes are most mobile, further research is needed.

Table 1.2. Synthesis of research results on the influence of size on the transport of microplastics in surface runoff. Coloured cells indicate the size fraction which were transported in the greatest numbers in surface runoff.

Author	Microplastic Size 1	Microplastic Size 2	Microplastic Size 3	Notes
Han <i>et al.</i> (2022)	250 μm	1 mm	-	Plastics sized 4 mm, 15 mm and 50 mm, were also studied but no plastics > 4 mm were delivered in surface runoff.
Rehm <i>et al.</i> (2021)	53-100 μm	250-300 μm	-	No statistical difference between the two sizes but more 250-300 μm were found in surface runoff
Zhang <i>et al.</i> (2022)	< 0.3 mm	0.3-1 mm	1-5 mm	

However, isolating the effect of size from other MP characteristics, such as morphology and polymer type, presents a significant challenge. Fewer studies have investigated the influence of MP morphology on MP transport in surface runoff and findings are inconsistent. While some research reports high quantities of films and fibres being transported compared to particles or fragments (Han *et al.*, 2022), others observe higher quantities of particles being transported as compared to films and fibres (Zhang *et al.*, 2022).

Similar to soil erosion, factors such as soil characteristics, rainfall intensity and slope likely play an important role in MP mobility in surface runoff. Recent research has shown that the overall erodibility of the soil influences the delivery of MPs (Rehm *et al.*, 2021). In Rehm *et al.* (2021) the transport of MPs in silty loam and loamy sand was compared, with loamy sand representing soils of lower erodibility due to its coarser texture compared to the finer, more easily eroded silty loam soils. They found loamy sand contained more MP per gram of sediment transported in surface runoff but silty loams eroded more sediment overall, resulting in nearly equal MPs transported from both soils. Soils with high organic matter content are generally less prone to erosion, because organic matter facilitates soil particle binding through aggregation (Ekwue *et al.*, 1993; Morgan, 2009). This pattern seemed to also be true for MPs, as soil amended with sewage sludge with high amounts of organic matter led to the erosion of very few MPs in surface runoff (Schell *et al.*, 2022).

The intensity of rainfall along with soil slope are critical factors governing the transport of soil particles (Morgan, 2009), however only two studies have investigated the impact of these factors on MP transport in surface runoff. Zhang *et al.* (2022) explored the influence of soil slope on MP transport in surface runoff and found a clear trend of increased slope increased the number of MPs transported in surface runoff. Han *et al.* (2022) examined the influence of rainfall intensity on MP transport and found that increased rainfall intensity, increased the number of MPs transported in surface runoff. Together this research aligns with research on soil erosion which follows the same patterns of increasing slope and rainfall intensity increases the amount of soil transport in surface runoff.

The residence time MPs have in soils can (1) change the characteristic of the MPs through degradation processes and (2) increase the interactions between MPs and soil particles resulting in aggregation. No research to date has investigated the effects of MP “age” or degree of degradation on mobilization and transport in surface runoff. One research study has been conducted investigating the vertical transport of aged MPs, but no comparison was made with pristine MPs (Yan *et al.*, 2020). The degree of MP aging could influence the transport in surface runoff and splash erosion as with increased age, MPs can become less hydrophobic and have rougher surfaces, thereby likely changing MP interactions with raindrops, surface runoff and surrounding soil particles (Liu *et al.*, 2019a). The second effect MP residence time has on transport is increased interactions between MPs and soil particles, resulting in aggregation (Yang *et al.*, 2022; Rehm *et al.*, 2021). It has been shown that through time as MPs are incorporated into aggregates they are transported in smaller amounts from soils in surface runoff (Rehm *et al.*, 2021).

1.4 Methods for detecting microplastics in soil

The complexities surrounding extraction and identification of MPs in soils has long been acknowledged as a reason little research exists describing MPs in soils (Rillig, 2012). Several MP identification methods require MPs to be separated from soil, so that mineral and organic soil materials do not interfere or distort signals from analytical equipment associated with approaches such as Raman spectroscopy, Fourier transform infrared spectroscopy (FTIR), or fluorescent microscopy (Bläsing and Amelung, 2018; Möller *et al.*, 2020). Currently, most research uses a 2-step extraction method for removing MPs from soil samples. First, a density separation which involves placing the soil containing MPs into a salt solution (for example NaCl or ZnCl₂) with a density higher than that of plastics, and removing the light density

particles from the solution (Bläsing and Amelung, 2018; Möller *et al.*, 2020). Second, soil organic material is removed from the light density particles sample so it will not interfere with MP signals from analytical equipment. This is done by choosing one of a variety of methods including but not limited to acid treatments, enzymatic digestions, or oxidative treatments (Bläsing and Amelung, 2018). No comprehensive or widely adopted method currently exists for MP analysis, which makes comparisons between research studies difficult as results can be a function of the sample processing and analytical equipment used to quantify MP analysis (Möller *et al.*, 2020).

Labelling MPs with carbon isotopes (Sander *et al.*, 2019; Taipale *et al.*, 2019), rare metals (Heinze *et al.*, 2021; Mitrano *et al.*, 2019), and fluorescent dyes (Caldwell *et al.*, 2021; Laermanns *et al.*, 2021) have been found to be effective alternatives to understand MP transformation and transport processes in soils, as complete MP extraction from the soil can be avoided. Using fluorescent particles has been shown to be a promising technique to understand particle movement during rainfall-induced erosion events (Hardy *et al.*, 2016, 2017; Laermanns *et al.*, 2021). Fluorescent particles, being a visual tracer, can not only be easily detected in soil and surface runoff samples, but also can be used to track the movement of particles over the soil surface giving insight into the rate and behaviour of particles during a rainfall-induced erosion event. Additionally, as the fluorescence emanating from the particles can be captured through photography, this avoids the need to disturb the soil or pause the rainfall simulations in order to collect data on the movement of the particles as is the case with other tracer methods (Guzmán *et al.*, 2013; Hardy *et al.*, 2017).

Complexity surrounding fluorescent particle detection during rainfall simulations has often led to compromises in the experimental design or data analysis. For example, Laermanns *et al.* (2021) used impervious surfaces in their rainfall simulations to ensure MP visibility throughout the experiment but by so doing blocked the environmentally realistic transport pathway of MPs moving into the soil profile. Hardy *et al.* (2017) used video imagery to measure the distance and speed of fluorescent sand particles over the soil surface. However, the complexity of accurately identifying the fluorescent particles led them to only include particles on the soil surface for more than 0.5 seconds and particles which were in at least 95% of the video frames in their data analysis. Particles which did not meet these conditions were considered to have been “buried” in the soil, submerged under water or splashed out of the box, therefore the fate nor the transport pathways of these particles were determined.

1.5 Summary and research gaps

In this literature review, the current knowledge surrounding the transport of MPs in agricultural soils through rainfall-induced erosion has been summarised and discussed. It is clear that several factors including, MP characteristics, soil and rainfall properties and MP residence time in the soil influence the probability of MP mobilization and transport from agricultural soil. However, the extent to which these factors and mechanisms influence MP transport are still not well understood, in part due to the lack of research. To date, research has not investigated how MP characteristics influence the transport pathways the MPs follow during a rainfall-induced erosion event (Figure 1.4). Specifically, MP transport vertically into the soil and in surface runoff is often investigated separately and no research has explored the transport of MPs in splash erosion. Additionally, little research on MP transport has explored how environmentally relevant conditions such as aged MPs and MPs bound in soil aggregates are transported in rainfall-induced erosion. Addressing these research gaps will benefit our understanding of MP transport in rainfall-induced erosion processes as well as aid in designing future experiments to further our understanding of MP transport from agricultural soils to freshwater ecosystems.

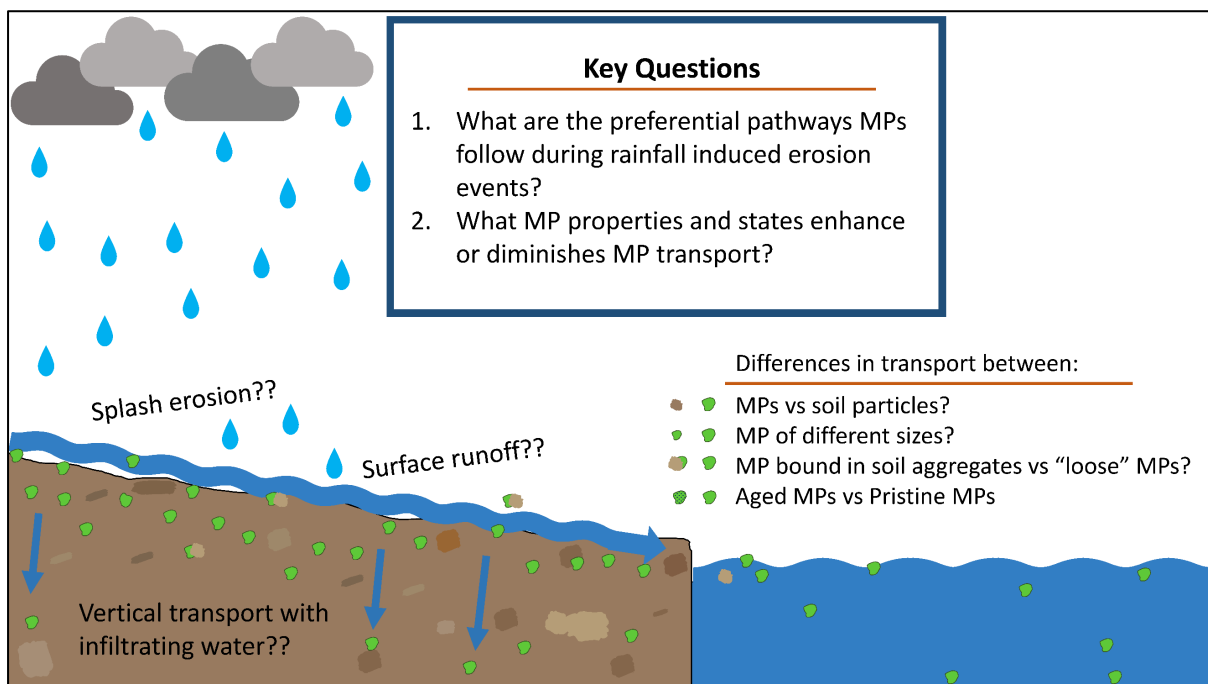


Figure 1.4. Conceptual diagram outlining key research gaps for microplastic (MP) transport in rainfall-induced soil erosion. Green particles represent MPs.

1.6 Thesis aims and objectives

This thesis examines the factors and mechanisms regulating the transport of MPs during rainfall-induced erosion, with a primary focus on surface runoff while also considering splash erosion and vertical transport. Through the development and application of highly innovative methodologies, this thesis aims to (1) investigate how MPs properties enhance or diminish the transport of MPs during rainfall-induced erosion, and (2) explore the transport pathways MPs follow as influenced by MP properties.

To meet these aims, the thesis addresses the following objectives:

1. To compare the transport pathways and rates of movement between MPs of various polymer types with natural soil particles during rainfall simulations (chapter 2);
2. To evaluate the transport pathways MPs of various size follow during rainfall simulations (chapter 3);
3. To investigate how the degree of MP aging affects aggregation and the transport of MPs during rainfall simulations (chapter 4).

1.7 Thesis structure

The thesis consists of 5 chapters, beginning with a general introduction chapter, followed by 3 data chapters presented as manuscripts, and concludes with a general discussion chapter. Chapters 2, 3, and 4 either have been submitted or are intended for submission in peer-reviewed journals.

Chapter 2 addresses objective 1 by conducting laboratory rainfall simulations to investigate the transport pathways three MPs and a fluorescently tagged sand particle follow in response to surface runoff and splash erosion. Vertical movement of particles into the soil profile is also examined. Novel methodologies developed in this research not only enabled the quantification of the number of each particle type in the transport pathway, but also allowed for the quantification of the rates of movement for each of the particle types.

Chapter 3 addresses objective 2 by performing rainfall simulations on plots located within an agricultural field. Building on knowledge gained in chapter 2, this experiment further investigates transport pathway of MPs but with a focus on varying MP size. The number of

MPs on the soil surface throughout the rainfall simulations is measured, alongside the number of MPs transported in surface runoff and the depth to which MPs are transported vertically into the soil profile. A laboratory rainfall simulation is included in the supplementary information (Appendix 2) to investigate the role of splash erosion on the MP transport patterns observed in the field experiment.

Chapter 4 addresses objective 3 by exploring methodologies to make laboratory rainfall simulations mirror environmental conditions, specifically by artificially accelerating MP aging and aggregation processes. Rainfall simulations are conducted to test the influence of MP age and aggregation on MP transport in surface runoff.

Chapter 5 provides a summary and analysis of the findings of this research and considers directions for future research.

2. The transport of microplastics from soil in response to surface runoff and splash erosion

Emilee Severe¹, Ben W. J. Surridge¹, Peter Fiener², Michael P. Coogan³, Rachel H. Platel³, Mike R. James¹, John Quinton¹

1. Lancaster Environment Centre, Lancaster University, Lancaster, UK
2. Institute of Geography, University of Augsburg, Alter Postweg 118, 86159 Augsburg, Germany
3. Department of Chemistry, Lancaster University, Lancaster, UK

Abstract

Erosion is hypothesised to be a significant process transporting microplastics (MPs) from soils to aquatic environments. However, the factors controlling this process are poorly understood. Using a unique combination of high-frequency photography and fluorescent particles, we investigated the transport of three MPs of varying polymer type during rainfall simulations: linear-low density polyethylene (LLDPE), polystyrene (PS); and polymethyl methacrylate (PMMA). We measured the movement of particles on the soil surface alongside the number of particles transported through splash erosion and surface runoff, comparing the behaviour of MPs to sand particles. Our results show that sand particles were preferentially retained in the soil after the rainfall simulations, while PS and PMMA were preferentially transported from the soil surface by splash erosion. The PS, PMMA, and sand particles were transported by surface runoff in nearly equal numbers, while significantly fewer LLDPE particles were transported in surface runoff. By comparing the movement of MPs to sand particles, results from our research establish a benchmark for evaluating MP mobility with current knowledge of soil particle movement. Understanding the transport processes controlling movement of MPs within soils is important not only for the redistribution of MPs within soils themselves, but also for the ultimate fluxes of MPs from soils to aquatic ecosystems.

2.1 Introduction

Plastic products have been widely used in agriculture since the 1960s (Kasirajan and Ngouajio, 2012), with an estimated 12.5 million tons of plastic currently used every year for food production across the globe (FAO, 2021). However, once added to soil, removing agricultural plastics is challenging because exposure to sunlight and other environmental factors fragment the plastics, creating smaller macro-, micro- or nano-scale plastics (Feuilloley *et al.*, 2005; Steinmetz *et al.*, 2016). Further, many agricultural soils receive plastic inputs from a range of sources that include biosolids, compost, road runoff and atmospheric deposition (Bläsing and Amelung, 2018; Brahney *et al.*, 2020; Cao *et al.*, 2021). As a consequence, microplastics (MPs) have been identified in soils with no obvious history of plastic input associated with agricultural production (Corradini *et al.*, 2021; Piehl *et al.*, 2018).

A growing body of literature suggests that surface runoff is an important process contributing to the transport of MPs throughout terrestrial environments and across boundaries between terrestrial and aquatic ecosystems (Crossman *et al.*, 2020; Lwanga *et al.*, 2022b; Nizzetto *et al.*, 2016a; Rehm *et al.*, 2021; Rehm and Fiener, 2024; Klaus *et al.*, 2024). Plastics have distinct properties compared to mineral soil particles, potentially leading to different behaviour during mobilization and transportation processes (Waldschläger *et al.*, 2022; Waldschläger and Schüttrumpf, 2019). First, plastics typically have densities similar to water ($\sim 1 \text{ g cm}^{-3}$), whereas mineral soil particles have an average density of $\sim 2.65 \text{ g cm}^{-3}$ (Blake, 2008). This difference in density is thought to be one of the most influential factors driving differences in transport between MP and mineral soil particles (Nizzetto *et al.*, 2016a; Rehm *et al.*, 2021; Waldschläger and Schüttrumpf, 2019).

Second, the physico-chemical properties of MPs, including hydrophobicity, plasticity and surface charge, are likely to influence MP detachment and transport in comparison to mineral soil particles. Moreover, these properties may change over time, due to multiple forms of MP aging which can influence interactions between MP and soil particles (Li *et al.*, 2024b). Research that directly investigates the influence of these MP properties on detachment and transport is lacking. However, research investigating soil erosion has shown hydrophobic soil particles to be more mobile than hydrophilic soil particles (Ahn *et al.*, 2013; Terry and Shakesby, 1993). Therefore, the level of MP hydrophobicity is likely to be an important

property influencing the transport behaviour of MPs in erosion events as compared to soil particles.

Finally, MPs currently represent an extremely broad term which includes plastics of all polymer types, morphologies, degrees of aging, and sizes from 1 μm to 5 mm (Kooi and Koelmans, 2019). These varying properties and states could lead to either more or less rapid MP transport rates compared to mineral soil particles. However, while some research has begun to focus on comparing the transport of MPs of various size, morphology and polymer type, robust comparisons to the transport behaviour of natural soil particles is lacking.

In this context, we sought to compare the movement of sand particles, a surrogate for mineral soil particles, with several types of MPs within the soil environment. Using fluorescent sand particles and MPs, we tracked the “real-time” movement of the particles during rainfall simulations, quantifying the rate and potential transport pathways (surface runoff, vertical flux into the soil, and splash erosion) of the MP and sand particles. Our research addressed two key questions. Firstly, how do the patterns of movement on the soil surface differ between various MP polymer types and mineral soil particles? Secondly, is there evidence for preferential transport pathways across various MP polymer types and mineral soil particles? We hypothesize that (1) MPs will show more rapid rates of movement from the soil surface compared to the sand particle throughout the rainfall event and (2) MPs of all polymer types will be preferentially eroded both through surface runoff and splash erosion as compared to the sand particle, due to physical and chemical differences between the particle types, for example, density and hydrophobicity. Understanding the similarities and differences in the transport processes affecting both MPs and mineral soil particles is important not only for estimating MP fluxes from terrestrial to aquatic ecosystems, but also for evaluating the effectiveness of erosion control practices in terms of reducing MP loads reaching aquatic ecosystems.

2.2 Methods

2.2.1 Experimental set-up

Metal soil boxes (width, length and depth of 24.5 cm x 50 cm x 10 cm) were packed with a loamy sand topsoil from Norfolk, UK which had been pre-screened to 4 mm (Bailey’s of Norfolk LTD). Particle size range distribution of the soil was $7.8 \pm 1.7\%$ clay; $7.6 \pm 0.4\%$ silt; $84.7 \pm 1.9\%$ sand. Organic matter content of the soil was not measured but another study using the same soil reported an organic matter content around 3% (Ripley, 2023). Soil boxes

were packed by adding ~3.6 kg of soil in five separate 2.2 cm layers then evenly spreading 500 mL of tap water on the surface with a watering can. This process was repeated until the soil reached a depth of 11 cm after which the soil box was covered with a lid and left for 24 hours to allow for homogenization of the water in the soil. This resulted in a dry bulk density of 1.3 g cm^{-3} and a volumetric water content of 19%.

Soil boxes were set at a 10-degree slope to reflect realistic environmental topography whilst ensuring runoff generation in a practical time frame. A 1 m x 1 m wooden frame covered in black geotextile fabric was placed beside the soil box, to determine the quantity of particles transported out of the soil box through splash erosion. Rainfall was simulated using a gravity-fed rainfall simulator (Figure 2.1) set at 50 mm h^{-1} with a Christiansen's coefficient of 84.5% (Christiansen, 1942). The simulator was mounted 3.27 m above the ground and produced raindrops ranging 0.9 mm- 3.5 mm with the mean raindrop size being 1.8 mm resulting in a kinetic energy of approximately $14.59 \text{ J m}^{-2} \text{ mm}^{-1}$.

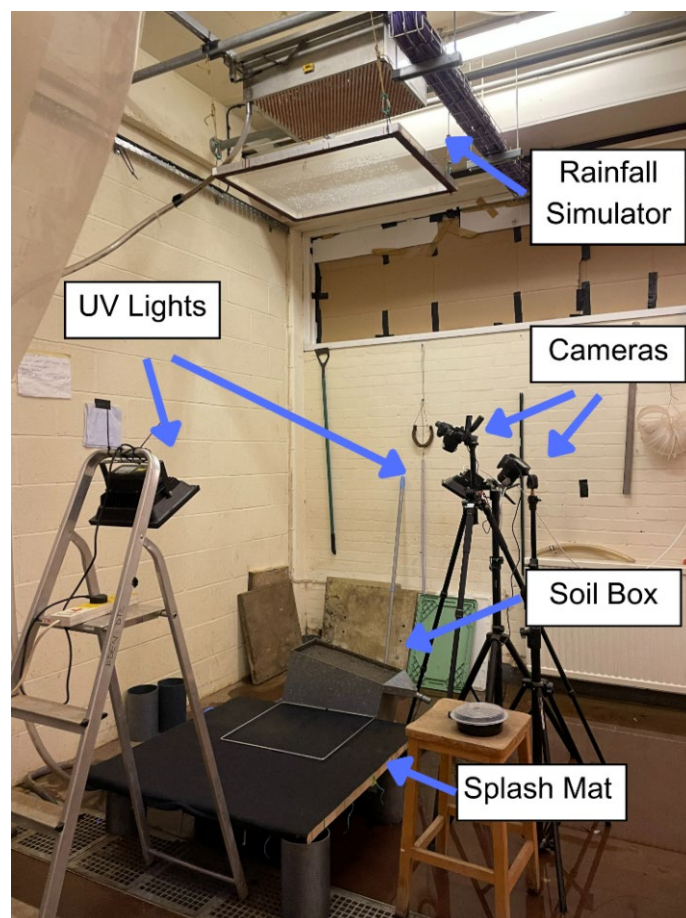


Figure 2.1. Laboratory set-up for simulation experiment.

The rainfall rate from this simulator is known to decline after a few hours of operation (Pryce, 2011), therefore the rainfall rate was measured before each rainfall simulation and no more than two rainfall simulations were conducted in one day. Overall, a mean rainfall rate of $49 \pm 2 \text{ mm h}^{-1}$ was recorded. While this rainfall rate is considered an extreme rainfall event in the UK (Blenkinsop *et al.*, 2017; Hand *et al.*, 2004), high rainfall rates are commonly used in erosion experiments in order to rapidly saturate the soil and to induce surface runoff, thereby facilitating the study of erosion processes (Novara *et al.*, 2012; Kinnell, 2009; Koch *et al.*, 2024).

2.2.2 Particle tracers

Four types of fluorescent particle were used in the research: linear low-density polyethylene (LLDPE); polymethyl methacrylate (PMMA); high-impact polystyrene (PS); and sand. Fluorescent PMMA (Simply Plastic Ltd.) and PS (Mark SG Enterprises Ltd.) were purchased commercially, and the polymer types were confirmed via FTIR. To create a fluorescent LLDPE particle, LLDPE (Sigma-Aldrich) was fused to a homogenous mixture with a modified lipophilic Rhodamine B derivative (see Section 2.2.3) and characterized by fluorescence spectroscopy. The sand particles used were comprised of a sand core with a green fluorescent coating (Hardy *et al.*, 2017) (Partrac Ltd.).

Density varied slightly between each of the particle types: LLDPE = 0.92 g cm^{-3} , PMMA = 1.19 g cm^{-3} , PS = 1.05 g cm^{-3} and the sand particles = 2.65 g cm^{-3} . All plastic types were milled using a Cryomill (Verder-Scientific) which gave the PMMA and PS a granular-like particle morphology (Figure 2.2). LLDPE assumed a thinner, flake-like particle morphology after milling, which is likely due to its higher plasticity compared to the PMMA and PS.

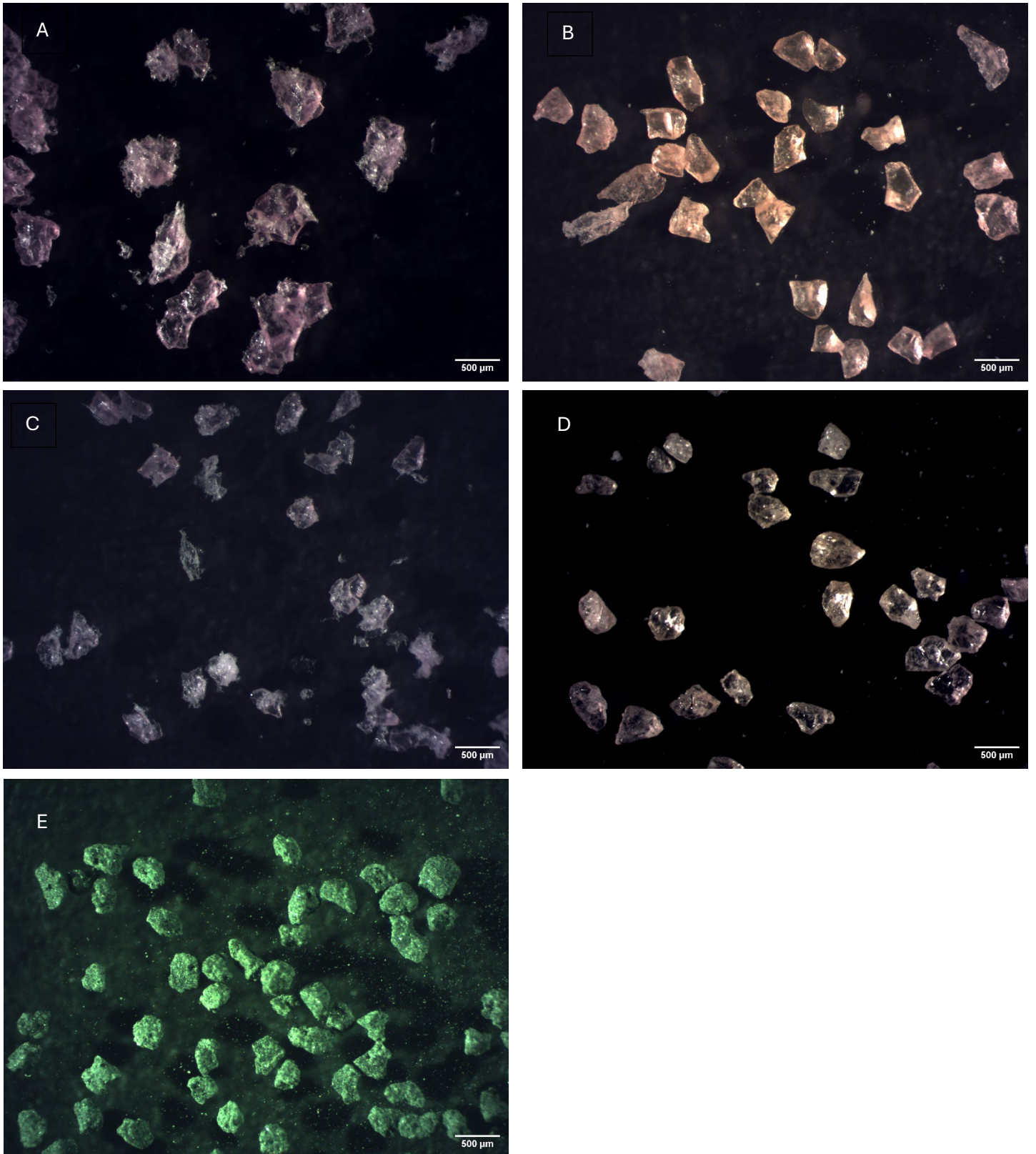


Figure 2.2. Images of the particles used in this experiment. Where image A represents linear low-density polyethylene large particle (LLDPE_L), B represents polymethyl methacrylate particle (PMMA), C represents linear low-density polyethylene small particle (LLDPE_S), D represents polystyrene particle (PS), and E represents the sand particle.

Each particle type was dry sieved using an automated shaker (Endecotts Ltd.) to target size ranges. LLDPE was sieved into two size ranges: small 250-355 μm (LLDPE_S) and large 500-600 μm (LLDPE_L). The PMMA, PS and the sand particles were sieved to 250-355 μm size range. The LLDPE_S particle proved difficult to detect and resulted in poor recovery during our experiments, causing us to exclude it from the research reported here (Section 2.2.4). A weight-to-particle number ratio was calculated for each particle type, and approximately 10,000 particles of each particle type were spread evenly on the surface of the soil within each soil box immediately before the soil box was placed under the rainfall simulator. Resulting in an approximate concentration of 81,630 MPs m^{-2} . The input concentration of 10,000 particles was arbitrarily chosen to ensure sufficient particles would be detected, without compromising the ability to detect individual particles on the soil surface. Estimates from images of the soil surface after the initial input of particles suggested a mean particle count of 9780 ± 976 . PS had the highest mean count of 10790 ± 347 particles, sand and PMMA had similar counts of 9590 ± 1381 and 9525 ± 814 particles, respectively, and LLDPE_L had the lowest mean count of 9219 ± 396 particles. Each particle type was placed in separate soil boxes, rather than combined particle treatments within individual soil boxes, and blank soil boxes without the addition of any particles were used to account for background fluorescence in the soil and reflection of UV light on the water during data collection (Section 2.2.5).

2.2.3 Preparation of fluorescent linear low-density polyethylene particles

To a solution of rhodamine B chloride (Sigma Aldrich) (25 mg, 0.052 mmol) in acetonitrile (2.5 mL) in a 10 mL round bottom flask equipped with a stirrer bar was added silver (I) trifluoromethane sulphonate (14 mg, 0.055 mmol) in acetonitrile (2.5 mL). The flask was flushed with nitrogen, sealed with a greased stopper loosely attached with rubber bands and the mixture stirred at ambient temperature for 10 minutes. The resulting thick suspension was filtered through celite, washed with 2 x 1 mL acetonitrile and concentrated under vacuum to give a very dark red solid that was used without further purification in the next step.

To a 500 mL round bottomed flask equipped with a large stirrer bar was added 20 g of linear low density PE pellets (Sigma Aldrich) and 250 mL of toluene. The mixture was heated in an oil bath set to 100 C with stirring, initially magnetic and then, as the mixture thickened, manual with a large spatula, and periodic addition of portions of toluene to maintain the volume as it was absorbed into the mixture. Once the beads were all uniformly swollen (ca.

30 minutes) 0.4 mL of a 0.01M solution of Rhodamine B Trifluoromethanesulphonate salt in acetonitrile was added dropwise with rapid stirring to disperse the highly coloured areas left after the immediate evaporation of the acetonitrile (CAUTION – over-rapid addition can lead to violent evaporation). Stirring was continued at 100 C until the swollen beads were uniformly coloured, and then the oil bath temperature was increased to 140 C and manual stirring continued until the mixture was homogenous (ca. 1 hour). Residual toluene was evaporated under a stream of compressed air, and then the mixture was allowed to cool to room temperature. The polymer was cut into 0.5-1 cm cubes and dried in a vacuum oven at 70 C overnight or to a constant mass.

2.2.4 LLDPE_S recovery

LLDPE_S particle (sized 250-355 µm) showed poor recovery in the images of the soil surface, splash mat, surface runoff and soil samples, with a total of <1% of particles inputted into the soil boxes accounted for. This poor recovery led us to exclude the LLDPE_S particle from the results. Both the LLDPE_L and LLDPE_S particles were dyed using Rhodamine B. Rhodamine B's excitation and emission peak wavelength is 546 nm and 567 nm, respectively. In order to fluoresce the MP and sand particles with multiple peak excitation wavelengths, a UV light with a peak emission of 365 nm was used. The commercially dyed MPs and sand particles were easily detectable, the LLDPE particles proved more difficult. As LLDPE_L particles had larger amounts of dye due to its larger size (500-600 µm), they were more readily detected than the LLDPE_S particles.

2.2.5 Image collection

Two cameras were used to capture images of both the particles moving over the soil surface and the particles transported out of the soil box via splash erosion during the rainfall simulations (Figure 2.4). A Canon EOS 850D camera with a 50 mm prime lens was used to capture images of the soil surface with an intervalometer (Neewer RS-60E3) programmed to take images every 10 seconds. Images were captured with the following settings: f/9.0, exposure 1 sec., ISO 320, RAW+ JPEG. The resolution of the images were 6000 x 4000 pixels. Camera was set at the base of the soil box approximately 50 cm away from the soil box and at a height of 140 cm.

An additional camera, a Canon EOS 500D, recorded images of a 50 cm x 50 cm sub-area of the 1 m x 1 m splash mat, marked with a metal quadrat, directly beside the soil box to record the number of particles transported through splash erosion over time. As for the soil surface

photography, a 50 mm prime lens was used, to photograph the area of the splash mat with an intervalometer (NeeWER RS-60E3) programmed to capture images every 60 seconds. Images were captured with the following settings: f/9.0, exposure 1 sec., ISO 200, RAW+JPEG. Prior to the start of the rainfall simulations, lenses on both cameras were autofocused with the laboratory room lights on, then switched to manual focus and the focus ring was manually secured to prevent focus drift due to shutter vibrations (Hardy *et al.*, 2016).

At the conclusion of each simulation, the entire 1 m² splash mat was photographed and used to calculate the total number of particles transported by splash erosion. The EOS 850D with a 50 mm prime lens was used to photograph the mat. The 1m² mat was divided into quarters using 50 cm² metal quadrats. Each quadrat was photographed separately with the camera at a height of approximately 210 cm in order to capture the whole sectioned area (Figure 2.3).

Two, 50-watt UV floodlights with a peak emission at 365 nm (Mark SG Enterprises) were used to excite the fluorescent dyes in the plastic and sand particles (Ehlers *et al.*, 2020). One floodlight was positioned to illuminate the soil box, and the other was positioned to illuminate the splash mat. When the entire 1 m² splash mat was photographed both of the UV lamps were repositioned to fully illuminate each section as it was photographed. Windows in the laboratory were blacked out to eliminate visible light from the room.



Figure 2.3 Camera and light set-up to photograph the 1m² splash mat at the conclusion of a rainfall simulation.

2.2.6 Surface runoff and soil samples

Once surface runoff began, the surface runoff leaving each soil box was subsampled every 5 minutes for 25 minutes. After collection, samples were immediately weighed before being placed in a drying cabinet (maximum temperature 50°C) until dry, then re-weighed to determine the volume of surface runoff and the mass of sediment transported from each soil box. Sediment and fluorescent particles were subsequently spread evenly on a dark surface, photographed, then manually counted to determine the number of fluorescent particles in each sample (Figure 2.4).

Four soil cores (diameter = 5.3 cm) were taken from each soil box following the rainfall simulation. The locations for core sampling were chosen using stratified random sampling to account for variations in particles downslope across the soil box. Soil samples were taken to a depth of 4 cm and sectioned every centimeter. Soil samples were then dried, spread thinly on a dark surface, photographed and the fluorescent particles in the images were manually counted (Figure 2.4).

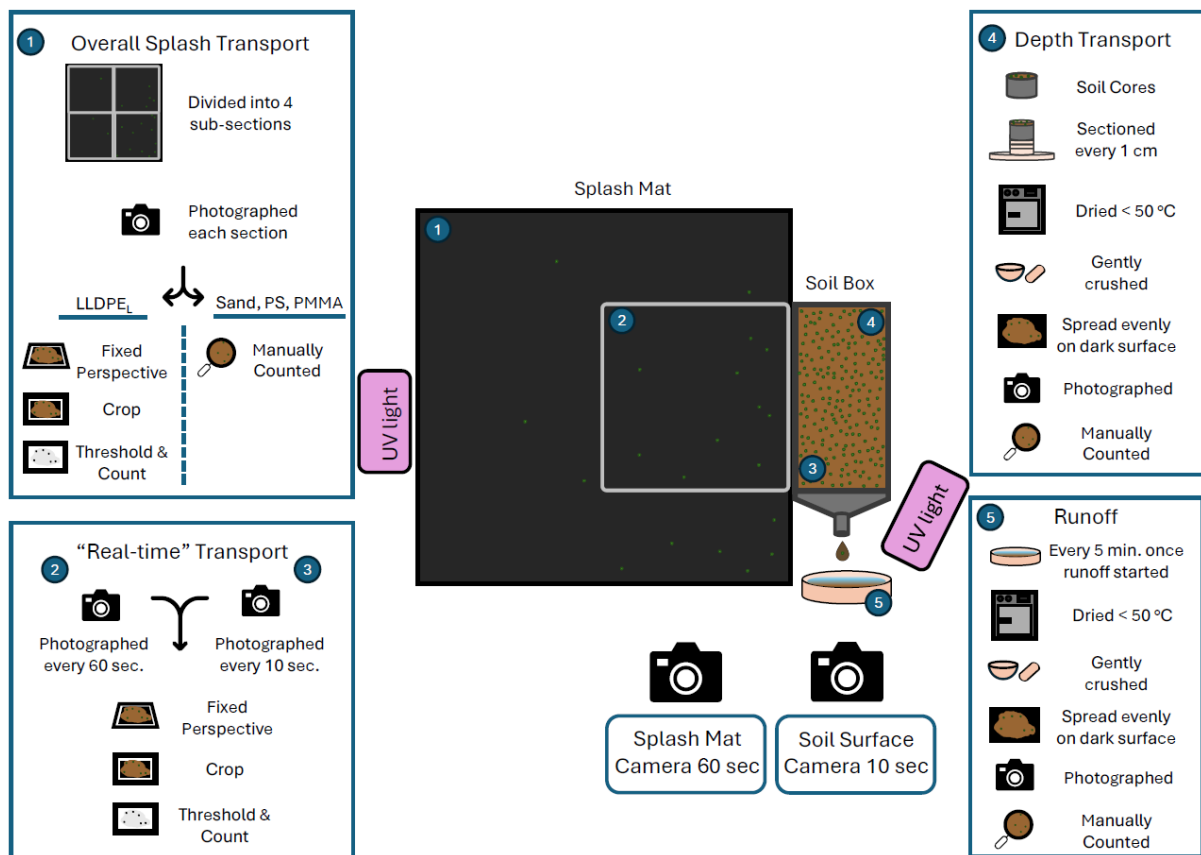


Figure 2.4. Diagram showing the experimental set-up, sample collection and sample processing. LLDPE_L; PMMA; PS; and SAND represents linear low-density polyethylene, polymethyl methacrylate, polystyrene and sand particles, respectively.

2.2.7 Image processing and analysis

All images were captured in RAW format and converted to TIFF (LZW compression) format using Adobe Photoshop. As the cameras could not be located to observe the soil box and splash mat surfaces orthogonally due to rainfall, perspective effects varied the size of the ground area represented by individual pixels within images. The Perspective Warp tool (stretch function) in Adobe Photoshop was used to resample the images, correcting for perspective in the images (Bowers and Johansen, 2002). Reference scales were placed at the top and bottom of the soil box and splash mat to validate the resampling.

Using Image J, each image was cropped just inside the edges of the soil box which created approximately a 24.5 cm x 50 cm area in the images. Splash mat images were cropped just inside the edges of the sub-area marked with a metal quadrat, creating an approximate 50 cm x 50 cm area in the images. Images were then processed through the Color Thresholding tool in Image J to quantify the particle counts of MP and sand in each image, using a HSB color space specific to each particle type. The Watershed Separation tool was then used to identify and separate potential adjoining particles.

Particles within the 1 m x 1 m splash mat were manually counted, except for the LLDPE particles which were counted with Image J thresholding. This was due to the splash mat images having a slightly lower camera resolution compared to images taken of the surface runoff and soil samples. The LLDPE particles had a slightly weaker fluorescence compared to the commercially purchased plastics with the chosen UV wavelength. Combined, these two factors led to analysis with Image J for the LLDPE images of the splash mat.

2.2.8 Color thresholding

Using the Color Thresholding tool in image J microplastics and sand particles were identified and counted. Color thresholding converts images from RGB to binary images by segmenting pixels to set values. The HSB color space was used in the segmentation of the image as it is robust against changes in illumination (Gonzalez and Woods, 2008). Different thresholds were used for the surface of the soil and the splash mat (Table 2.1). As the rainfall simulation progressed through time, the surface runoff reflected the light of the UV lamp, so thresholds which excluded pixels of high brightness values and retained high saturation values were used.

Table 2.1. Threshold ranges for particle detection as used in image J. LLDPE_L; LLDPE_S; PMMA; PS; and SAND represents linear low-density polyethylene size large, linear low-density polyethylene size small, polymethyl methacrylate, polystyrene and sand particles, respectively.

Soil Surface				Splash Mat			
Particle	Hue	Saturation	Brightness	Particle	Hue	Saturation	Brightness
LLDPE _L	20-225 “pass” or band-reject	85-255	45-255	LLDPE _L	20-225 “pass” or band-reject	85-255	35-255
LLDPE _S	20-195 “pass” or band-reject	85-255	40-255	LLDPE _S	20-225 “pass” or band-reject	70-255	30-255
SAND	50-130	40-255	65-255	SAND	50-130	85-255	45-255
PMMA	0-55	30-255	150-255	PMMA	0-55	30-255	85-255
PS	0-55	55-255	150-255	PS	0-55	60-255	70-255

2.2.9 Performance evaluation

Because of the dynamic nature of the soil surface and particles during the rainfall simulations, it was challenging to quantify the effectiveness of the image-based detection of particles on the soil surface and splash mat. Due to changes in the soil surface throughout the simulations and the onset of water flowing on the soil surface, it is possible that there were some particles on the surface of the soil that remained undetected using the approach developed for our research.

To quantify the effectiveness of the image analysis process, particles in the images of the soil boxes and splash mats before, during and after the rainfall simulation were manually counted and used as ground truth. Performance of the image analysis was evaluated by calculating the recall, precision and f-score for each particle type as shown in Table 2.2. Recall, precision and f-score are calculated on a scale of 0 to 1, with 1 reflecting the highest performance. Recall describes the percentage of particles detected which were correctly classified (true positive/ (true positive +false negative)). Precision describes the proportion of the positives detected that were correctly classified as particles (true positive/ (true positive +false positive)). F-score considers both the precision and the recall to measure the proportion of particles which were correctly classified in the images ($2*((\text{precision}*\text{recall})/(\text{precision} +\text{recall}))$). Overall, for the soil surface, all particles had a f-score > 0.88 meaning over 88% of particles were correctly classified. The splash mat showed similarly high rates of detection for sand, PMMA and PS (f-score > 0.97), with LLDPE_L showing the lowest f-score of 0.81.

Table 2.2. Table showing the correct and incorrect identification of fluorescent particles in images. LLDPE_L; PMMA; PS; and SAND represents linear low-density polyethylene size large, polymethyl methacrylate, polystyrene and sand particles, respectively.

Soil Surface				Splash Mat			
Particle	Recall	Precision	F-score	Particle	Recall	Precision	F-score
LLDPE _L	0.887	0.882	0.885	LLDPE _L	0.885	0.746	0.810
SAND	0.838	0.978	0.903	SAND	0.973	0.971	0.972
PMMA	0.882	0.979	0.928	PMMA	0.994	0.995	0.994
PS	0.792	0.997	0.883	PS	0.993	0.994	0.994

2.2.10 Effectiveness of the image-based detection method

The dynamic nature of the soil surface, including variations in surface roughness and the onset of surface runoff, and the movement of particles during the rainfall simulations, makes it challenging to detect particles on the soil surface using image-based detection methods. To ensure patterns of particle movement on the soil surface observed in this research can be attributed to transport processes and not simply artifacts of the detection method, we used blank soil boxes without any particles added to the soil.

Figure 2.5 shows the number of particles detected on the surface of the blank soil boxes for each particle type. The number of particles detected on the blank soil surface never exceeded 800 particles for any particle type. The number of particles detected on replicate box 1, was much higher for the LLDPE_L, LLDPE_S and PMMA particles compared to all the other replicates. This was not reflected for the PS and sand particles. When replicate box 1 is excluded from the data the number of particles does not exceed 400. There was a pattern of more particles detected on the images of the surface of the blank soil boxes in the latter end of the simulations. The number of particles detected on the splash mat from the blank soil boxes was relatively low with LLDPE_L, PMMA, PS and sand particles consistently detecting less than 25 particles. LLDPE_S on the other hand constantly detected more than 25 particles over the course of the simulation.

Correlating the patterns of decrease on the soil surface (Figure 2.6) with the number of particles identified in each transport pathway gives evidence that images of the soil surface reflect transport patterns and not artefacts of the detection method. For example, the largest decrease in particle number on the soil surface occurred in the first 10 minutes of the rainfall simulation (Figure 2.6), and visual inspection of the respective images showed that only 3 of the 16 soil boxes had evidence of a layer of water on the surface at this time. Therefore,

interference in the detection method due to water on the soil surface is believed to be unlikely. Likewise, after surface runoff began, the number of particles transported from the soil boxes in surface runoff and splash erosion approximately accounts for the decrease in particle number observed on the soil surface (Figures 2.6 and 2.8.) However, the LLDPE_L had the weakest fluorescence signal than all other particles, as the optimal wavelength to excite the Rhodamine dye (~500 nm) was not used in the experiment, but rather a UV light with a peak wavelength of 365 nm. For this reason, it was difficult to distinguish LLDPE_L from soil in the images, which resulted in a lower recovery from the images compared to the other particle types.

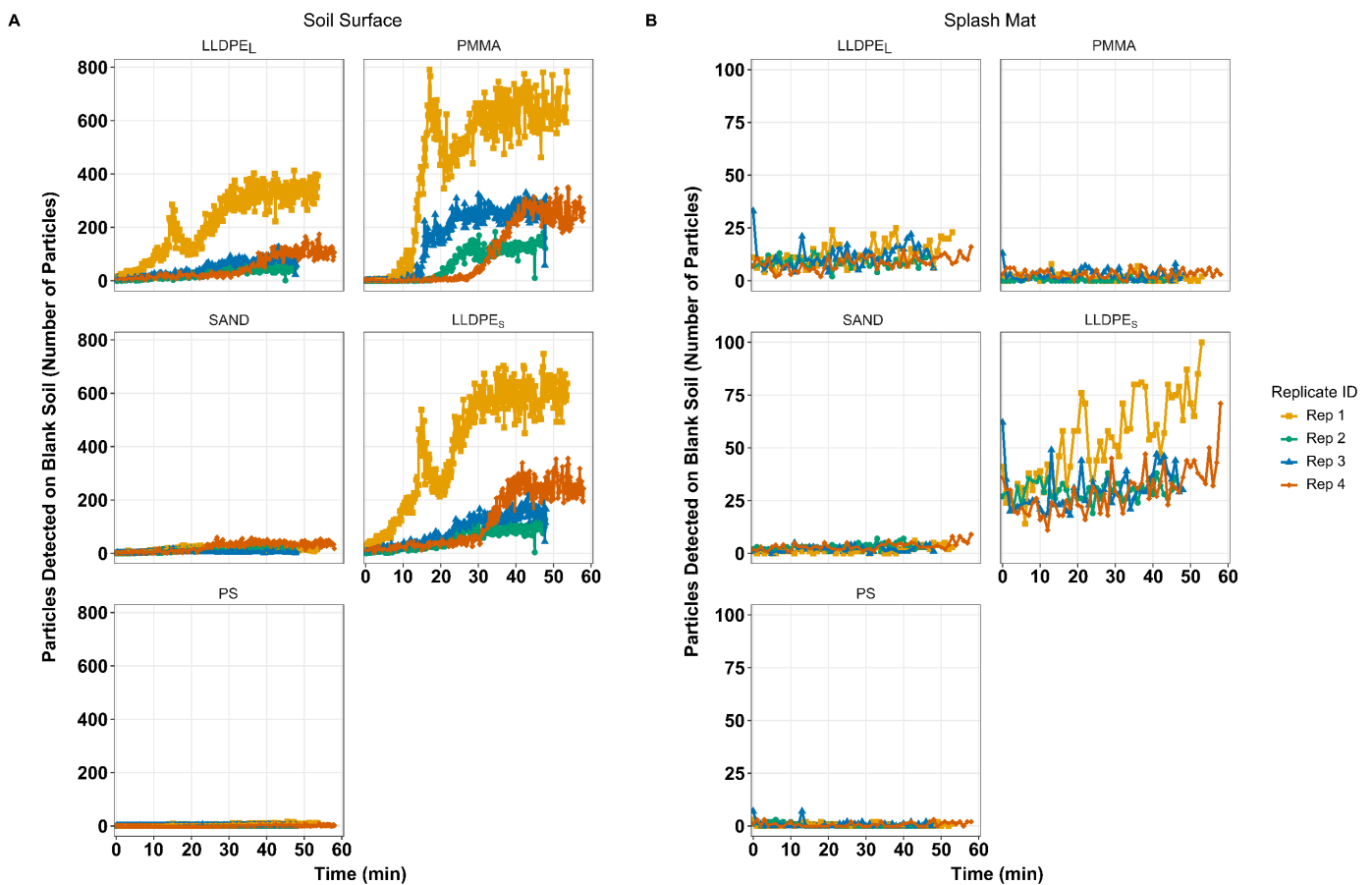


Figure 2.5. Graphs showing the number of particles detected in the image analysis process on blank soil throughout the rainfall simulation (n=4). Panel A shows particles on the surface of the soil box and panel B shows the particles on the splash mat. Each line represents a different replicate. LLDPE_L; PMMA; PS; SAND; and LLDPE_S represents linear low-density polyethylene large size, polymethyl methacrylate, polystyrene, sand particles, and linear low-density polyethylene small size respectively.

2.2.11 Statistical analysis

This experiment followed an independent measures design, with the sand particle serving as a reference material to compare the differences between MP and sediment movement. This approach was chosen in order to isolate the effects of particle composition on transport dynamics in rainfall-induced erosion. Each trial was conducted under controlled environmental conditions, with multiple replicates ($n=4$). The independent variable was particle type, while the dependent variables were the number of particles transported and the rate of transport from the soil surface. Data were analysed to determine whether MP particle movement significantly deviated from that of the sand particle, providing insight into their transport dynamics.

Statistical analysis was performed using R Statistical Software version 4.3.1 (R Core Team, 2023). Histograms of the data were visually inspected and normality was tested using D'Agostino-Pearson's K^2 test to a 0.05 significance. Analysis of variance test (ANOVA) was used to test for differences between treatments when the data were normally distributed along with a Tukey's post-hoc test. When data were not normally distributed, Kruskal-Wallis tests were used along with a Wilcoxon rank-sum post-hoc test. The holm method was used in the Wilcoxon post-hoc tests to reduce the likelihood of type 1 errors. Data regarding the real-time movement of particles from the soil surface were log-transformed and fit to a linear model. The coefficients noted as "B" were compared by using 95% confidence intervals. Residuals of the linear models were found to fit a normal distribution, both visually with Q-Q plots and with D'Agostino-Pearson's K^2 test to a 0.05 significance. Data are reported as mean \pm standard deviation unless otherwise noted.

2.3 Results and Discussion

2.3.1 Using photography to track the real-time movement of fluorescent particles

Previous research has utilized fluorescent particles to study the movement of MP and soil particles during erosion events (Han *et al.*, 2023; Hardy *et al.*, 2017; Laermanns *et al.*, 2021). However, the use of impervious surfaces in some research (Han *et al.*, 2023; Laermanns *et al.*, 2021) limits our understanding of MP transport during erosion events by excluding the potentially significant pathway of vertical transport into the soil profile (Heinze *et al.*, 2024; O'Connor *et al.*, 2019). Our research builds upon this work, to not only track MP movement on the soil surface, but also to identify key transport pathways taken by particles during erosion events.

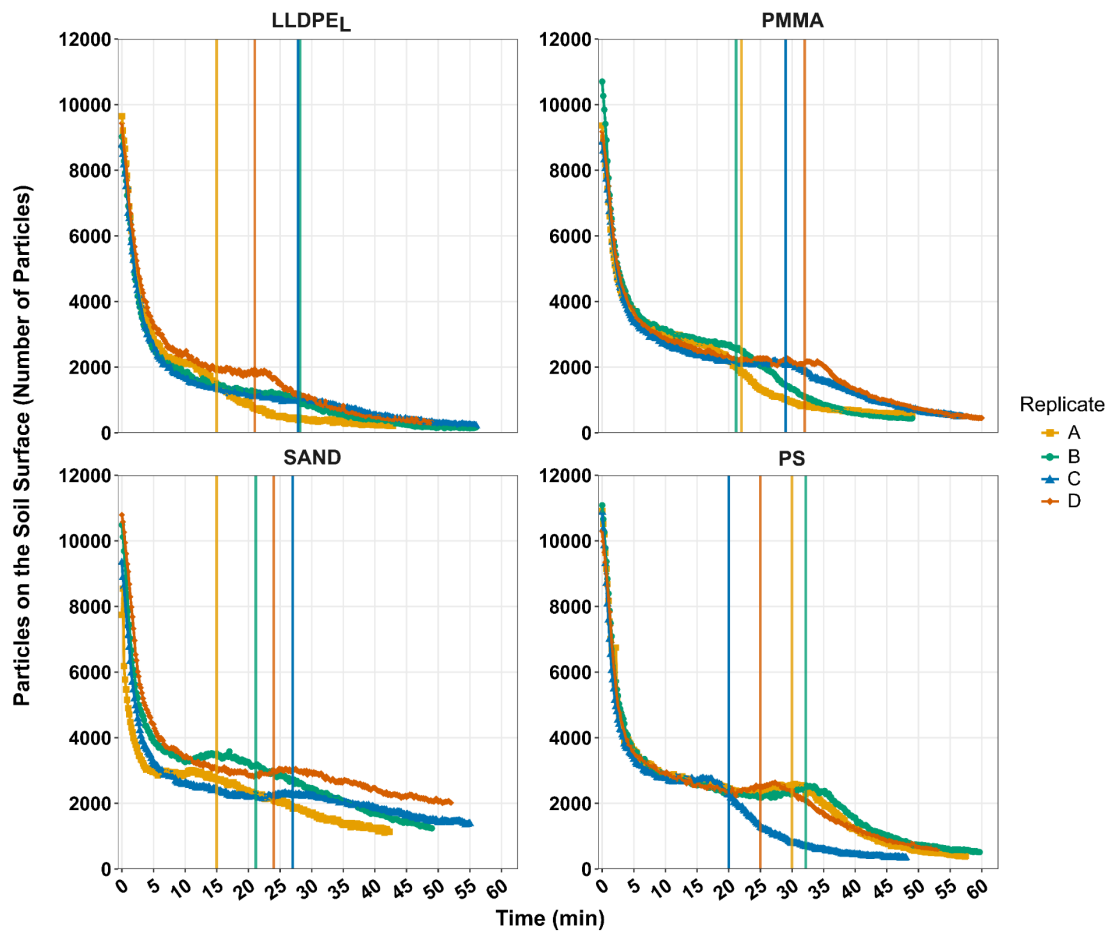


Figure 2.6. Number of particles on the soil surface through time ($n=4$). Vertical lines indicate the start of surface runoff delivery for each replicate. LLDPE_L; PMMA; PS; and SAND represents linear low-density polyethylene, polymethyl methacrylate, polystyrene and sand particles, respectively.

The dynamic nature of both the soil surface, including variations in surface roughness and the onset of surface runoff, and of the particles during the rainfall simulations, makes it challenging to detect fluorescent particles on the soil surface using image-based detection methods (Hardy *et al.*, 2017). It is possible that there were particles on the surface of the soil that remained undetected using the approach we developed. However, we remain confident that the patterns of particle movement on the soil surface that are reported can be attributed to transport processes, and do not simply reflect artifacts of the detection method (Section 2.2.10).

The number of particles detected on the soil surface through time revealed two distinct phases of particle movement on the soil surface (Figure 2.6). Firstly, an initial period of exponential decline in particle number on the soil surface followed, secondly, by a more gradual, linear decrease in particle number. The transition between these two phases was linked to the onset of surface runoff reaching the end of the soil box, which ranged between 15 and 32 minutes, with a mean start time of 24 minutes and 15 seconds.

To compare the rates of decrease in particle number detected on the soil surface between each particle type, data were split between the phases of movement prior to surface runoff and after surface runoff began, then log transformed and fit to linear models (Figures 2.7A & 2.7B). Slope coefficients from the linear models were compared between treatments and the lack of overlap in 95% confidence interval values were used as evidence of significant differences in slope coefficients. Prior to surface runoff initiation, LLDPE_L showed the most rapid rate of decline (B= -0.69), followed by PMMA (B= -0.43), PS (B = -0.42), and then sand (B = -0.37) (Figure 2.7A). All slope coefficients had a p-value < 0.001. All particle types, apart from PMMA and PS had significant differences in slope coefficients (LLDPE_L [-0.70, -0.67], PMMA [-0.44, -0.42], sand [-0.39, -0.36], PS [-0.43, -0.41].)

A similar pattern was found after the onset of surface runoff (Figure 2.7B). All MP particle types: PS (B = -0.029; 95% CI [-0.030, -0.028]); LLDPE_L (B = -0.029; 95% CI [-0.029, -0.028]); and PMMA (B = -0.025; 95% CI [-0.026, -0.024]) were associated with faster rates of decline compared to the sand particles (B = -0.011; 95% CI [-0.012, -0.010].) All slope coefficients had a p-value < 0.001.

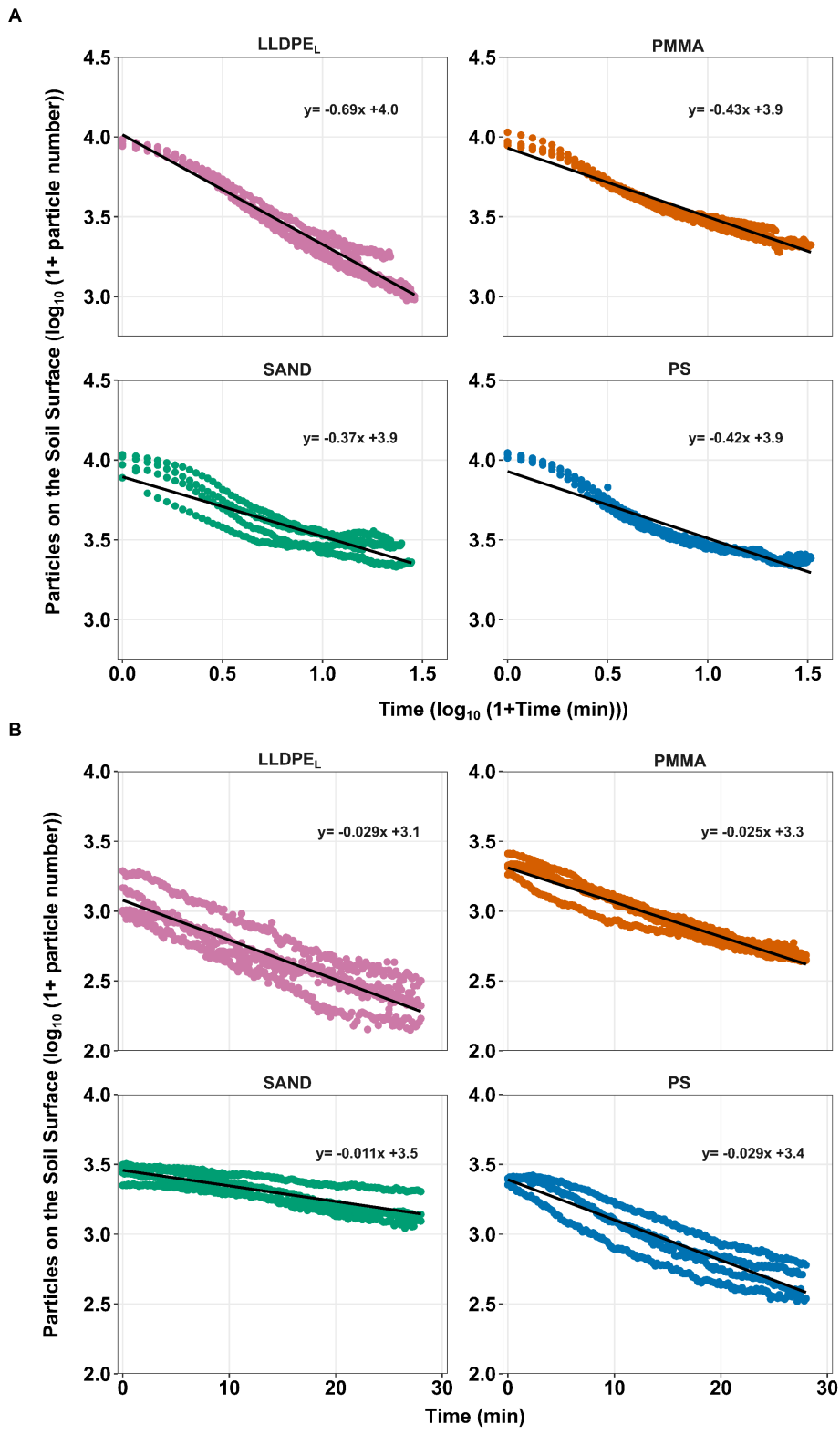


Figure 2.7. Log transformed data showing the rate of decline in number of particles from the soil surface. Panel A shows the decline in number of particles on the surface prior to surface runoff. Panel B shows the decline in numbers of particle from the surface after the onset of surface runoff. Data from four replicates are shown for each particle type in each panel. Comparisons between the linear models in panel A and panel B should not be made due to the difference in x-axis. LLDPE_L; PMMA; PS; and SAND represents linear low-density polyethylene, polymethyl methacrylate, polystyrene and sand particles, respectively (n=4).

The movement of particles by splash erosion differed significantly between particle types (Figure 2.8). The highest rate of particle accumulation on the splash mat was associated with PS (B= 12.40), followed by PMMA (B= 8.23), LLDPE_L (B= 4.62), and finally sand (B= 4.29). Each coefficient describing particle accumulation on the splash mats differed significantly between treatments, except for LLDPE_L and sand (95% CI: PS [11.89, 13.01]; PMMA [7.64, 8.82]; LLDPE_L [4.01, 5.23]; sand [3.65, 4.92].) For MP treatments following the start of surface runoff, there was a slight increase in the rate of MP transport to the splash mat, a pattern which was not repeated for the sand particle treatment.

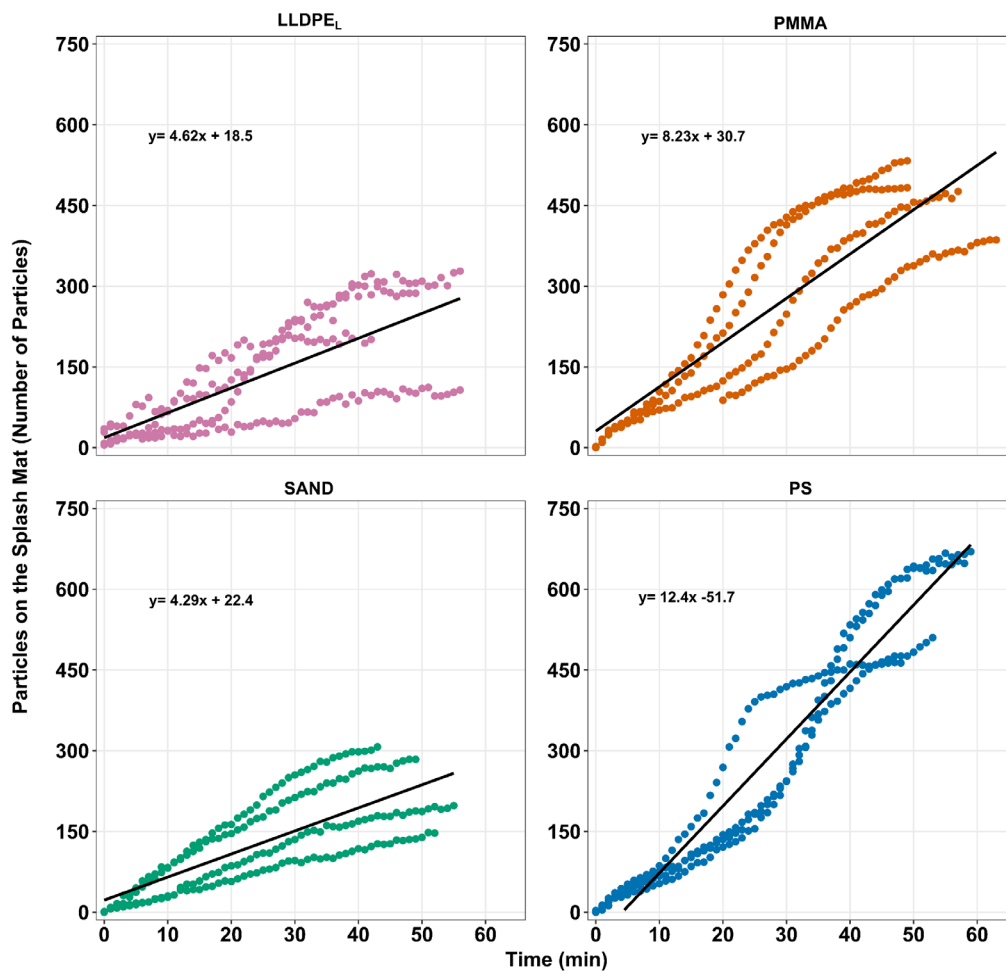


Figure 2.8. Number of particles on the 50 cm² section of the splash mat through the full rainfall simulation. Each panel shows results from four replicates with each line representing a single replicate (n=4). For the MPs there is an increased rate of accumulation on splash mat when surface runoff begins; this pattern is absent for the sand particle. LLDPE_L; PMMA; PS; and SAND represents linear low-density polyethylene, polymethyl methacrylate, polystyrene and sand particles, respectively.

Estimates of the number of particles transported by splash erosion (up to 50 cm radius from the edge of the soil box) were compared to the initial exponential decrease in particle number detected at the soil surface, to assess whether splash erosion could explain this decrease (Figures 2.6 and 2.8). A single timepoint at 600 seconds was used for this comparison, as this was prior to any surface runoff and therefore the reduction in particle number on the soil surface could not be attributed to surface runoff processes. Across all particle types, between 70 to 80% of particles (~7000-8000 particles) disappeared from the surface of the soil box in the first 600 seconds of the rainfall simulation. Because only 3 to 5% of particles (~300-500 particles) were estimated to be transported out of the soil box by splash erosion during this period, splash erosion cannot explain the exponential reduction in particle number on the soil surface reported above.

The primary hypothesis for the reduction in particle number on the soil surface is raindrop impact incorporating particles into the soil. Raindrops can transform the surface of a soil by creating small depressions (Beczek *et al.*, 2018; Mouzai and Bouhadeh, 2003; Zhao *et al.*, 2015), breaking up soil aggregates and filling soil pores (Ellison, 1950; Laburda *et al.*, 2021; Legout *et al.*, 2005), compacting the soil (Ellison, 1950; Mouzai and Bouhadeh, 2003) and selectively transporting particles due to size (Legout *et al.*, 2005; Leguédois *et al.*, 2005; Sadeghi *et al.*, 2017). A combination of these processes could be responsible for the decreases in particle number on the soil surface, by creating a mixing process at a microscale which incorporated the particles into the near surface soil layer. This mixing process may also reduce the likelihood of particle transport in surface runoff, by moving the particles from the surface into the soil matrix. Further, once mixed within the soil, particles could be transported by water infiltrating vertically into the soil profile prior to surface runoff, thereby removing the particles from the erodible layer. The faster rates of decrease on the soil surface prior to surface runoff for MPs compared to sand indicates that MPs are more readily mixed with the soil than sand particles, which could potentially limit MP transport from the soil in surface runoff. However, as our research was conducted in repacked soil boxes, particles likely remained in the erodible layer with vertical movement into the soil profile more limited than under field conditions (Rehm *et al.*, 2021).

2.3.2 Microplastic transport in surface runoff

Across all treatments a mean surface runoff rate of $55.4 \pm 21.3 \text{ mL min}^{-1}$ was delivered from the soil boxes with no significant differences between each treatment ($F(3,92) = 1.28$, $p =$

0.29). Runoff rates through time likewise showed no notable variation in surface runoff across all soil boxes (Figure 2.9A). The mean sediment transport rate across all treatments was $1.7 \pm 1.3 \text{ g min}^{-1}$ with no significant differences between each treatment ($\chi^2(3) = 1.93, p = 0.59$). The amount of sediment transported from the plot throughout the rainfall simulation showed no substantial variation between particle type (Figure 2.9B).

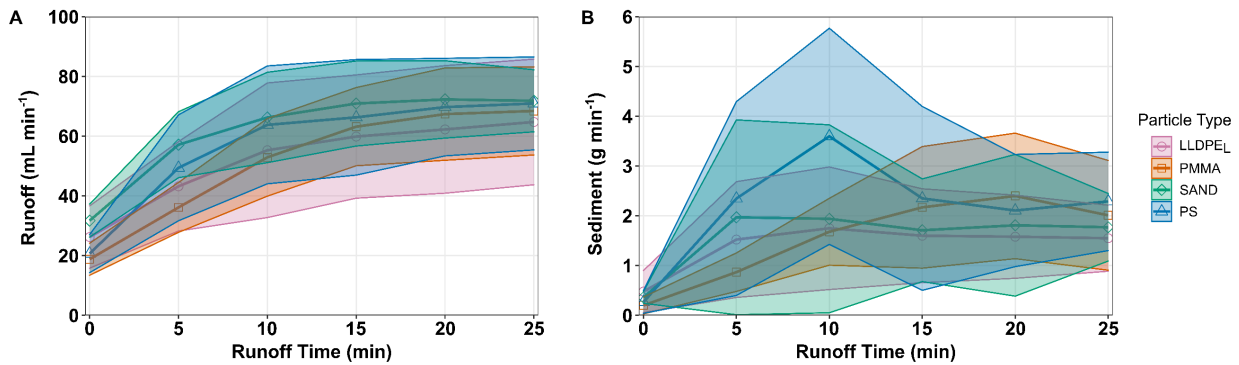


Figure 2.9. Surface runoff (A) and sediment flux (B) during the rainfall simulations. Data is LLDPE_L; PMMA; PS; and SAND represents linear low-density polyethylene, polymethyl methacrylate, polystyrene and sand particles, respectively (n=4).

The concentration of PMMA and PS in surface runoff was higher in the first 10 minutes following the start of surface runoff, compared to either the sand or LLDPE_L particles (Figure 2.10). The concentration of sand particles transported from the soil boxes in surface runoff remained relatively constant throughout the simulations, whereas all MP particle types showed lower concentrations in surface runoff as the rainfall simulation progressed. The overall number of particles transported in surface runoff differed significantly between particle type ($F(3,12) = 12.72, p = 0.005$). Post-hoc testing showed that the number of PMMA, PS and sand particles transported in surface runoff were not significantly different at 910 ± 203 , 1082 ± 162 and 1159 ± 192 , respectively, whilst the total number of LLDPE_L particles collected in surface runoff was significantly lower at 473 ± 118 ($p < 0.02$).

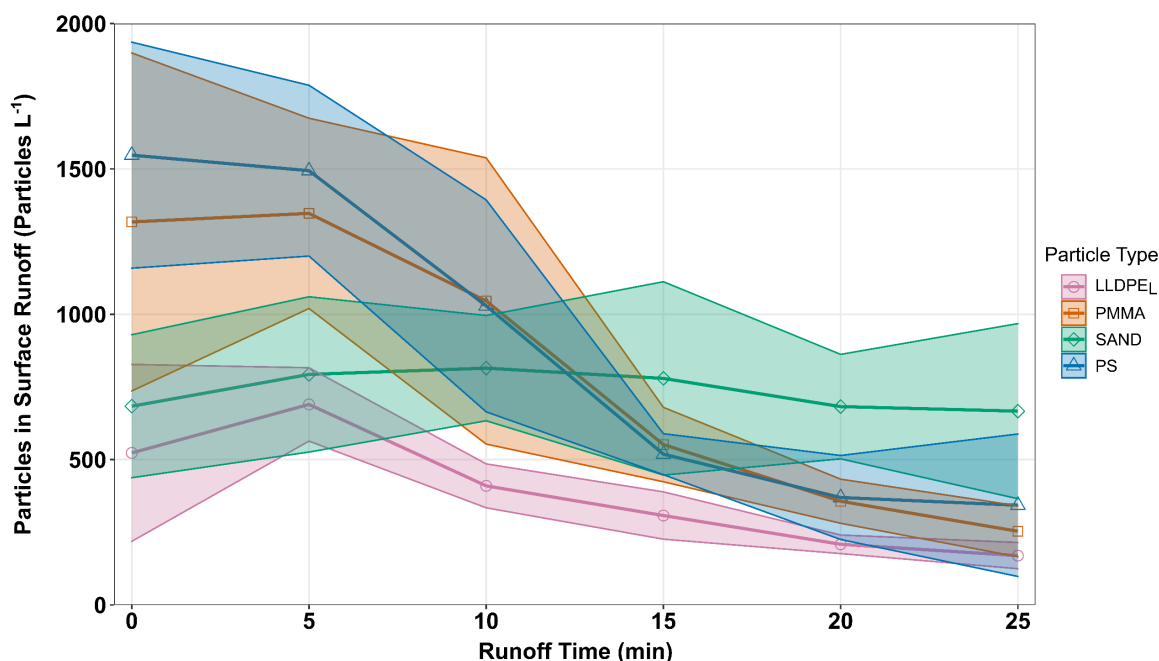


Figure 2.10. Number of particles per litre of surface runoff through time. Time 0 marks time since surface runoff commencement. Lines represent the mean number of particles while the shaded regions mark \pm one standard deviation. LLDPE_L; PMMA; PS; and SAND represents linear low-density polyethylene, polymethyl methacrylate, polystyrene and sand particles, respectively (n=4).

Once surface runoff commenced, sand particles displayed a significantly slower decrease in particle number at the soil surface as compared to the MPs (Figure 2.7B). We believe that this reflects higher rates of MP loss from the soil boxes compared to loss of sand particles, due to the combination of: (i) a flush of MPs delivered from the soil boxes in the first 10 minutes of surface runoff which was not matched by the sand particle treatment in this time period (Figure 2.10); (ii) preferential splash erosion of MPs compared to sand particles (Figure 2.8). Rehm *et al.* (2021) also noted similar patterns of high MP transport in the early stages of surface runoff which subsequently declined dramatically due to an exhaustion of MPs in the erodible soil layer.

2.3.3 Retention and transport into the soil profile

Based on data from soil cores collected following the end of each rainfall simulation, sand particles were preferentially retained in the soil, at 3432 ± 1434 particles, compared to all MP types which remained below 1600 particles (Figure 2.12). A Kruskal-Wallis test indicated significant differences in the number of particles retained in the soil among different particle types ($\chi^2(3) = 11.71, p = 0.008$), though post-hoc testing did not show statistically significant differences between any pairs of particle types ($p > 0.17$). Across all particle types, rarely did any particle penetrate below the first centimeter of the soil profile (Figure 2.11).

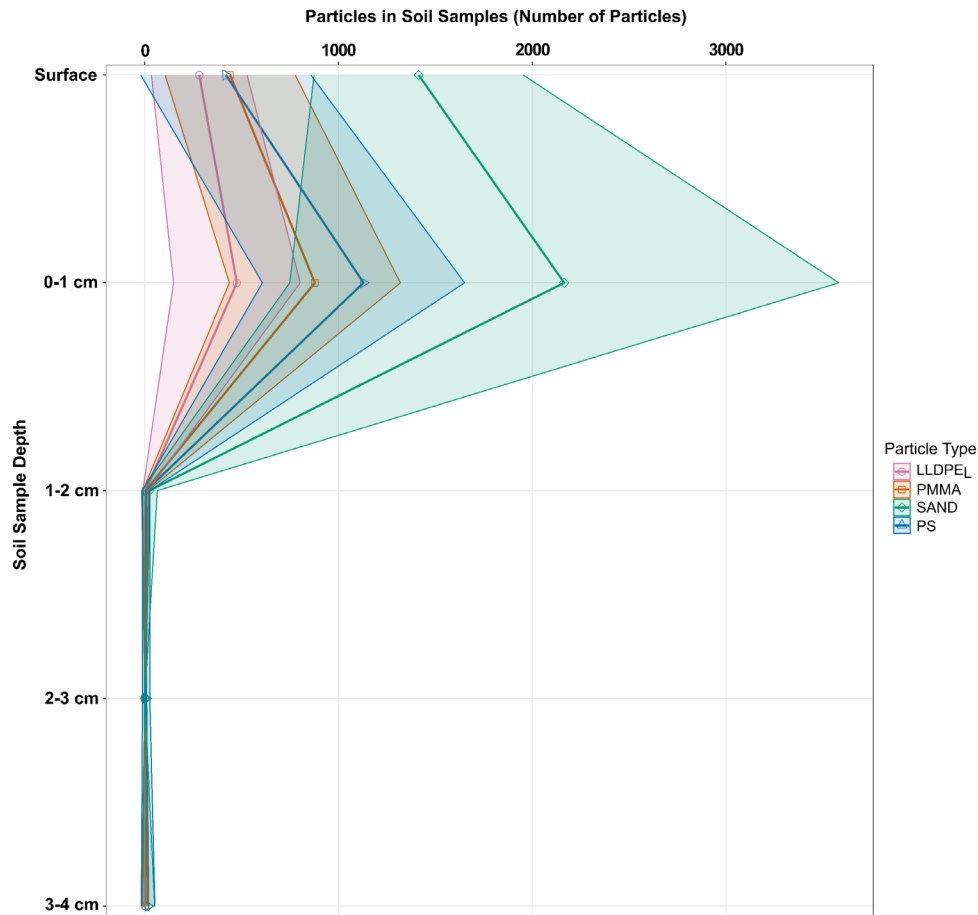


Figure 2.11. Vertical movement of MPs through the soil profile to a 4 cm depth. Dark lines represent the mean while the shaded regions mark \pm one standard deviation. Surface particles were counted once sampling core was in the soil then ultimately subtracted from particles found in the 0-1 cm depth class. Rarely were any particles found in the soil below a 1 cm depth. LLDPE_L; PMMA; PS; and SAND represents linear low-density polyethylene, polymethyl methacrylate, polystyrene and sand particles, respectively (n=4).

2.3.4 Microplastic transport via splash erosion

The number of particles transported via splash erosion was a function of particle type ($F(3,12) = 25.36, p < 0.0001$), with post-hoc tests showing a greater number of PMMA and PS particles, 3742 ± 353 and 4569 ± 625 respectively, being transported outside of the soil boxes, as compared to only 1874 ± 481 sand particles and 1561 ± 765 LLDPE_L particles ($p < 0.003$). Particle type had no significant effect on the distance from the soil box that particles were transported via splash erosion up to 1 metre ($F(3,12) = 0.591, p = 0.63$).

After surface runoff began, there was an increase in the rate of MP transport from the soil boxes through splash erosion, compared to the rate of sand particle transport via this

mechanism (Figure 2.8). This observation is consistent with past research on soil particles which shows that thin films of water on the surface of a soil can increase the number of particles transported via splash erosion, as compared to dry soils (Allen, 1988; Brodowski, 2010; Fernández-Raga *et al.*, 2017; Palmer, 1964). However, the sand particle treatment itself did not reflect this pattern in our research. This could be due to the relatively large size of the sand particle used in this research compared to other soil particles. There are two potential explanations for why the MPs were more mobile as compared to the sand particle. Firstly, MPs in this research having densities ranging from 0.92-1.19 g cm⁻³ and hydrophobic properties (relative to sand particles) are likely to be buoyant in water, thereby needing less kinetic energy to transport them outside of the soil box via splash erosion as compared to sand particles. Second, when sand particles are transported by splash erosion the higher density of the sand results in shorter transport distances once surface runoff commenced i.e. within the boundaries of the soil boxes. The density of soil particles has been shown to be a controlling factor determining whether or not these particles are transported via splash erosion, or in surface runoff (Kinnell, 2005, 2009). Our results are consistent with research investigating the transport of soil particulate organic carbon that has a similar density to plastics, which found soil organic carbon was more likely to be transported via splash erosion as compared to mineral particles (Beguiría *et al.*, 2015).

2.3.5 Mass balance

A mass balance was constructed by summing particle numbers found in the surface runoff, on the splash mat as a result of splash erosion and retained in the soil itself at the end of the rainfall simulation (Figure 2.12). This total particle number was then compared with the initial assumption that 10,000 particles had been input to the soil prior to the start of the rainfall simulations. The PMMA, PS and sand particles had the highest recovery rates at 5977 ± 437 (59.8%), 7220 ± 726 (72.2%) and 6466 ± 1525 (64.7%) particles, respectively. The LLDPE_L particle had the lowest recovery rate at 2794 ± 847 (27.9%) particles.

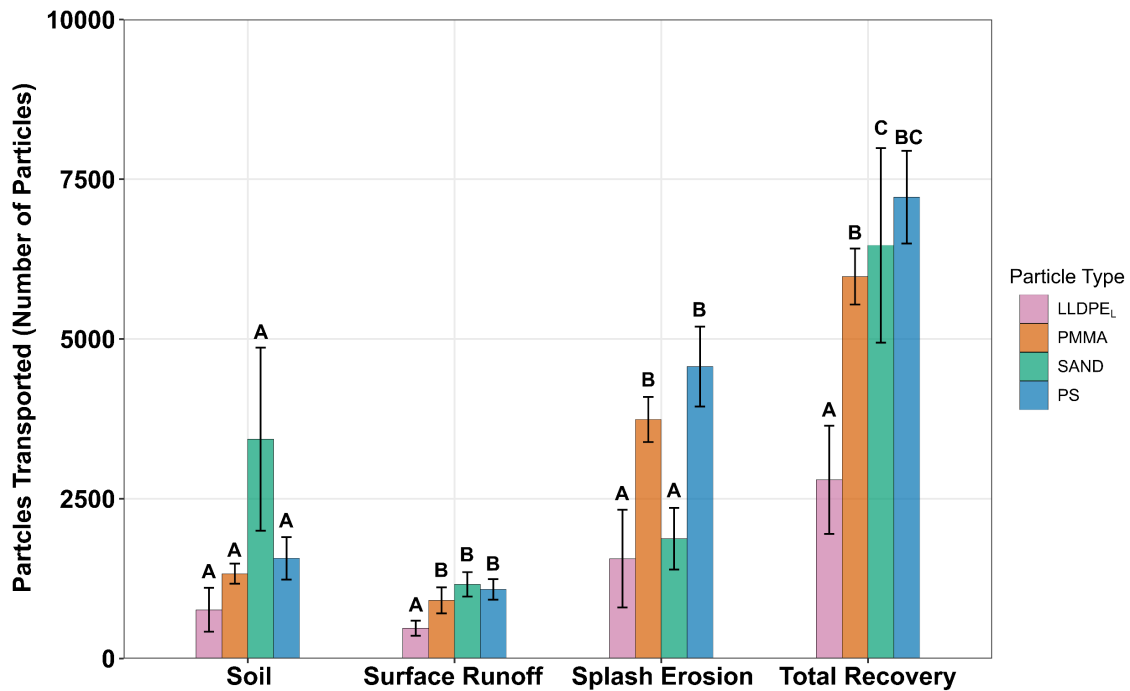


Figure 2.12. Particles found in each transportation compartment measured. Error bars represent ± 1 standard deviation. LLDPE_L; PMMA; PS; and SAND represents linear low-density polyethylene, polymethyl methacrylate, polystyrene and sand particles, respectively (n=4).

The discrepancy in the mass balance, where no single particle type achieved 100% recovery, could be attributed to several factors. First, the use of weight-to-particle number ratios may have introduced uncertainties in our estimates of the total number of particles input to the soil surface at the start of the simulations. For example, PS consistently had a slightly higher number of particles detected by the camera on the soil surface at time 0 than the other treatments, which may explain why slightly more PS was recovered than PMMA. Second, not all areas of particle deposition were captured using the measurement approach we developed. For example, it was observed that particles accumulated on a 3 cm vertical edge between the soil surface and the top of each soil box, but as the camera was not able to capture images of the edge these particles were not accounted for. Additionally, it is possible that particles were transported by surface runoff out of the soil box before the first surface runoff sample was collected. Lastly, in the case of LLDPE_L limitations of the image-based particle detection method as discussed above likely contributed to a lower recovery rate as compared to all other particle types.

2.3.6 Comparing transport pathways between different microplastics

In this experiment, PS and PMMA demonstrated nearly identical transport rates and dominant transport pathways. These particles were very similar in physical characteristics, sharing the

same morphology and size, though they possess slightly different densities. There were several significant differences in transport pathway (Figure 2.12), and number of particles detected on the surface of the soil throughout the rainfall simulation (Figure 2.6), when comparing the PS and PMMA particles to the LLDPE_L particles. The lower recovery rate of LLDPE_L in the mass balance and the difficulty in distinguishing these particles from the background soil, likely contributed to differences observed in the transport pathways and rates of movement over the soil surface compared to PS and PMMA. However, the larger size, greater plasticity, and flake-like morphology of LLDPE_L compared to PS and PMMA could have also played a role in the faster rates of decline from the soil surface prior to surface runoff (Figure 2.7A) and the number of particles in each transport pathway (Han *et al.*, 2023; Zhang *et al.*, 2022). With a higher plasticity, LLDPE_L may “bend” with the impact of raindrops rather than being transported short distances (on the mm-cm scale within the soil box), resulting in more extensive mixing of LLDPE_L with the near-surface soil compared to either the PMMA and PS particles. There were also significantly fewer LLDPE_L particles detected in the surface runoff as compared to PS and PMMA particles. Research investigating MP transport in surface runoff has generally shown that MP particles with larger surface areas, such as LLDPE_L in our research, are less likely to be mobilized in surface runoff (Zhang *et al.*, 2022; Han *et al.*, 2022).

Understanding the influence of morphology and polymer type on MP mobilization and transport is complex, because morphology is often at least partly related to polymer type. Additionally, polymer type has several characteristics, aside from density, which could influence particle movement i.e., plasticity, surface charge, and hydrophobicity. Presently, it is unclear whether marginal differences in density or hydrophobicity between MPs make a significant difference to transport processes (Lehmann *et al.*, 2021b), and these are priority areas for future research.

2.3.7 Erosion as a mechanism for microplastic transport to terrestrial and freshwater ecosystems

In this research, we sought to compare the transport processes affecting MP and sand particles during erosion events, by undertaking laboratory-scale rainfall simulations. The use of small soil boxes in erosion experiments is valuable for gaining detailed understanding of erosion processes (Mutchler *et al.*, 1994), although it is imperative that the results from these experiments are placed in context with erosion events affecting agricultural soils under large-scale field conditions. For example, in the research we report here, sand and MP particles

were observed in nearly equal numbers in surface runoff. Although this result may suggest that MP and sand particles are transported in relatively equal numbers within surface runoff, it is important to note that the particles which were transported outside of the soil box via splash erosion in our experiments would have been entrained in surface runoff under field conditions. Therefore it is likely that under large-scale field conditions, MPs would have been transported in greater numbers than sand particles in surface runoff (Rehm *et al.*, 2021). Additionally, while we report little evidence of MP or sand particles moving below 1 cm depth in the soil profile during our experiments, other research has demonstrated that MPs can be relatively mobile vertically within the soil profile, migrating to depths greater than 10 cm (Heinze *et al.*, 2024; Li *et al.*, 2024a; O'Connor *et al.*, 2019; Weber *et al.*, 2022; Weber and Opp, 2020; Xing *et al.*, 2021). Further research is recommended to test the controls on vertical movement of MP particles into soil profiles under large-scale field conditions.

There is a pressing need for more research investigating the processes controlling MP transport during erosion events and how the transport of MPs differs from naturally occurring soil particles. While there are several physical and chemical differences between MPs and natural soil particles, much of the recent research has focused on understanding how differing physical characteristics (i.e. size, morphology, density) between various MPs influence their movement (Han *et al.*, 2022; Rehm *et al.*, 2021; Zhang *et al.*, 2022). Future research should also aim to understand how chemical differences (e.g. hydrophobicity, plasticity, surface charge) between soil particles and MPs influence transport processes in erosion events. This research will not only help provide accurate estimates of the magnitude of MPs transported from terrestrial to aquatic ecosystems but also aid in devising effective strategies to mitigate this transport.

The findings from this research demonstrates that MPs have a more rapid and preferential transport during rainfall-induced erosion events than naturally occurring soil particles. Recent models estimate that erosion processes from terrestrial landscapes transports a greater mass of MPs per year to freshwater ecosystems than effluent from wastewater treatment plants (Norling *et al.*, 2024; Rehm and Fiener, 2024). These findings emphasize the significant role of erosion as a transport mechanism for MP entering aquatic ecosystems. Reducing MP transport to aquatic environments may be achieved through management practices aimed to reduce soil erosion such as using cover crops, vegetative buffer strips and restoring riparian areas. Implementing strategies such as these can help reduce runoff and stabilize soil thereby limiting MP mobilization from the terrestrial environment to aquatic ecosystems.

2.4 Conclusion

Erosion is thought to be an important process mobilizing and transporting MPs throughout terrestrial environments and across boundaries between terrestrial and aquatic ecosystems. In this research, we took a process-based approach to compare the mechanisms enhancing or constraining MP mobilization and transportation through soil during laboratory rainfall simulations to compare the movement of MPs to sand particles. Using fluorescent particles and high-frequency photography our results revealed two distinct processes of particle movement on the soil surface. First, a rapid decline (approximately 70-80%) in the number of particles on the soil surface for both MPs and the sand particles in the first 10 minutes of the rainfall event prior to runoff exiting the plot. This rapid decrease was attributed to a mixing process driven by raindrop impact to the soil surface. Second, once runoff was generated from the plots both MP and sand particles showed a second gentler decline in the number of particles from the plot. Overall, the results provided sufficient evidence to support the first hypothesis of this experiment in that there was a clear pattern of the number of MPs decreasing from the soil surface at faster rates compared to sand particles both prior and after the commencement of overland flow.

Along with quantifying the real-time movement of particles, the number of particles transported through splash erosion and surface runoff, alongside the depth to which particles infiltrate into the soil profile were also measured. A greater number of sand particles were estimated to be held in the soil after the rainfall event as compared to all MP types. Splash erosion proved to be the preferential pathway of transport for PMMA and PS, whereas sand and LLDPE_L particles were transported in lower numbers due to splash erosion. Both the sand particle and all MPs had a nearly equal number of particles transported from the soil due to surface runoff. Though, during an erosion event in an agricultural field soil particles transported via splash erosion are entrained in surface runoff, therefore MPs would show an enrichment compared to sand particles in surface runoff. Overall, the results provided insufficient evidence to support the second hypothesis that MPs of all particle types would be preferentially eroded in surface runoff and splash erosion compared to the sand particle owing to the LLDPE_L MP being transported in lower numbers compared to the sand particle.

These results highlight distinct differences in the rates and transportation processes of MPs in comparison with sand particles. Rainfall-induced erosion is an important mechanism transporting MPs throughout the terrestrial environment and subsequent deposition into aquatic ecosystems. The findings from this research prompts several further questions

including whether interventions aimed to reduce soil erosion will also reduce MP transport. While plastic products provide a wide range of benefits for farmers, caution is needed to reduce the potentially negative consequences of MP accumulation in agricultural soil and transport to aquatic ecosystems.

2.5 Acknowledgements

This project has received funding from the European Union's Horizon 2020 research and innovation programme under the Marie Skłodowska-Curie grant agreement No 955334. The authors would like to thank Dom Williams, Erik Hughs and Ian Wimpenny at the Henry Royce institute for their help with developing a protocol for Cryomilling plastics. We also thank Vassil Karloukovski for his technical support and Mengyi Gong for her advice on statistical analysis. Lastly, we would like to express our appreciation to Partrac for providing the fluorescent sand tracer.

3. Rainfall-induced lateral and vertical microplastics transport of varying sizes in agricultural fields

Emilee Severe¹, Saunak Sinha Ray², Wang Li³, David Zumr², Tomáš Dostál², Josef Krasa², Florian Wilken⁴, Peter Fiener⁴, Ahsan Maqbool⁵, Christine Stumpp³, Ben W.J. Surridge¹, José Alfonso G Gómez⁵, Chrisian Zafiu⁶, John Quinton¹

1. Lancaster Environment Centre, Lancaster University, Lancaster, UK
2. Czech Technical University in Prague, Faculty of Civil Engineering, Prague, Czech Republic
3. Institute of Soil Physics and Rural Water Management, University of Natural Resources and Life Sciences Vienna, Muthgasse 18, 1190 Vienna, Austria
4. Institute of Geography, University of Augsburg, Alter Postweg 118, 86159 Augsburg, Germany
5. Institute for Sustainable Agriculture, CSIC, Cordoba 14004, Spain
6. Institute of Waste Management and Circular Economy, University of Natural Resources and Life Sciences Vienna, Muthgasse 18, 1190 Vienna, Austria

Abstract

Agricultural soils, particularly those utilizing plastic products for crop production, are increasingly recognized as a source for microplastics (MPs) in both surface waters and groundwater. Surface runoff is thought to be a significant mechanism transporting MPs to surface waters, while infiltrating water through the soil is thought to be a significant process transporting MPs vertically in the soil profile. However, the majority of studies investigating the movement of MPs have investigated either the transport of MPs in surface runoff or infiltration into the soil profile, but not both in tandem. In this research, the transport pathways MPs followed during a rainfall event were investigated. MPs of three different size ranges (53-63 μm , 125-150 μm and 425-500 μm) were tracked during a field-based high intensity rainfall simulation (60 mm hr^{-1}). Using a combination of fluorescent particles and high-frequency photography, we measured the depth to which MPs migrated into the soil profile, the number of MPs which were transported in surface runoff, and we also tracked the number of MPs on the soil surface throughout the rainfall simulation. Our results show that the majority of MPs were retained in the soil, with MPs of all sizes migrating to an 8 cm depth after one hour of rainfall simulation. Approximately 20% of MPs sized 125-150 μm and 425-500 μm MP were transported from the soil in surface runoff. Images of the soil surface throughout the rainfall simulations revealed a decline in the number of MPs that were detected on the soil surface prior to the start of surface runoff, which indicates that MPs were mixed into and buried beneath the soil surface due to the impact of raindrops. Results from this research not only give insight into two MP transportation pathways from soil, but also

provide evidence as to how MPs of varying sizes influence the transport of MPs from soils to freshwater environments.

3.1 Introduction

Microplastics (MPs), currently defined as pieces of plastic less than 5 mm in size, have been frequently detected in freshwater ecosystems, including both groundwater and surface waters across the globe (Samandra *et al.*, 2022; Strungaru *et al.*, 2019; Umeh *et al.*, 2024). The accumulation of MPs in freshwater ecosystems is of concern due to their demonstrated negative impacts on aquatic organisms (Scherer *et al.*, 2020; Vázquez and Rahman, 2021; Ziajahromi *et al.*, 2018) and the potential risks MPs pose to human health through ingesting MPs via drinking water (Koelmans *et al.*, 2019; Kosuth *et al.*, 2018; Prata *et al.*, 2020; Yan *et al.*, 2022). Amongst the various means by which MPs are entering freshwater ecosystems, soils are increasingly recognized as a significant source (Norling *et al.*, 2024; Rehm *et al.*, 2021; Rehm and Fiener, 2024; Su *et al.*, 2022; Wang *et al.*, 2022a).

In 2019 alone, approximately 708 kt of plastic were used for agricultural production in the EU, with polyethylene (PE) being the most common polymer type (Pereira *et al.*, 2021). Products containing plastics, such as polytunnels, mulching films, polymer coated fertilizers and irrigation tape, are used to increase crop production while simultaneously decreasing pesticide, irrigation and fertilizer inputs (Cusworth *et al.*, 2022; FAO, 2021). However these plastic products fragment, through various means into macro-, micro- and nano- sized plastic pieces which are challenging to remove entirely from the soil (Feuilleley *et al.*, 2005; Maqbool *et al.*, 2024). Additionally, agricultural soils may be contaminated with MPs through secondary sources, for example: sewage sludge (Corradini *et al.*, 2019; Zubris and Richards, 2005), compost (Braun *et al.*, 2023; Weithmann *et al.*, 2018), tire wear particles from nearby roads (Sommer *et al.*, 2018), litter (Braun *et al.*, 2023) and atmospheric deposition (Brahney *et al.*, 2020).

Due to this multitude of input sources and very long half-lives of most conventional plastics (Chamas *et al.*, 2020) MPs accumulate in soils, resulting in a large MP sink. However, soils may also be an important source of MPs for both surface water bodies (Rehm *et al.*, 2021) and groundwater (Samandra *et al.*, 2022; Moeck *et al.*, 2022), particularly following heavy rainfall when infiltration and surface runoff may lead to the export of MPs to these water bodies. In chapter 2, MPs were found to be readily transported in splash erosion and surface runoff processes. Few MP were found to be transported vertically in the soil past 1 cm,

though this was attributed to small pore space in the repacked soil boxes (Chapter 2). Several factors may influence which transport pathway (i.e. laterally over the soil in surface runoff, or vertically into the soil profile) MPs travel along during rainfall events, including soil conditions such as bulk density, soil erodibility and MP characteristics. Among these, MP size likely plays a critical role in determining the transport pathway and ultimate fate of the MP during erosion events (Rehm *et al.*, 2021; Zhang *et al.*, 2022).

However, current understanding of size-dependent transport pathways is limited as most research is laboratory based, uses limited MP size ranges, and investigates either MP transport in surface runoff or percolation into the soil profile but not both potential transport pathways in tandem. All research to date which has investigated the effect of size on MP transport in surface runoff has found that, generally, MPs >1000 μm and <250 μm show less mobility than MPs sized 250-1000 μm (Han *et al.*, 2022; Rehm *et al.*, 2021; Zhang *et al.*, 2022). The current research on the influence of size on the vertical movement of MP into the soil under field conditions is mixed, with some studies showing clear size-dependent transport trends (Rehm *et al.*, 2021) while others show no patterns of size-dependent migration (Heerey *et al.*, 2023; Heinze *et al.*, 2024). Research that did find size dependent transport reported that MPs sized 53-63 μm migrated deeper in the soil compared to MP sized 250-300 μm , over the period of 1.5 years as affected by simulated rainfall and natural conditions such as bioturbation (Rehm *et al.*, 2021).

The aim of this research was to simultaneously investigate the relative roles between lateral and vertical MP fluxes during simulated rainfall events in field conditions. It was not logistically feasible to investigate splash erosion in this research but as splash erosion was found to be a very influential transport pathway in chapter 2, a small laboratory splash erosion experiment was conducted to account for this movement (Appendix 2). To determine how MP size effects the transport pathways followed during a rainfall simulation, three size ranges (53-63 μm , 125-150 μm , and 425-500 μm) of fluorescent MPs were used. We hypothesized that: (i) MPs of each size range will show a preferential transport pathway, with a greater number of the largest MP size (425-500 μm) being preferentially transported in surface runoff due to less interaction with soil particles and limited vertical transport as compared to the smaller MP sizes (125-150 μm and 53-63 μm); and (ii) MPs sized 125-150 μm will infiltrate to greatest depth into the soil profile, because vertical transport of the 425-500 μm MPs will be hindered due to small pore sizes within the soil matrix, and the 53-63

μm MPs will adhere to surrounding soil particles and therefore be retained in the top layers of soil.

3.2 Methods

3.2.1. Site description and experimental set-up

Rainfall simulations took place on a farm near Řisuty which is approximately 30 km northwest of Prague in the Czech Republic at coordinates $50^{\circ}13'2.0''\text{N}$, $14^{\circ}1'2.2''\text{E}$. The soil is classified as a cambisol of a loamy texture consisting of 18.3% clay, 33.8% silt, and 47.9% sand and an organic carbon content ranging from 1.2% - 1.5%. A mean porosity was measured to be 0.48. More information about the field site can be found in Jeřábek *et al.* (2022); Li *et al.* (2022); and Stašek *et al.* (2023). Five, 1 m x 1 m experimental plots were prepared on a uniformly north-oriented 9° slope. Vegetation was manually removed from the fallow soil, and the soil was tilled using a rototiller to a depth of 10 cm.

Fluorescent polyethylene (PE) microspheres (Cospheric LLC) of three differing size ranges and colors 425-500 μm (red), 125-150 μm (green) and 53-63 μm (yellow) were used. The 125-150 μm and 53-63 μm MPs had densities of 1.00 g cm^{-3} while the 425-500 μm MP had a slightly higher density of 1.09 g cm^{-3} . Fluorescent particles were chosen for convenient sample analysis and to track the movement of the MPs over the soil surface using a novel, high frequency photographic approach throughout the rainfall simulation (Chapter 2 and Appendix 1).

A homogeneous mixture of soil and MP particles was created by adding 1.35×10^5 MP particles sized 53-63 μm and 125-150 μm and 1.24×10^5 of MP sized 425-500 μm into 12.5 kg of topsoil sieved to 1.5 cm. In total, 3.94×10^5 MPs were mixed into the soil, creating a 0.058% w/w mixture and a concentration of $3.94 \times 10^5\text{ MPs m}^{-2}$. The MP-soil mixture was applied evenly to the plot to create a 1 cm topsoil layer. Once the MP-soil mixture had been applied to the plots, the topsoil was compacted to ensure uniform initial conditions across all plots, using a 50 kg rolling press applying a pressure of approximately 20 kPa.

Soil moisture in the topsoil (<6 cm) was measured before the rainfall simulation and 15 minutes after the wet run (see below), using a soil moisture sensor (ML3 ThetaProbe, Delta-T devices, UK) at six locations within each plot.



Figure 3.1. Image showing the preparation for rainfall simulation on the 1 m x 1 m plot. Camera at the base of the plot used for detecting microplastics on the surface of the plots.

Rainfall was applied with a pressure-fed swinging nozzle rainfall simulator as described by Kavka & Neumann (2021) at a rainfall intensity of 60 mm hr^{-1} (Figure 3.1). This simulator produces raindrops with a kinetic energy of $4.14 \text{ J m}^{-2} \text{ mm}^{-1}$ and Christiansen's uniformity coefficient of 93%. A simulation procedure similar to Neumann *et al.* (2022) and Stašek *et al.* (2023) was followed. Rainfall simulation on each plot comprised of three phases: (i) a "dry run" simulation executed at "dry" ambient soil moisture lasting 30 minutes after surface runoff commenced; (ii) a 15 minute interval where the simulator was turned off to facilitate infiltration and sediment deposition; (iii) a second "wet run" simulation on the wet soil for 30 minutes after surface runoff commenced at the same settings. The time of rainfall initiation and subsequent surface runoff generation were recorded.

Deuterated water was utilized as a conservative tracer to trace the extent to which simulated rainwater infiltrated into the soil profile. Exactly, 50 mL Deuterium oxide (99.96 atom % D, Sigma-Aldrich) was added to a 1000 L water reservoir ($\delta^2\text{H}$, $-64.2 \pm 0.56 \text{ ‰}$) which was used

to supply water for the rainfall simulations. Approximately 200 L of water was applied per plot for the rainfall simulation. Water samples were taken during the experiment for each plot, and the $\delta^2\text{H}$ ratio was measured for identical tracer input across each plot. Furthermore, soil near the plots were sampled before experiments, to get the background soil water $\delta^2\text{H}$ signature.

3.2.2. Observations during the simulation and sample collection

To observe the MP particle movement during the rainfall simulations, the surface of the soil containing the fluorescent MPs was imaged throughout the rainfall simulation using UV photography methods (Appendix 1). Images of the soil surface were captured every ~10 seconds during each simulation using a Canon EOS 850D camera. An 18-55 mm zoom lens set at a focal length of 26 mm was used and the following camera settings were set: $f/7.1$, exposure 1 second and ISO 320. For each plot, the camera was set 78 cm from the bottom boundary of the plot, at a height of 165 cm. Simulations were performed overnight, in the absence of natural light, and plots were illuminated by a 365 nm wide beam UV 50-watt flood lamp (Mark SG Enterprises). Due to technical difficulties with the UV lamp during the rainfall simulation on the first plot, results from that plot were omitted from analysis of surface movement of MPs.

During both the dry and wet runs, surface runoff leaving the bottom edge of the plots were collected in glass bottles with tin caps every 2.5 minutes and time of collection was recorded.

A stainless-steel column (length: 13 cm; inner diameter: 6.5 cm) with openings on two sides at every 2 cm was used to collect soil samples. Soil samples were collected from plots number 1 and 2 and the other plots were left intact to study the long-term MP transport. To obtain a representative MP retention profile per plot, composite soil sampling was used and samples were taken from 5 different locations (one sample on each corner, and one sample in the middle of the 1 m x 1 m plot). The soil was too wet for sampling after 1 hour of rainfall simulation, therefore, soil samples were taken after 5 hours. Soil water isotopic signature and MPs were analysed within the following depth increments: -2, -4, -6, -8, -11, and -13 cm to reveal the water flow and MP retention profile.

3.2.3. Sample analysis and microplastic extraction

3.2.3.1 Microplastic soil surface movement image processing and analysis

Images were captured in RAW format and converted to TIFF format (LZW compression) using Adobe Photoshop. Due to the position of the rainfall simulator, the camera could not be located orthogonally in relation to the plots. Therefore, a single pixel in the foreground of the images (or front of the plot) represented a larger spatial area than the pixels in the background (or rear of the plot). The Perspective Warp tool (stretch function) in Adobe Photoshop was used to resample the images, correcting the perspective in the images (Bowers and Johansen, 2002). Photogrammetry targets were placed outside of the plots to validate the resampling (Collins and Gazley, 2017).

Each image was cropped to a 3400 x 3400-pixel area in Image J which is equivalent to 0.98 m x 0.98 m area, giving a ~ 1 cm buffer from the borders of the plot. These 1 cm buffer areas were created to remove MPs stuck to the borders of the plot from the image and remove the potential edge effects of the border on MP retention or removal (Mutchler *et al.*, 1994).

To enhance the visibility of the particle colors, the maximum brightness intensity for each image was adjusted. This type of image adjustment is widely accepted as long as care is taken to not over-saturate the brightness intensity and thus lose data in the images (Cromey, 2010). As our images were very dark (on a scale of 0-255, mean brightness intensity ~ 8.6), such adjustment was warranted. As the brightness intensity of each image varied slightly, average values needed to readjust the maximum brightness value were calculated and the maximum brightness value was adjusted to 135 in Image J.

Images were then processed through the Color Thresholding tool in Image J to quantify the number of MPs in each image, using a HSB color space specific to each particle size. The 53-63 μm particle was not considered in our analysis of the surface movement as it could not be detected by the digital camera. The following thresholds were set for each of the following MPs: 425-500 μm (red) MPs: hue= 45-220 (“pass” or band-reject), saturation= 55-255, brightness= 85-255; 125-150 μm (green) MPs: hue= 45-95, saturation= 45-255, brightness= 45-255. The watershed separation tool was then used to detect and separate potential adjoining particles (Figure 3.2).

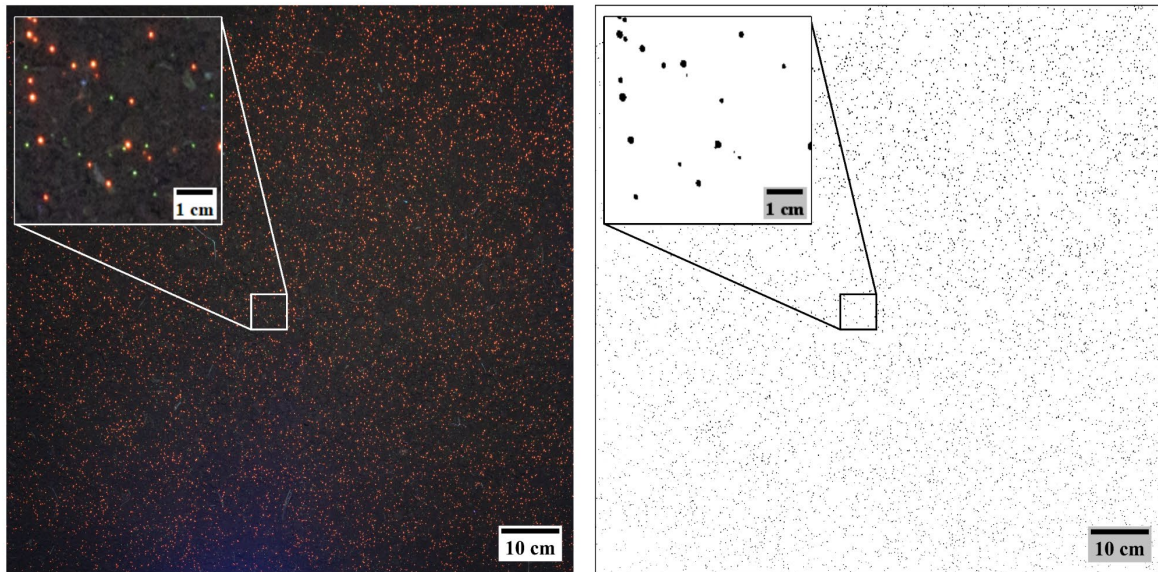


Figure 3.2. Images demonstrating the particle detection from the images of the soil surface. Image of the soil surface after perspective correction and cropping (left). Thresholded image detecting the 425-500 μm (red) MPs, black dots are detected microplastics (right).

The dynamic nature of the soil surface (i.e. variable surface microtopography, surface flows of water) during the rainfall simulation made it difficult to quantify the effectiveness of MP detection. However, a small validation plot was prepared in an identical manner to the other plots described above, with a known number of MP particles spread on the surface of the plot and photographed. In the validation plot, of the 60 MPs sized 425-500 μm and 441 MPs sized 125-150 μm which were spread on the surface, 51 (85%) of the 425-500 μm and 132 (30%) of the 125-150 μm were visible in the images. Due to the porous nature of the soil and due to surface topography, it is likely that the particles which were not detected in the validation plots, migrated into the soil profile or were hidden from view of the camera after being spread on the soil surface.

To determine the effectiveness of correctly identifying MPs detected in the images; subsections of the images from the main 1 m x 1 m plots before, during and after the rainfall simulations were manually counted and considered as ground truth data in this study. Performance was assessed by calculating the f-score for each particle size. The f-score takes into account both the proportion of particles detected and the proportion of the detected particles which were correctly labelled in the thresholding procedure. F-score is calculated on a scale of 0-1 where 1 indicates the best performance. The 425-500 μm MP had an f-score of 0.94 and the 125-150 μm MP had an f-score of 0.82 meaning that 94% and 82% of 425-500

μm MPs and 125-150 μm MPs respectively, which were visible in the images, were correctly classified.

3.2.3.2 Runoff and sediment analysis

After collection, bottled runoff samples were weighed then placed in an oven at 60°C for 24-32 hours, then re-weighed to determine the mass of sediment and the volume of runoff delivered from the plots. To determine the number of MPs in each sample, 100 ml of distilled water was added to the dried sediments in the bottles, followed by ultrasonication (40 kHz) and overhead stirring (500 rpm) for 5 minutes each to dislodge settled sediments and release entrapped MPs. Samples were wet sieved (1 mm, 500 μm , 425 μm , 150 μm and 125 μm) to separate the fluorescent MPs and sediments by sizes. Sampling bottles were decanted and sieved using distilled water over a period of 5 min. The material remaining on the 425 μm and 125 μm sieves was filtered onto separate filter papers (pore size 0.7 μm) and oven-dried at 40 °C.

Samples from the filter paper were spread as a thin layer onto an opaque black tray (30 cm x 45 cm). A portable darkroom (Ilford Photo), with a 365 nm wide beam UV 50-watt flood lamp (Mark SG Enterprises) angled at 45 degrees and a digital camera (Sony Alpha model $\alpha 6000$), placed at a vertical distance of 55 cm above the sampling tray were used to capture darkroom images of the prepared samples. Camera settings were fixed at: f/5.6, exposure 0.2 seconds, and ISO 100.

The color thresholding tool in Image J was used to detect the number of each MP size in the plots using the HSB color space. The following thresholds were set for each of the following MPs: 425-500 μm (red) MPs: hue= 0-45, saturation= 0-255, brightness= 130-255; 125-150 μm (green) MPs: hue= 50-145, saturation= 0-255, brightness= 130-255. Following the thresholding, the watershed separation tool was used to detect and separate adjacent particles, which may have been erroneously counted as one MP. A shape threshold was then applied to select particles with a circularity of 0.95-1.0, with 1.0 being a perfect circular shape. To count the number of MPs which were clustered together in the images, the area of each MP particle was divided by the median area of the MP (specific for each size range) in order to estimate the number of individual MPs within clusters.

A pretest was conducted to assess the efficiency of the MP identification process and to determine recovery rates. A soil sample from the field was sieved to 2 mm, and 10 g of the sieved soil was mixed with five different concentrations of MPs (0.05%, 0.1%, 0.2%, 0.5%,

and 1.0% w/w), with three replicates for the 125-150 μm and the 425-500 μm MPs. These samples underwent the same processes described above. The mean recovery rates were $84.9 \pm 3.6\%$ ($n = 15$) for the 125-150 μm MPs and $91.2 \pm 2.8\%$ ($n = 15$) for the 425-500 μm MPs. The 425-500 μm MP had an f-score of 0.93 and the 125-150 μm MP had an f-score of 0.89 meaning that 93% and 89% of 425-500 μm MPs and 125-150 μm MPs respectively, which were visible in the images, were correctly classified.

3.2.3.3 Soil sample microplastic extraction and analysis

The density of MPs applied to the soil plots in this experiment was less than 1.1 g cm^{-3} . Therefore, saturated NaCl (1.2 g cm^{-3}) was selected for density separation to extract MPs from collected soil samples, which is cost-effective and non-toxic. Collected soil samples were placed in 1000 mL beakers, with 400 mL saturated NaCl and 2 mL H_2O_2 (30 %) added. A glass stirring rod was used to stir the beaker, and to ensure the soil sample and added solution were well mixed. The supernatant was then collected into a 500 mL beaker after overnight settlement. As the MPs used were fluorescent, a UV lamp was used to ensure residual MPs were not left on glassware. The entire process was repeated 3 times to maximize the extraction efficiency. Considering the wide particle size range (53 μm to 500 μm), the collected supernatant was then further sieved into different fractions by using sieves with openings of 53 μm , and 500 μm , respectively. Afterward, collected MPs were filtered through a vacuum filtration system using regenerated cellulose filters (47 mm diameter, 8 μm pore size). All filters were then analysed with a confocal laser scanning microscope (SP8, Leica).

Water and soil samples were analysed for $\delta^2\text{H}$ with a Cavity Ring-Down Isotope Spectrophotometer (Picarro L2130-i) with a precision of $\pm 1 \text{ ‰}$. The Water-vapor equilibration method was employed to test the soil water isotopic signature. Briefly, soil samples were collected in double resealable zipper bags with air pushed out and stored in the fridge (4 $^\circ\text{C}$) before measurement to avoid soil moisture loss due to evaporation. To ensure water-vapor equilibrium in the headspace, collected soil sample bags were inflated with dry synthetic air and left for 3 days at laboratory conditions (20-22 $^\circ\text{C}$). After that, the bag was punctured with a needle that connected to the Picarro L2130-i laser analyser which was used to quantify isotope levels (Boumaiza *et al.*, 2023; Wassenaar *et al.*, 2008).

3.2.4. Data analysis

To understand the relationship between soil and MP transport, an enrichment ratio (ER) was calculated using the equation reported in Rehm *et al.* (2021). In short, the mean MP concentration transported in the surface runoff was divided by the mean MP concentration in the topsoil. A value > 1 indicates a preferential transport or enrichment of MPs in sediments transported in surface runoff and a value < 1 indicates a reduction in the concentration of the MPs transported in sediments compared to the concentration of MPs in the topsoil.

This experiment followed an independent measures design. This approach was chosen in order to isolate the effects of MP size on MP transport as well as identify transport pathways MP follow during a simulated rainfall-induced erosion event. Each trial was conducted under controlled environmental conditions with multiple replicates ($n=5$). The independent variables were MP size and transport pathway, while the dependent variables were the number of particles transported and the rate of transport from the soil surface.

All results are reported as mean \pm standard deviation unless otherwise noted. Statistical analysis was conducted using R Statistical Software version 4.3.1 (R Core Team, 2023). Data normality and homogeneity were tested visually by inspecting histograms and using Kolmogorov-Smirnov and D'Agostino-Pearson's K^2 test to a 0.05 significance. When data were normally distributed Welch's t-tests were carried out to check for significant differences between treatments. When data were not normally distributed, Kruskal-Wallis tests were used along with Wilcoxon rank sum post-hoc tests to determine significant differences between treatments. Change point analysis of the mean and variance was used to identify time points where the mean rate of change and variance changed significantly for particles detected on the soil surface. Change points were calculated using the Pruned Exact Linear Time (PELT) method in the R change point package (Killick and Eckley, 2014). As change point analysis requires regularly intervalled data, the number of MPs for each time point were averaged between plots and used in the analysis.

3.3 Results

3.3.1 Patterns of microplastic movement on the surface of the soil

Images taken of the soil surface revealed the number of MPs present on the surface throughout the rainfall simulations. Across all plots, there were approximately 64% fewer 125-150 μm MPs (2819 ± 738) detected on the soil surface compared to the 425-500 μm MPs

(7834 ± 540) before the start of the rainfall simulations. Figure 3.3 reports changes in the number of particles detected on the soil surface during the rainfall simulations, expressed as a percentage of the number of particles detected prior to the start of the rainfall simulations.

During the dry runs, the 425-500 μm MPs showed a steady decline in particle number on the soil surface at the beginning of the simulation, followed by a period of relative stability, whereas the 125-150 μm MPs were associated with a sharper rate of disappearance from the soil surface at the beginning of the simulation, followed by a period of relative stability. There was a $95.9 \pm 1.8\%$ and $79.6 \pm 1.6\%$ reduction in the 125-150 μm and 425-500 μm MPs, respectively, from the soil surface over the course of the dry run simulation (Figure 3.3). In the wet runs, there was a $13 \pm 9.7\%$ increase in the 425-500 μm MPs detected at the soil surface, and a $6.2 \pm 5.3\%$ decrease in the 125-150 μm MPs detected at the soil surface (Figure 3.3). Overall, there was no significant difference in the percentage change between particle sizes ($\chi^2(1) = 0.89, p = 0.34$), but a significant difference was observed between the dry and wet conditions ($\chi^2(1) = 11.29, p = 0.0008$). As the mean time for runoff generation was $4 \text{ minutes and } 13 \text{ seconds} \pm 55 \text{ seconds}$, the disappearance of the particles in the first 4 minutes of the rainfall simulation cannot be solely attributed to particles being transported from the plot via surface runoff.

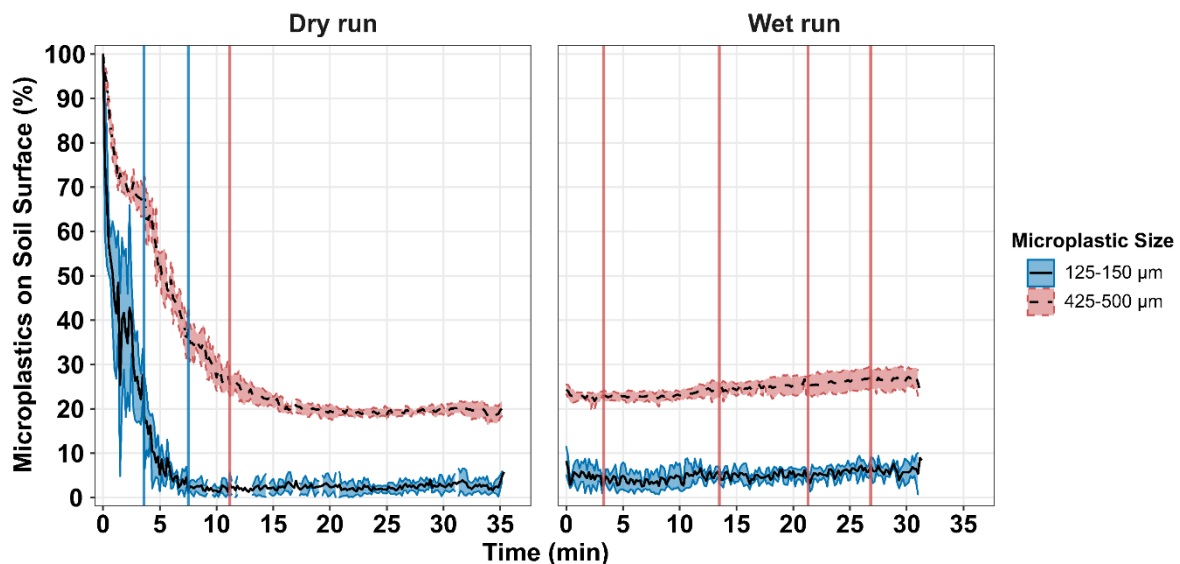


Figure 3.3. Microplastics (MPs) visible on the surface of the plots throughout the duration of rainfall simulations. MP concentration is shown as percentage of particles with respect to the initial number of MPs detected on the soil surface for each plot and particle size. Black lines represent the mean particle number from all the plots and the shaded areas represent one standard deviation from the mean for each MP size ($n=4$). Red vertical lines indicate changepoints for the 425-500 μm MP and blue vertical lines indicate changepoints for the 125-150 μm MP.

A changepoint analysis of mean and variance was conducted to identify points at which the mean rate and variation of the rate of change in the number of particles detected on the soil surface shifted significantly. During the dry runs, 125-150 μm particles had a changepoint near that of runoff commencement, at 3 minutes and 40 seconds, as well as a changepoint later in the simulation at 7 minutes and 30 seconds. The 425-500 μm MPs had one significant changepoint in the dry runs at 11 minutes and 10 seconds after the start of the rainfall simulation. This confirms that the number of 425-500 μm particles on the surface steadily declined throughout the simulation, and that the start of surface runoff did not enhance the disappearance of these sized MPs from the soil surface significantly. In contrast, the 125-150 μm MPs detected at the soil surface showed multiple changepoints throughout the dry run simulations, indicating more variable rates of decline at the soil surface. In the wet run simulations, changepoints were identified at 3 minutes 20 seconds, 13 minutes and 30 seconds, 21 minutes and 20 seconds, and 26 minutes and 50 seconds for the 425-500 μm MPs, showing the variable rates of increase of particles in this size range at the soil surface. No changepoints were detected for the 125-150 μm MPs in the wet runs, indicating a lack of significant changes in the number of these sized particles detected on the soil surface.

In the dry run prior to surface runoff, there was a $39 \pm 10\%$ (3100 ± 913 MPs) decrease in 425-500 μm MPs and $91 \pm 4\%$ (2573 ± 734 MPs) decrease in the 125-150 μm MPs detected on the soil surface (Appendix 2 Figure S3.2). After runoff commenced, there was a further $40 \pm 9\%$ (2724 ± 489 MPs) and $5 \pm 4\%$ (254 ± 172 MPs) decrease in MPs on the soil for the 425-500 μm MPs and 125-150 μm MP, respectively.

3.3.2 *Microplastic delivery in surface runoff*

Across all plots, no substantial variation was detected in the initial soil moisture conditions prior to the dry run rainfall simulations, with the mean volumetric water content (VWC) being $14.0 \pm 1.3\%$. The time it took each plot to generate steady runoff in the dry runs varied slightly, ranging from 3-6 minutes after the start of rainfall, with the mean start time for runoff being 4 minutes and 13 seconds \pm 55 seconds. The mean topsoil VWC for the wet run simulations was $25.8 \pm 3.2\%$. During the rainfall simulations, runoff coefficients of 0.29 ± 0.01 ($n = 5$) and 0.37 ± 0.02 ($n = 5$) were produced for dry and wet runs, respectively. Similar runoff volumes and little variability in runoff rates were observed across all five replicate plots (Figure 3.4). Overall, the mean runoff rates for wet runs (0.94 ± 0.12 L min^{-1}) were statistically higher than those for dry runs (0.74 ± 0.17 L min^{-1}) ($t(111.02) = -7.29, p <$

0.001). In general, the dry and wet runs sediment delivery rates followed the surface runoff dynamics (Figure 3.4), wherein an initial flux of sediment movement was observed at the start of runoff, and sediment delivery peaked around the same time as peak runoff. A higher mean sediment delivery was observed in the wet runs $7.76 \pm 1.35 \text{ g min}^{-1}$ than in the dry runs $6.75 \pm 1.44 \text{ g min}^{-1}$ ($t(114.15) = -3.90, p = 0.0002$).

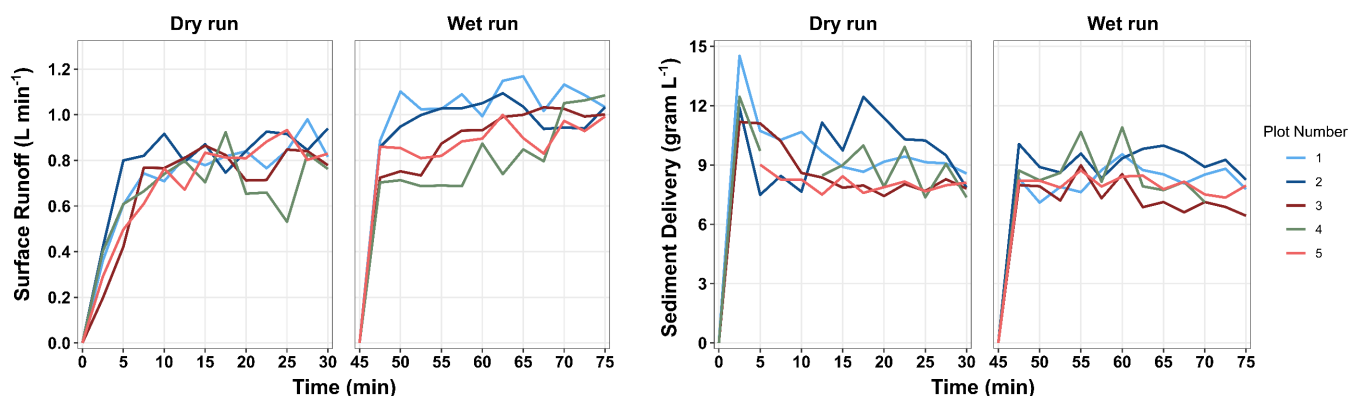


Figure 3.4. Surface runoff and sediment flux during the rainfall simulations across the five plots ($n=5$). The x-axis shows the time scale of the rainfall simulation (0-30 minutes dry run, 15 minutes of break, and 45-75 minutes wet run). Missing data points in plot 4 are visible, these values were outliers and were excluded from the analysis as the values were twice that of the mean sediment concentration and did not relate to other measured parameters suggesting there may have been an error.

The number of MPs transported from the plots in surface runoff peaked in the first 10 minutes of surface runoff then declined as the rainfall simulation progressed (Figure 3.5). This pattern held true for both the dry and wet runs. During the dry run simulation, $854 \pm 411 \text{ MP L}^{-1}$ and $861 \pm 358 \text{ MP L}^{-1}$ of the MPs sized 425-500 μm and 125-150 μm , respectively, were transported from the plots in surface runoff (Figure 3.5). The wet runs had lower concentrations of MPs transported from the plots in surface runoff at $259 \pm 119 \text{ MP L}^{-1}$ and $280 \pm 160 \text{ MP L}^{-1}$ for MPs sized 425-500 μm and 125-150 μm , respectively. Statistically significant differences in MP delivery in surface runoff were not observed between the size fractions in either dry or wet runs ($F(1, 236) = 0.13, p = 0.72$). However, there was a statistically significant difference in the number of overall MPs delivered per litre between the dry and wet runs with wet runs delivering fewer MPs ($F(1, 236) = 247.12, p < 0.001$). Overall, MPs transported in the surface runoff represented $18.8 \pm 0.5\%$ for the 125-150 μm MPs and $20.0 \pm 0.1\%$ for the 425-500 μm MPs of the total number of particles initially inputted into the plots.

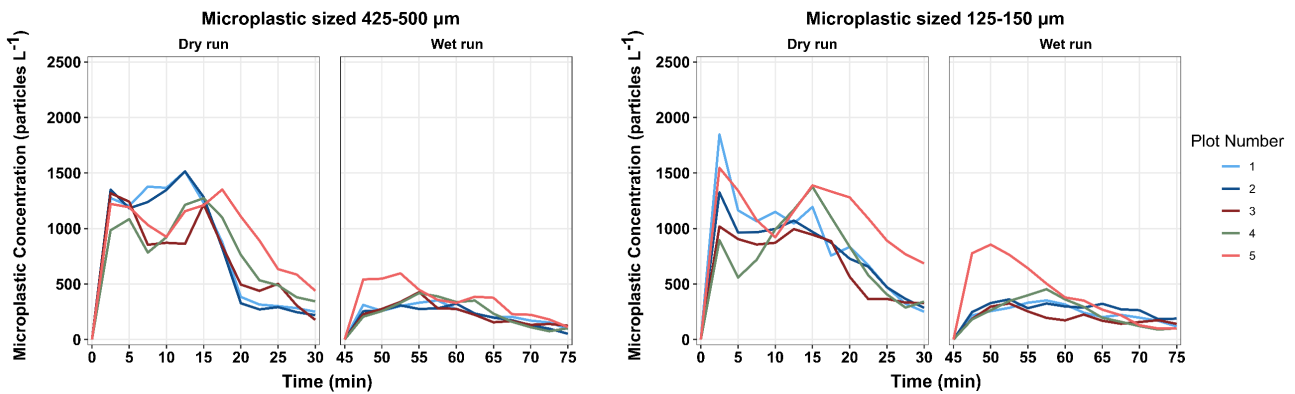


Figure 3.5. Microplastic (MP) sizes 425-500 μm and 125-150 μm transported in surface runoff across the five plots ($n=5$). The x-axis shows the time scale of the rainfall simulation (0-30 minutes dry run, 15 minutes of break, and 45-75 minutes wet run).

Mean enrichment ratios for MPs after both the dry and wet runs showed strong evidence of preferential erosion for the 425-500 μm and 125-150 μm , at 6.2 ± 4.5 and 5.8 ± 3.9 respectively (Figure 3.6). No significant difference was observed in the enrichment ratios between the two MP sizes across both dry and wet runs ($\chi^2(1) = 0.22, p = 0.64$). Overall, enrichment ratios for the dry runs were 9.3 ± 4.6 and 8.6 ± 3.6 for 425-500 μm and 125-150 μm MPs, respectively, whilst for wet runs these ratios were 3.2 ± 1.4 and 3.1 ± 1.8 for 425-500 μm and 125-150 μm MPs, respectively. Wet runs had significantly lower enrichment ratios 3.2 ± 1.6 than the dry runs 9.0 ± 4.1 for both MP sizes ($\chi^2(1) = 117.83, p < 0.001$).

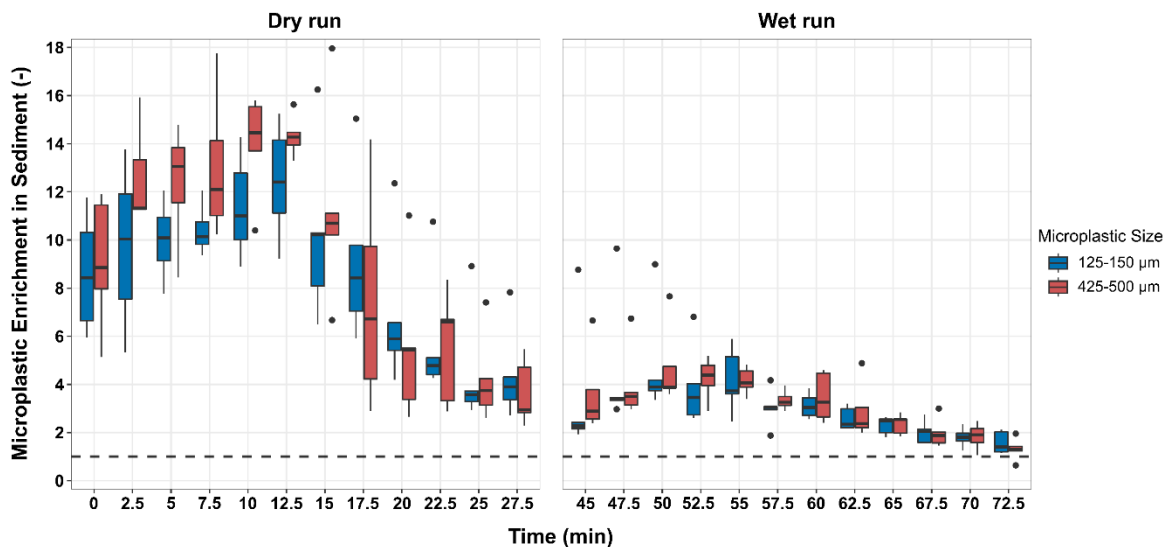


Figure 3.6. Enrichment ratio of 425-500 μm and 125-150 μm microplastic (MP) in delivered sediments across rainfall simulations on all five plots for dry and wet runs ($n=5$). Boxes show the median, 1st, and 3rd quartiles; whiskers represent the minimum and maximum values. An enrichment factor greater than 1 in all simulations indicates preferential erosion of MP. The dashed line marks the initial concentration in the topsoil ($<1\text{ cm}$) as a factor 1.

3.3.3 Vertical tracer movement and retention profile of microplastics

As the mass of collected soil samples varied, the concentration of MPs of different size ranges was normalized into particle number per kg of soil (Figure 3.7). In each plot, the 53-63 μm and 125-150 μm MPs each had an input of 10811 particles per kg of soil and the 425-500 μm had an input of 9919 particles per kg soil prior to the start of the rainfall simulations. Most of the MPs remained in the 0-2 cm layer, with fewer particles found as depth increased. No MPs were detected in the soil below 8 cm depth. Overall, larger numbers of 425-500 μm MPs were detected in every soil layer as compared to either the 125-150 μm or 53-63 μm MPs, including in the 6-8 cm soil layer (Figure 3.7).

Deuterium, ($\delta^2\text{H}$), was used to trace the extent to which rainwater infiltrated into the soil profile. An average isotope value of $229.3 \pm 1.08 \text{ ‰}$ was observed, indicating a similar isotopic signature of deuterated rainwater across all plots (Appendix 2 Figure S3.3a). Infiltration of the labelled water was visible in the upper soil depth (0-6 cm), whereas the contribution of labelled water diminished in the deeper soil layers (8-13 cm) (Appendix 2 Figure S3.3b), indicating that the infiltrating water reached 8 cm depth after one hour of simulated rainfall. Further information regarding $\delta^2\text{H}$ can be found in appendix 2 supplementary information section 3.1.

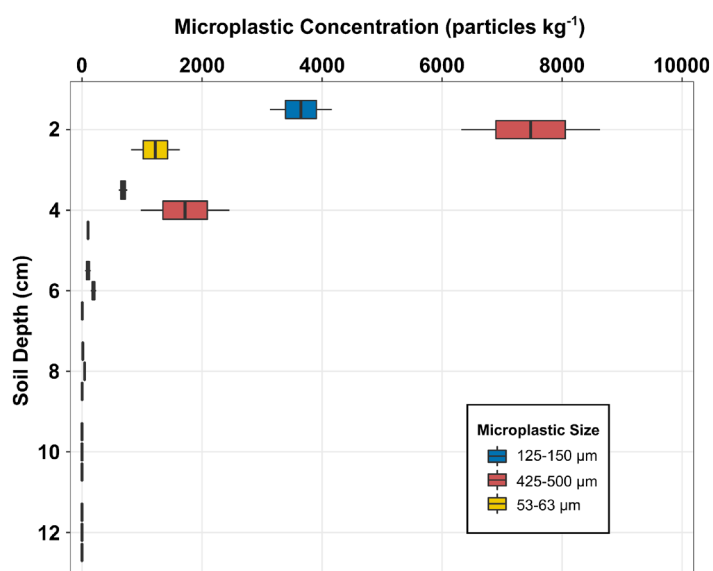


Figure 3.7. The number of detected microplastics (MPs) by the mass of soil. Boxes show the median, 1st, and 3rd quartiles; whiskers represent the minimum and maximum values (n=2).

3.4 Discussion

3.4.1 Pathways and rates of microplastic transport

Images of the soil surface through time revealed various patterns of MP transport from the soil surface. In the dry runs prior to surface runoff, there were substantial decreases in particle numbers detected on the soil surface, reaching 39% for 425-500 μm MPs and 91% for the 125-150 μm MPs of the particle numbers prior to the start of the rainfall simulations. As these decreases occurred prior to surface runoff, the most probable explanation for the decrease in particle number is the impact of raindrops on the soil surface. While it is possible that MPs were transported out of the plots through splash erosion processes (Chapter 2), visual inspection of the area surrounding the plot indicated a very small proportion of MPs were lost from the plots through this transport mechanism. Further, laboratory experiments following the rainfall simulation indicated that small numbers of MP particles were transported via splash erosion processes (Appendix 2 Supplementary Information section 3.2). Therefore, we believe that the most probable explanation for the substantial reduction in MPs detected at the soil surface during the rainfall simulations is that MPs were incorporated into the soil matrix by raindrops mixing the near-surface layer of the soil. Once mixed with the soil, MPs could be transported vertically into the soil profile by infiltration (Li *et al.*, 2024a).

In our research, most MPs remained in the 0-2 cm soil layers, with decreasing numbers of MPs found as soil depth increased. Following a similar pattern to $\delta^2\text{H}$, MPs of all size ranges were identified in soil layers as deep as 8 cm after 1 hour of rainfall simulation, indicating infiltrating water is a vector for MP transport vertically into the soil profile. However, no MPs were identified in the 8-13 cm layers of the soil. Previous research has found similar patterns in which the majority of MPs input to a soil remaining in the upper layers of the profile, with decreasing numbers of MPs in the deeper soil layers after rainfall simulations (Schell *et al.*, 2022; Zhang *et al.*, 2022).

Patterns of MPs transported in surface runoff in both the wet and dry runs, showed that MPs were transported in higher numbers in the initial stages of surface runoff compared to the latter stages (Figure 3.5). This contrasts the pattern of sediment transported from the plots which did not decrease throughout the simulations (Figure 3.4). This aligns with results from chapter 2 which also found soil particles, specifically sand, was transported in relatively constant concentration throughout the rainfall simulations, whereas MPs showed lower concentrations in surface runoff in the latter part of the rainfall simulations. A similar initial

flux of MPs from the soil in the first few minutes of surface runoff has been reported in previous research (Rehm *et al.*, 2021). Enrichment ratios showed MPs have preferential transport compared to soil in this research for both MPs sized 125-150 μm and 425-500 μm . Mean enrichment ratios of 9.3 for the 425-500 μm and 8.6 for the 125-150 μm were recorded during the dry runs, while the wet runs showed smaller enrichment ratios of 3.2 for the 425-500 μm and 3.1 for the 125-150 μm . These enrichment ratios fluctuated through time mirroring the fluxes of MPs throughout the simulation. One explanation of the observed fluctuations in both the MPs transported in surface runoff and the enrichment ratios could be MPs vertical transport into the soil during the simulation which would remove MPs from the erodible layer.

Overall, the dry run simulations delivered significantly more MPs than the wet run simulations (Figure 3.5), even though the wet run simulations had consistently higher amounts of surface runoff and sediment transported from the plots. This discrepancy could be due to a combination of factors, including the preferential transport of MPs in surface runoff, leading to their depletion from the soil, as well as MPs being transported vertically in the soil profile during the dry run simulation and thus being removed from the erodible layer.

3.4.2 The relationship between microplastic size and transport

Much ambiguity surrounds MP transport processes as MPs themselves represent a diverse and everchanging range of polymer types of varying morphologies, sizes and levels of degradation (Kooi and Koelmans, 2019). Some attention has been given to the influence of size in determining the probability and rate of MP transport into the soil profile and over the soil surface. These studies, along with the findings reported in our research, indicate that both horizontal and vertical movement of MPs in the soil as influenced by size does not follow an inverse, linear relationship between MP size and mobility. Rather MPs may follow a similar mobility pattern as soil particles, in which the smallest size particles, i.e. clay (< 2 μm), and the larger particles, such as sand (20 μm - 2000 μm), are typically less mobile than the mid-size particles, such as silt (2 μm -20 μm) (Martinez-Mena *et al.*, 2000). This is because clay particles have strong interactions with the soil matrix due to physico-chemical sorption to other elements of the soil matrix, therefore less likely to detach and sand particles having a larger mass are harder to mobilize as compared to silt particles. However, currently not enough empirical evidence exists to postulate the exact size ranges at which the probability of MP transport increases or decreases. Additionally, it is important to note that factors other

than size can determine MP mobility i.e. MP morphology, density, soil type and time in the soil.

While in our research, there was no significant difference in the number of MPs sized 125-150 μm and 425-500 μm transported from the plots via surface runoff, a slightly larger proportion of MPs sized 425-500 μm ($20.0 \pm 0.1\%$) were transported from the plots compared to MPs sized 125-150 μm ($18.8 \pm 0.5\%$). Similarly, Rehm *et al.* (2021) found no significant difference in the number of MPs sized 53-100 μm and 250-300 μm transported from field plots via surface runoff. However, these authors also reported a slightly larger number of the 250-300 μm MPs transported in the surface runoff. Han *et al.* (2022) found more plastics sized 250 μm transported from soil through surface runoff than plastics sized 1 mm, 4 mm, 15 mm and 50 mm, with no plastics > 4 mm delivered in surface runoff. Zhang *et al.* (2022), found MPs sized < 0.3 mm were transported in greater numbers than MPs sized 0.3-1 mm and 1-5 mm, though the number of MPs sized < 0.3 mm were only transported in slightly higher number than MPs sized 0.3-1 mm. Whilst research to date reported a mixed influence of particle size on MP transport in surface runoff, it seems clear that MPs < 1 mm is more likely to be transported than MPs > 1 mm in surface runoff.

The transport of MPs vertically through the soil profile as influenced by MP size is better constrained in comparison to transport over the soil surface via surface runoff, although many studies have been conducted in columns with sieved soil, sediment or glass beads which have a homogeneous size and shape. These studies report clear trends of deeper vertical movement for MPs of decreasing size (Li *et al.*, 2024a; O'Connor *et al.*, 2019; Qi *et al.*, 2022; Ranjan *et al.*, 2023). There is less research investigating the vertical movement of MPs in natural soils. In our research, we found clear evidence that MPs across the size ranges 53-63 μm , 125-150 μm and 425-500 μm were transported as deep as water infiltrated into the soil profile (8 cm). Although a larger number of 425-500 μm MPs were recovered in the soil samples at all depths as compared to the MPs sized 53-63 μm and 125-150 μm , we believe this could be due to a heterogeneous distribution of MPs in the soil plots after the rainfall simulation and not the influence of MP size. Research conducted by Du *et al.* (2024) compared the vertical migration ability of MPs in 3 size ranges and found that 25-147 μm were the most mobile followed by 0-25 μm and then 147-250 μm MPs. Rehm *et al.* (2021) found a similar pattern in their experiment were the 53-100 μm were more mobile vertically in the soil as compared to 250-300 μm . Another research study found MPs < 0.3 mm were the most mobile vertically in the soil followed by MPs 0.3 mm- 1 mm with MPs 1-5 mm being the least mobile (Zhang

et al., 2022). Results from our research and these studies indicate that the transport of MPs vertically in the soil does not necessarily follow the pattern, which is often seen in column experiments where, as MP size decreases the depth MPs are transported increases. Future work should be done on MPs of more size ranges to understand at which sizes the probability of MP transport increases or decreases.

3.4.3 Transport of microplastics to groundwater and surface waters

Our research demonstrates that MPs may be transported with infiltrating water vertically into the soil profile and are enriched compared to soil particles in surface runoff during erosion events. This mobility increases the risk that MPs may be transported from agricultural soils and delivered to freshwater ecosystems. This is particularly concerning in regions with intensive agricultural activity that utilises plastics to support crop production.

Given the widespread use of plastic materials in agriculture and the persistence of many MPs in the environment, the results of this study underscore the need for improved management practices to mitigate the export of MPs from terrestrial into aquatic ecosystems. While there is evidence that some interventions to reduce soil erosion also reduce the lateral transport of MPs, for example increasing vegetation density, these effects have been shown to be dependent on polymer size and morphology (Forster *et al.*, 2023; Han *et al.*, 2022). In regard to the vertical movement of MPs, previous research demonstrates that soil management practices and MP incorporation into aggregates may limit MP transport vertically through the soil profile (Heinze *et al.*, 2024; Rehm *et al.*, 2021). Further research should be conducted to test the effectiveness of these and other strategies to reduce MP transport both vertically into the soil and laterally over the soil surface.

3.5 Conclusion

Microplastics (MPs) are a contaminant of emerging concern, transported through diverse ecosystems across the globe. In this research, we investigated the transport of MPs of various sizes from agricultural soil during erosion processes induced through rainfall. The results from this research show that MPs are simultaneously transported both vertically into the soil profile with infiltrating water and laterally in surface runoff during heavy rainfall events. Though, the majority of MPs were retained in the soil, indicating that soils could be considered sinks as well as sources for MP pollution. MPs sized 125-150 μm and 425-500 μm exhibited distinct patterns of movement from the surface of the soil but ultimately were transported in surface runoff in nearly equal numbers. This result provides insufficient

evidence to support our first hypothesis that MPs sized 425-500 μm would be transported in higher numbers in surface runoff compared to MPs sized 125-150 μm . MPs of each size range 53-63 μm , 125-150 μm , and 425-500 μm were each detected in the soil as deep as 8 cm, providing insufficient evidence to support our second hypothesis that there would be a size dependant vertical transportation. These results challenge the current assumption that as MP size decreases the likelihood of MP mobility increases, underscoring the complexity of MP transport dynamics in soils. While further research is needed not only to deepen our understanding of how MPs are transported within and from soils, steps should be taken to reduce the amount of MPs entering into agricultural soils in order to limit global MP pollution.

3.6 Acknowledgements

This project has received funding from the European Union's Horizon 2020 research and innovation programme under the Marie Skłodowska-Curie grant agreement No 955334. The authors would like to express their sincere appreciation to Martin Neumann, and Tomas Laburda at CVUT for their technical support as well as Mengyi Gong for her advice on time series statistical analysis.

4. Microplastics detachment and transport from soil as influenced by polymer age and aggregation within the soil

Emilee Severe¹, Quynh Nhu Phan Le¹, Ahsan Maqbool², Ben Surridge¹, Crispin Halsall¹, Jose A. Gomez², John Quinton¹

1. Lancaster Environment Centre, Lancaster University, Lancaster, UK
2. Institute for Sustainable Agriculture, CSIC, Cordoba 14004, Spain

Abstract

Surface runoff is an important process transporting microplastics (MP) from agricultural soils. Although in recent years a handful of studies have quantified the movement of MPs in surface runoff, many of them lack environmental relevance as they use pristine MPs that have not been stored or degraded in the environment prior to the experiment. Microplastics which have fragmented in the environment from larger macroplastics can be physically and chemically different compared to pristine MPs. The changes to polymers within the environment include, but are not limited to, increased surface roughness, alterations to polymer surface chemistry, and decreased hydrophobicity. In this research, we compare the rate of aggregation and transportation of pristine and chemically-aged polystyrene MPs during rainfall simulations. Additionally, we quantified the proportion of both aged and pristine MPs incorporated into soil aggregates after several wet-dry cycles and the influence wet-dry cycles had on MP mobilization. Our results showed that the chemical oxidizing process did not age the polystyrene as effectively as the reference polymer, polyethylene. Wet-dry cycles incorporated approximately 1-3% of MPs into soil aggregates. No significant differences were found in the number of MPs transported in surface runoff between pristine and aged MPs. Similarly, no difference was found in the number of MPs which were transported in surface runoff between soils which underwent wet-dry cycles. The results from this research add to the growing body of work describing the movement of MPs in the environment and are among the first to attempt to investigate the impact of polymer age on MP mobility in surface runoff and the influence of MP age on incorporation into soil aggregates.

4.1 Introduction

Agricultural soils are considered to be a major source of diffuse pollution to aquatic environments, releasing contaminants such as nutrients, sediments and agrochemicals (He *et al.*, 2014; Kreuger, 1998). Microplastics (MPs), defined as pieces of plastic < 5 mm in length, are a contaminant of emerging concern, which have been discovered in agricultural soils in varying amounts (Cusworth *et al.*, 2024; Piehl *et al.*, 2018; Zhang *et al.*, 2023). MPs in high concentrations have been shown to be harmful not only to terrestrial and aquatic biota (Edwards *et al.*, 2023; Palmer & Herat, 2021) but also potentially to soil productivity (Maqbool *et al.*, 2023; Ullah *et al.*, 2021) and human health (Prata *et al.*, 2020; Yang *et al.*, 2021).

Globally, it is estimated that 22.2 million metric tonnes of plastic waste are emitted into the environment every year (Cottom *et al.*, 2024). Once in the environment these large pieces of plastic can degrade and fragment into MPs, through mechanical (Maqbool *et al.*, 2024), microbial (Hadad *et al.*, 2005; Munhoz *et al.*, 2024; Yoshida *et al.*, 2016), and photooxidation processes (Andrady *et al.*, 2022; Beltrán-Sanahuja *et al.*, 2021; Chamas *et al.*, 2020; Rodriguez *et al.*, 2020). These processes not only reduce the size of the plastic, they also influence the physical and chemical properties of the polymer, in some cases making them less hydrophobic, less electronegative and developing higher surface roughness as compared to pristine plastics (Du *et al.*, 2023; Liu *et al.*, 2019b). These changes in physical and chemical properties are thought to change the way the environmentally degraded or “aged” MP interacts with water and soil particles (Yang *et al.*, 2024), thereby potentially changing the aggregation and transportation behaviour of MPs in soil.

Surface runoff is an important process transporting MPs from agricultural soils to freshwaters (Klaus *et al.*, 2024; Norling *et al.*, 2024; Rehm *et al.*, 2021; Rehm and Fiener, 2024).

Although some more recent research has focussed on the transportation of MPs in surface runoff in recent years, this work often uses pristine MPs inputted into soil immediately before rainfall simulations. This is not reflective of MPs in the environment because: (1) as discussed above MPs in the environment are often aged; and (2) MPs are often found in soil aggregates in various proportions in the environment (Rehm *et al.*, 2021; Yang *et al.*, 2022; Zhang and Liu, 2018).

Research has found that MPs stored in soil for extended periods of time were transported in surface runoff to a lesser extent than MPs placed in soil directly before rainfall (Rehm *et al.*,

2021). This was mostly attributed to MPs interacting with soil particles leading to incorporation of MPs in soil aggregates. However, research investigating the vertical transport of aged MPs has found that aged MPs are more mobile than pristine MPs (Liu *et al.*, 2019a; Li *et al.*, 2024b), although this has not been tested in surface runoff transport processes.

Creating conditions reflective of the environment is difficult as time is needed for MPs to age and become incorporated within soil aggregates. However, alternative methods may be employed to accelerate the aging and aggregation of MPs so that environmentally realistic transport research can be undertaken in a shorter period of time. Specifically, heat-activated oxidative processes have been shown to be a rapid, yet effective method to accelerate MP aging (Liu *et al.*, 2019b). This process is able to change the hydrophobicity and the surface roughness of MPs to extents typically seen over years in the environment but following only days of accelerated aging treatment. Additionally, wet-dry cycles are commonly used in laboratory experiments to simulate aggregation, as wet-dry cycles facilitate both chemical and microbial processes which induce aggregation formation in soil (Bronick and Lal, 2005). Research has shown wet-dry cycles to be an effective method to bind MPs to soil aggregates even in sterile soil (Lehmann *et al.*, 2019).

In this context, we aimed to investigate how MPs move in surface runoff when the factors of polymer age and aggregation are considered. We tested the methods outlined in Liu *et al.* (2019b) to accelerate the aging process of commercial fluorescent polystyrene (PS) MPs and used wet-dry cycles to promote interactions between MPs and soil particles. We quantified the proportion of both aged and pristine MPs incorporated into soil aggregates prior to rainfall simulations. Using fluorescent MPs not only enabled rapid quantification of the number of MPs transported via surface runoff, but also allowed us to track the movement of MPs over the surface of the soil through UV photography methods (Appendix 1, Chapters 2 and 3). We hypothesize that aged MPs will have decreased movement as compared to pristine MPs because increases in surface roughness of the aged MPs will “grip” or “snag” soil particles as it is being transported. Similarly, the decreased hydrophobicity will likely reduce the transport of aged MPs because they will be slightly less buoyant and more resilient to detachment and transport by raindrops. We also hypothesize that aged MPs are more likely to form aggregates than pristine MPs, due to rough surfaces which act as binding points and decreased hydrophobicity increases interactions with water and soil particles, this increased aggregation subsequently reducing MP transport. Through this research, we examine and

report methods which should enable more environmentally-relevant research to be undertaken that investigates MP aggregation and transport in surface runoff.

4.2 Methods

4.2.1 Microplastics and accelerated aging process

Polystyrene (PS) was utilised in this experiment as it is a common polymer used in society and is also used in some agricultural applications (PlasticsEurope, 2019). Though various forms of polyethylene (PE) and polypropylene make up the majority of plastic products used in agriculture (FAO, 2021; Scarascia-Mugnozza *et al.*, 2011), PS has been found abundantly in agricultural soils ranging from 8-16% of macro- and microplastic pieces detected in agricultural soil both in terms of the number of MPs and in terms of MP mass (Piehl *et al.*, 2018; Yu *et al.*, 2021)

Fluorescent high impact PS granules (Mark SG Enterprises Ltd.) were purchased from a commercial supplier. The polymer type was verified as PS using Fourier transform infrared spectroscopy (FTIR) and density was measured as 1.053 g cm^{-3} by gas pycnometry using pure helium. The PS was cryogenically milled, then dry sieved to 250-355 μm using an automatic sieve shaker (Endecotts).

The method described in Liu *et al.* (2019b) was used to accelerate the aging of PS by chemical oxidization. In short, 0.5 g of PS MPs as described above were placed into glass beakers containing 20 mL of 100 mM freshly made $\text{K}_2\text{S}_2\text{O}_8$ solution adjusted to pH 7.0. Beakers were then placed in a thermostatic water bath at 70 °C. Every 12 hours, 20 mL of $\text{K}_2\text{S}_2\text{O}_8$ solution was added to the beakers and MPs were filtered and rinsed every 2 days. In total, MPs remained in the $\text{K}_2\text{S}_2\text{O}_8$ solution for 5 days in order to equate to 4 years of environmental degradation (Liu *et al.*, 2019b). A small sample of spherical PE MPs (Cospheric Ltd.) sized 250-300 μm also underwent the aging process as a reference to compare with the PS.

4.2.2 Evaluating microplastic aging

Microplastic aging was evaluated using FTIR spectroscopy, thermogravimetric analysis (TGA) and differential scanning calorimetry (DSC), and scanning electron microscope (SEM) imaging (Ainali *et al.*, 2021; Binda *et al.*, 2024). The FTIR measurements were carried out using an Agilent Cary 630 FTIR (Agilent Technologies Inc., Danbury, CT, USA). An attenuated total reflection (ATR accessory, diamond substrate) was used to confirm

polymer types and potential aging effects on the polymer surface functional groups (penetration depth $\sim 2 \mu\text{m}$ at 1700 cm^{-1}). The FTIR spectra were gathered in the $650\text{--}4000 \text{ cm}^{-1}$ range, with 64 accumulated scans and a 2 cm^{-1} spectral resolution. After collection, each spectrum underwent baseline correction and normalization at the 2912 cm^{-1} (PE) and 2929 cm^{-1} (PS) peaks using Spectragryph software.

The TGA-DSC analysis was performed with a SDT Q600 TGA-DSC instrument (TA Instruments). Approximately, 15 mg of MPs were weighed into a tared alumina crucible and set on the sample beam. Samples were heated at $10 \text{ }^\circ\text{C min}^{-1}$ from room temperature to $1000 \text{ }^\circ\text{C}$ and during analysis the sample was purged by compressed air at 50 mL min^{-1} .

For SEM analysis, MPs samples were mounted on gold plated SEM pin stubs and analysis was carried out by using a JEOL JSM-7800F SEM. The plastics were coated with 10 nm of gold before measurement to enhance electric conductivity (Quorum Technologies Q150RES (magnetron type)). Images were taken of various MPs in several locations to detect visible signs of aging.

4.2.3 Experimental set-up

Wooden soil boxes (length, width and depth of $52 \times 26 \times 10 \text{ cm}$) with drainage holes were lined with a black geotextile woven membrane and packed with soil to a dry bulk density of 1.24 g cm^{-3} . The soil, a sandy loam classified as a petrocalcic palexeralf, was collected from a long-term experimental site near Benacazón, Spain (Guzmán *et al.*, 2010). The soil was screened to 5 mm before use in this experiment. The particle size distribution of the soil was $11.8 \pm 0.8\%$ clay; $8.5 \pm 0.6\%$ silt and $79.7 \pm 0.8\%$ sand, with an organic matter content of $1.6 \pm 0.5\%$ (Guzmán *et al.*, 2010). Soil boxes were set to a 10° slope to reflect realistic environmental topography whilst ensuring runoff generation in a practical time frame.

Exactly 0.15 grams of MPs (approximately 10,000 particles) were evenly mixed with 5.03 kg of soil to constitute an MP-soil mixture in the top 3 cm of soil (0.003% w/w or $73,960 \text{ MPs m}^{-2}$). This concentration of MPs was chosen as it reflects the concentrations of MPs which have been detected in arable soils (Cusworth *et al.*, 2024; van den Berg *et al.*, 2020; Yu *et al.*, 2021; Zhang *et al.*, 2023).

Rainfall was simulated using a nozzle-type rainfall simulator, as described in Alves Sobrinho *et al.* (2008) with the Veejet 80.150 nozzle and set to an intensity of 60 mm hr^{-1} . Rainfall

simulations had a duration of 30 minutes after surface runoff commenced and samples of surface runoff were taken every 2.5 minutes.

4.2.4 Wet-dry cycles

To investigate the influence of MP-soil aggregation on MP transport in surface runoff, 10 soil boxes (5 boxes each containing either aged or pristine MPs) were subjected to wet-dry cycles and 10 soil boxes (5 boxes each containing either aged or pristine MPs) were not put through wet-dry cycles, but were brought to a similar soil moisture to the wet-dry treatment prior to rainfall simulations through capillary action (Figure 4.1).

Soil boxes in the wet-dry treatments were put through four wet-dry cycles over fourteen days to facilitate the incorporation of MPs into soil aggregates. Soil was wet through capillary action to approximately 40% gravimetric water content (GWC), which is slightly above field capacity for this soil, then dried in an oven at 55 °C to approximately 25% GWC, or just below field capacity for this soil. In the no wet-dry cycle treatment, soils were brought to approximately 25% GWC through capillary action prior to rainfall simulation.

To evaluate the proportion of pristine and aged MPs bound to soil aggregates in the wet-dry cycles, two small containers (diameter and depth 11.5 cm x 10 cm), one containing aged MPs and the other containing pristine MPs, was filled with soil and MPs to the same concentration as the soil boxes. These containers went through the same wet-dry treatment as described above for the soil boxes. After the wet-dry cycles, the soil was air-dried and 600 g of soil in 200 g replicates for the aged and pristine MPs were sieved to 4.75 mm, 2 mm, 1 mm, 0.5 mm, 0.355 mm, 0.25 mm size fractions using an automatic sieve shaker (Endecotts Ltd.) for 60 seconds at 40% power. Each soil aggregate fraction was then gently crushed using a mortar and pestle and the number of MPs in each aggregate size fraction were counted in a dark room with a UV light. Soil boxes which had no wet-dry cycles were assumed to have 0 MPs adhered to soil aggregates.

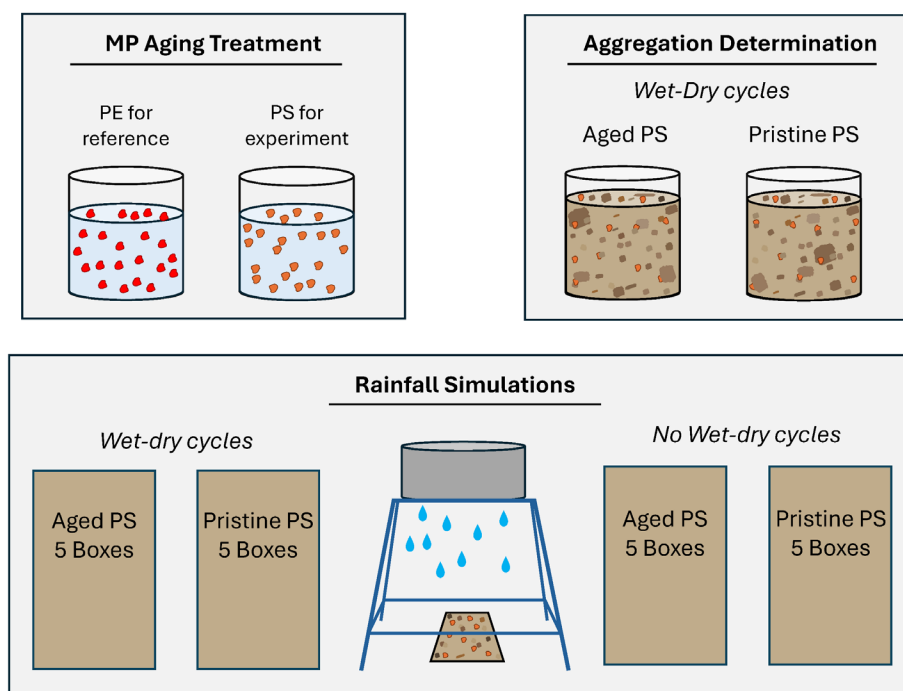


Figure 4.1. Diagram of the experimental set-up showing the microplastic (MP) aging treatment, the determination of how many MPs were bound to soil aggregates, and the rainfall simulations. PE and PS represents polyethylene and polystyrene, respectively.

4.2.5 Image collection and processing

As the MPs were fluorescent, the number of MPs on the soil surface could be quantified throughout the duration of each rainfall simulation. A Canon EOS 850D camera with a 50 mm prime lens was set at the base of the soil boxes and captured images of the soil surface every 10 seconds using an intervalometer (Neewer RS-60E3). The camera was set to capture images in RAW format at the following settings: $f/9$, exposure 1 sec. and ISO 320. The camera was auto focused with natural lighting, then switched to manual focus and the focus ring was manually secured to prevent focus drift due to shutter vibrations (Hardy *et al.*, 2016). A 50-watt UV floodlight with a peak emission of 365 nm (Mark SG Enterprises Ltd.) was secured above the soil box to excite the fluorescent dye in the MPs. Several tarps were placed over the rainfall simulator and camera to decrease ambient light.

Images were converted into TIFF format (LZW compression) using Adobe photoshop. As the camera could not be located directly over the soil box due to rainfall, perspective effects varied the size of the ground area represented by individual pixels within each image. To rectify this, the Perspective Warp tool, which is a stretch function in Adobe Photoshop was

used to resample the images, correcting for perspective in the images (Bowers and Johansen, 2002). Images were then cropped to just inside the edges of the soil box (representing an area of approximately 52 cm x 26 cm) using Image J. The Color Thresholding tool in Image J was then used to identify the fluorescent MPs on the soil surface in the images. Using the HSB color space, particles were identified using the following threshold values: Hue= 0-55, Saturation= 70-255, and Brightness= 80-255. The Watershed Separation tool was subsequently used to identify and separate adjoining particles.

The effectiveness of MP identification in the images was determined using the same procedure outlined in chapters 2 and 3. As the pristine and aged MPs had identical color signals in the images, the effectiveness of MP identification for both polymers was considered together and an overall f-score of 0.93 was recorded meaning approximately 93% were correctly classified.

4.2.6 Microplastics in surface runoff

After collection, surface runoff samples were immediately weighed to quantify the mass of runoff water transported from the plots. Surface runoff samples were then filtered through a vacuum filtration system and were oven dried at 55 °C. Once dry, the filter paper containing sediments and MPs were weighed. Sediments and MPs were then separated from the filter paper and gently crushed using a mortar and pestle. Sediments and MPs were then spread thinly on a piece of black cardstock paper and manually counted using a 50-watt UV floodlight with a peak emission of 365 nm (Mark SG Enterprises Ltd.).

4.2.7 Statistical analysis

This experiment followed an independent measures design. This approach was chosen in order to isolate the effects of microplastic age and aggregation with soil (through wet-dry cycles) on MP transport dynamics in rainfall-induced erosion. Each trial was conducted under controlled environmental conditions with multiple replicates (n=5). The independent variables were MP age and aggregation with the soil, while the dependent variables were the number of particles transported and the rate of transport from the soil surface. Data were analysed to determine whether MP particle movement significantly deviated between treatments providing insight into their transport dynamics.

Statistical analysis was carried out using R Statistical Software version 4.3.1 (R Core Team, 2023). Data normality was tested by using D'Agostino-Pearson's K^2 test to a 0.05

significance. When data was normally distributed, analysis of variance (ANOVA) were used to test differences between treatments, followed by Tukey's post-hoc tests where required. Kruskal-Wallis tests were used to test differences between treatments when data were not normally distributed, along with Wilcoxon rank-sum post-hoc tests. Both ANOVAs and Kruskal-Wallis tests were performed to a 0.05 significance. Change point analysis of the mean and variance were used to evaluate the time series data of the number of MPs on the surface of the soil. Change point analysis is often used to identify instants where there are significant shifts in the data points in time series. Change points were calculated from the mean of each treatment using the AMOC (At Most One Change point) method in the R change point package (Killick and Eckley, 2014). All results are reported as mean \pm one standard deviation.

4.3 Results

4.3.1 Evaluation of microplastic aging and wet-dry cycle methodologies

Both, TGA-DSC and FTIR were used to quantify the differences between the pristine and aged PS MPs. The PE MPs which underwent the same treatment were analysed alongside the PS MPs as a reference. The TGA-DSC analysis showed no difference between the derivative thermogravimetric (DTG) curves of the aged and pristine PS (Figure 4.2A). However, there were considerable differences between DTG curves of the aged and pristine PE MPs (Figure 4.2A). The aged PE demonstrated new peaks and shelves in the DTG curves between 300°C to 500°C underlining substantial changes in polymer thermic properties. The FTIR analysis also showed no differences between the pristine and aged PS but slight differences between the pristine and aged PE (Figure 4.2B). The aged PE displayed new absorption peaks around wavelength 3300 to 3600 cm^{-1} which is indicative of the formation of hydroxyl (OH) groups through oxidative degradation.

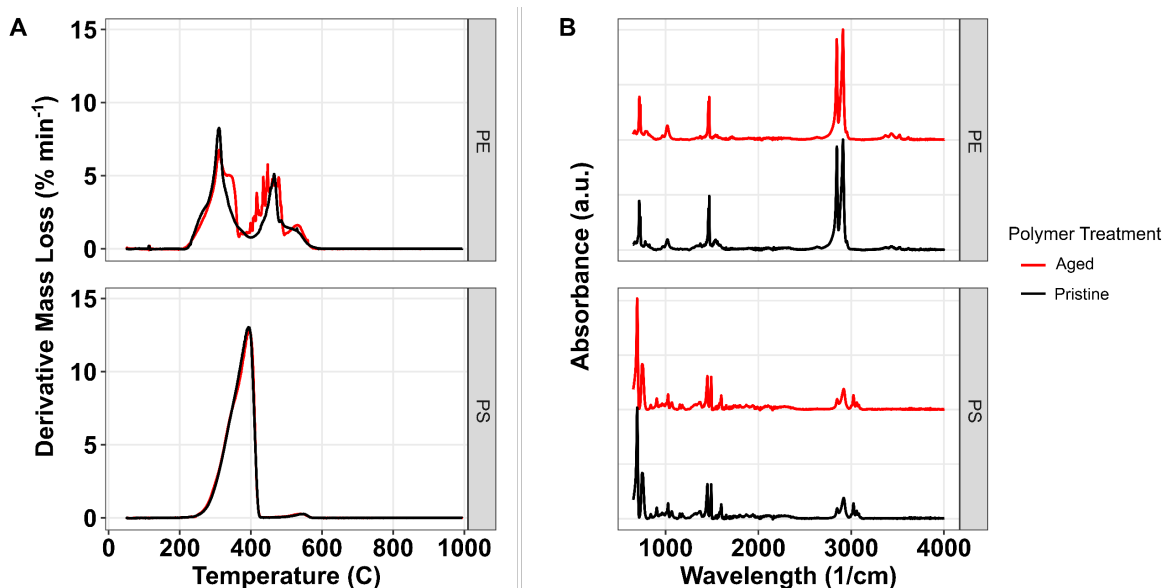


Figure 4.2. Thermogravimetric analysis and differential scanning calorimetry (TGA-DSC) analysis showing the derivative thermogravimetric (DTG) curve (A) and Fourier transform infrared spectroscopy (FTIR) spectra of both the polyethylene (PE) and polystyrene (PS) microplastics (MPs) (B). The DTG curve represents the rate change of mass (% min⁻¹) with respect to temperature in Celsius. The FTIR spectra showing the absorbance by wavelength. Red lines representing aged MPs and black lines represent pristine MPs.

The SEM images of the polymer surfaces visually confirmed the patterns of degradation in the FTIR and TGA-DSC analysis (Figure 4.3). Both the pristine and aged PS have moderately smooth surfaces with ridges on the polymer surfaces in the SEM images, however no additional signs of degradation were found on the aged PS MP compared to the pristine PS MP (Figure 4.3A and 4.3B). Pristine PS MPs seemed to have more nano-sized particles adhered to the surface as compared with the aged PS. In contrast, the pristine PE had a notably smoother surface as compared to aged PE MP which showed significant peeling and pits on the polymer surface (Figures 4.3C and 4.3D).

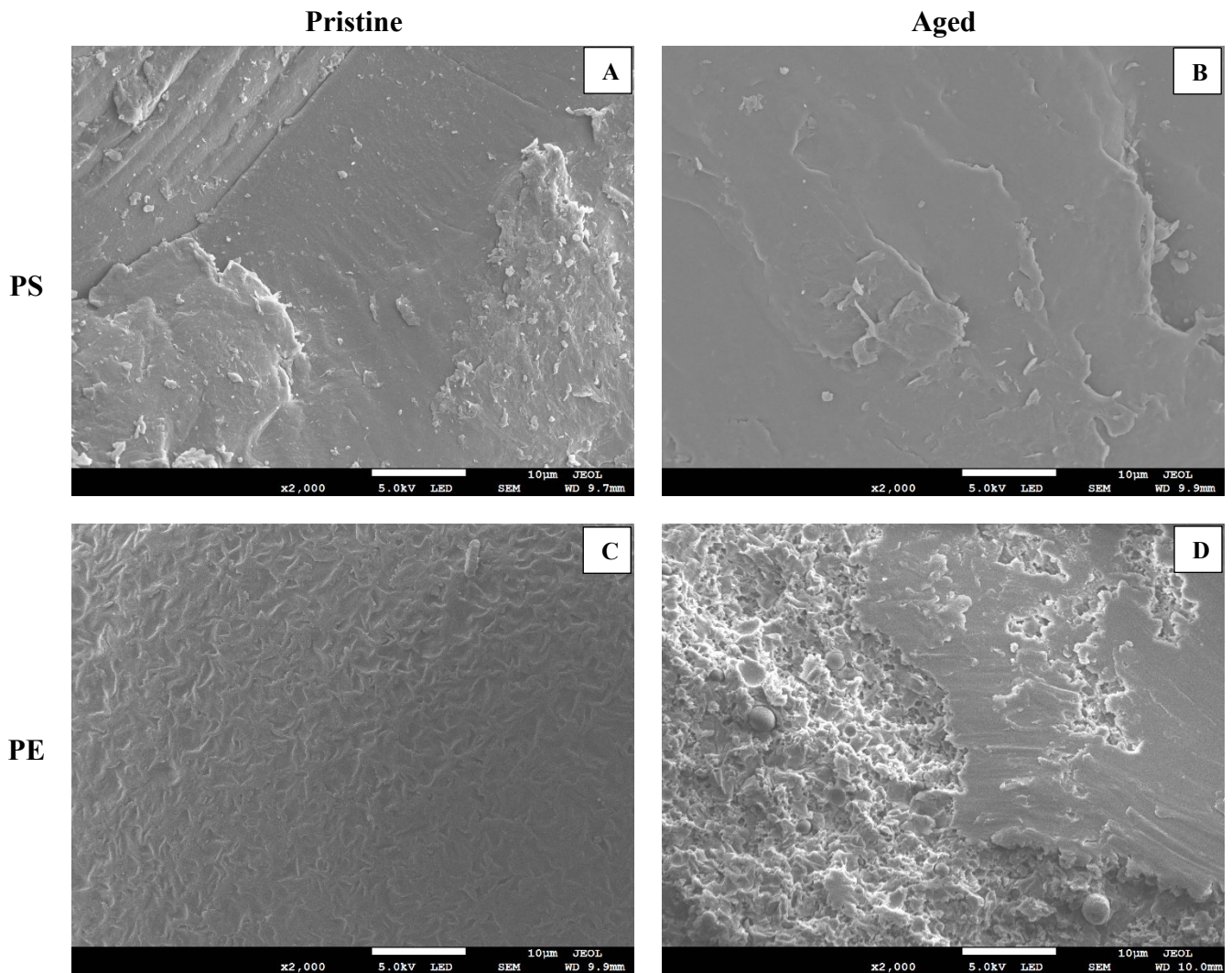


Figure 4.3. SEM images of pristine PS (A), aged PS (B), pristine PE (C), and aged PE (D). Working distance (WD), magnification, and 10 μm scale bar indicated on the bottom of each respective images. PE signifies polyethylene and PS signifies polystyrene.

Approximately 1-3% of PS MPs placed in the soil were bound to soil aggregates due to the wet-dry cycles (Table 4.1). No significant difference was detected in the number of MPs found in aggregates between pristine MPs and aged MPs ($\chi^2(1) = 0.052, p = 0.82$). There was no significant pattern of MPs binding into one aggregate size fraction over the other.

Table 4.13 Microplastics (MPs) found in soil aggregate fractions. Soil mass refers to the mass of soil in grams for each sieved aggregate size fraction. # MPs indicates the number of MPs found in each aggregate size fraction. % MPs indicates the proportion of MPs in each aggregate size fraction in relation to the total number of MPs recovered for all sizes. As the MPs were sieved to 0.25-0.355 mm prior to the experiment any MPs found below 0.355 mm were considered loose in the soil and MPs found in the larger aggregate size fraction were assumed to be bound to soil aggregates.

	Aggregate Size (mm)	Pristine Microplastics (MPs)			Aged Microplastics (MPs)		
		Soil Mass (g)	# MPs	% MPs	Soil Mass (g)	# MPs	% MPs
Bound	> 4.75	9.7 ± 0.3	1 ± 1	0.1 ± 0.2	11.1 ± 3.9	1 ± 2	0.2 ± 0.4
	2-4.75	44.0 ± 1.0	1 ± 1	0.2 ± 0.2	43.6 ± 1.7	3 ± 2	0.5 ± 0.4
	1-2	23.0 ± 1.1	1 ± 1	0.2 ± 0.2	23.2 ± 1.4	0 ± 0	0 ± 0
	0.5-1	15.9 ± 0.5	2 ± 2	0.5 ± 0.3	15.9 ± 1.1	3 ± 3	0.5 ± 0.6
	0.355-0.5	4.8 ± 0.7	4 ± 2	0.7 ± 0.4	5.1 ± 0.5	8 ± 3	1.7 ± 0.6
Loose	< 0.355	102.3 ± 1.9	507 ± 41	98.3 ± 0.9	100.6 ± 1.9	494 ± 36	97.1 ± 1.2

4.3.2 Patterns of movement on the soil surface

In this research, images of the soil surface showed gentle declines in the number of MPs from the soil surface throughout the rainfall simulations. The means and standard deviations of the number of MPs on the soil surface showed no substantial differences between treatments throughout the duration of the rainfall simulations (Figure 4.4). In each treatment, there was a pattern of more rapid decline in the first 4-15 minutes of the rainfall simulation followed by a gentle decline. The average start time to surface runoff was 3 minutes (minimum= 1 minute and maximum = 7 minutes). Change point analysis showed a significant shift in the mean and variance in the number of particles on the soil surface at 6 minutes and 40 seconds, 14 minutes and 40 seconds, 6 minutes and 10 seconds and 4 minutes and 40 seconds for Wet-Dry Aged MP, Wet-Dry Pristine MP, No Wet-Dry Aged MP, and No Wet-Dry Pristine MP, respectively (Figure 4.4). This shows that in the initial stages of the rainfall simulation the number of MPs on the soil surface decreased faster than in the latter stages of the rainfall simulation.

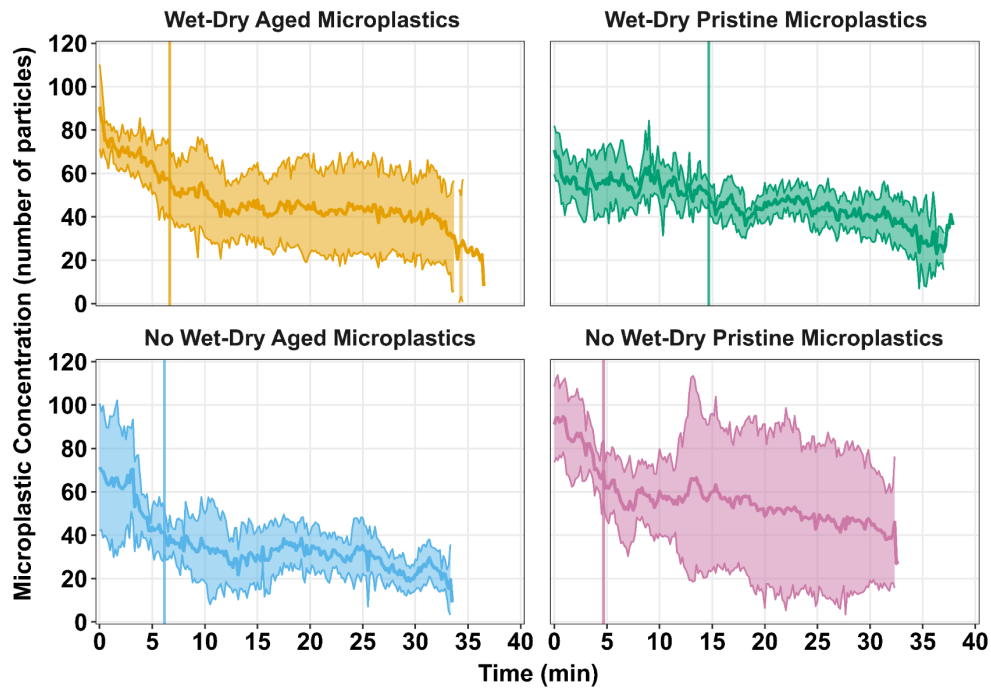


Figure 4.4. The number of microplastics (MPs) on the surface of the soil throughout the rainfall simulations ($n=5$). Dark lines represent the mean number of particles and the shaded regions represent \pm one standard deviation. Vertical lines indicate the changepoint for each treatment.

4.3.3 Microplastic transport in surface runoff

There were significant differences in means between the surface runoff rates between treatments ($F(3, 232) = 14.94, p < 0.001$) (Figure 4.5A). Post-hoc testing showed that the treatments which underwent wet-dry cycles had significantly less average surface runoff $0.065 \pm 0.019 \text{ L min}^{-1}$ compared to treatments that did not undergo wet-dry cycles $0.079 \pm 0.014 \text{ L min}^{-1}$ ($p < 0.005$). Further investigation found that initial soil moisture varied significantly between treatments ($F(3, 236) = 64.57, p < 0.001$), with the no wet-dry cycle treatments having a lower GWC than the wet-dry cycle treatments prior to the start of rainfall simulations ($p < 0.0001$) (Figure 4.5B). For the sediment transported from the soil boxes, there were no significant differences between the treatments ($\chi^2(3) = 4.26, p = 0.23$). Across all treatments a mean sediment transport rate of $1.51 \pm 0.85 \text{ g min}^{-1}$ was recorded.

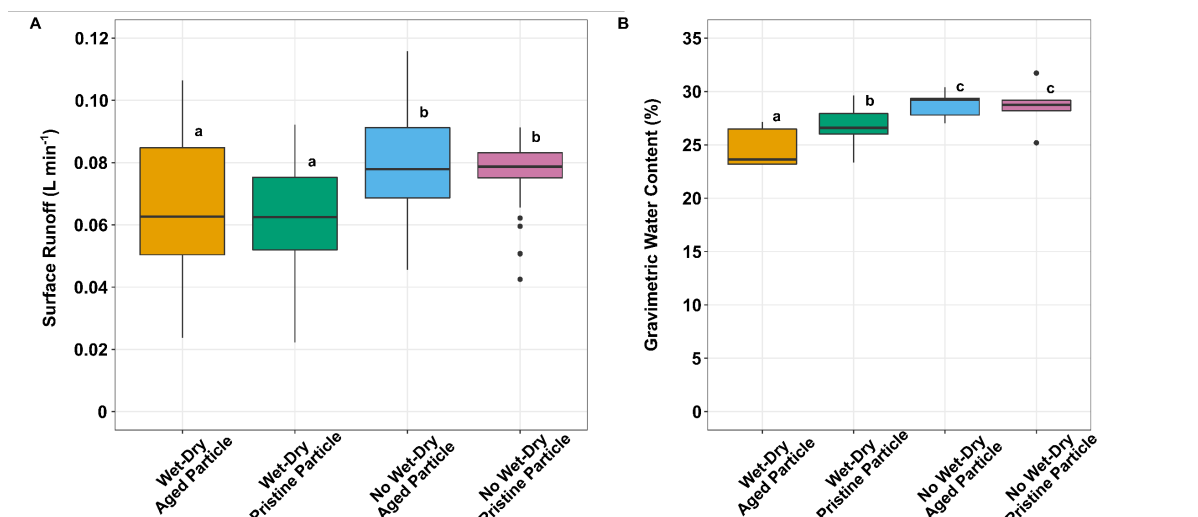


Figure 4.5. Surface runoff transported from the soil boxes in litres per min (A). Gravimetric water content (GWC) of the soil boxes before being placed under the rainfall simulator (B). Letter on the boxplots indicate significance ($p < 0.05$). For all data $n=5$.

Across each treatment, the number of MPs transported from the soil boxes in surface runoff demonstrated similar patterns through time (Figure 4.6A). Each treatment showed a general pattern of a higher concentration of MPs transported in the surface runoff in the first 5 minutes of the rainfall simulation as compared to later time points. However, the aged MPs that underwent wet-dry cycles did not follow this pattern, instead showing more erratic and slightly higher concentrations of MPs transported through time as compared to the other treatments.

The wet-dry cycle treatments appeared to be associated with greater total transport of MPs in surface runoff than the no wet-dry cycle treatments, but ultimately no significant difference between the mean number of MPs transported in surface runoff across the treatments was found ($F(3,16) = 1.12, p = 0.37$) (Figure 4.6B). For soil boxes that had wet-dry cycles imposed before rainfall simulation, the aged and pristine MPs had 189 ± 68 MPs and 139 ± 58 MPs transported from the soil boxes in total, respectively, while soil boxes that did not have the wet-dry cycles imposed transported 142 ± 44 aged MPs and 141 ± 20 pristine MPs in total.

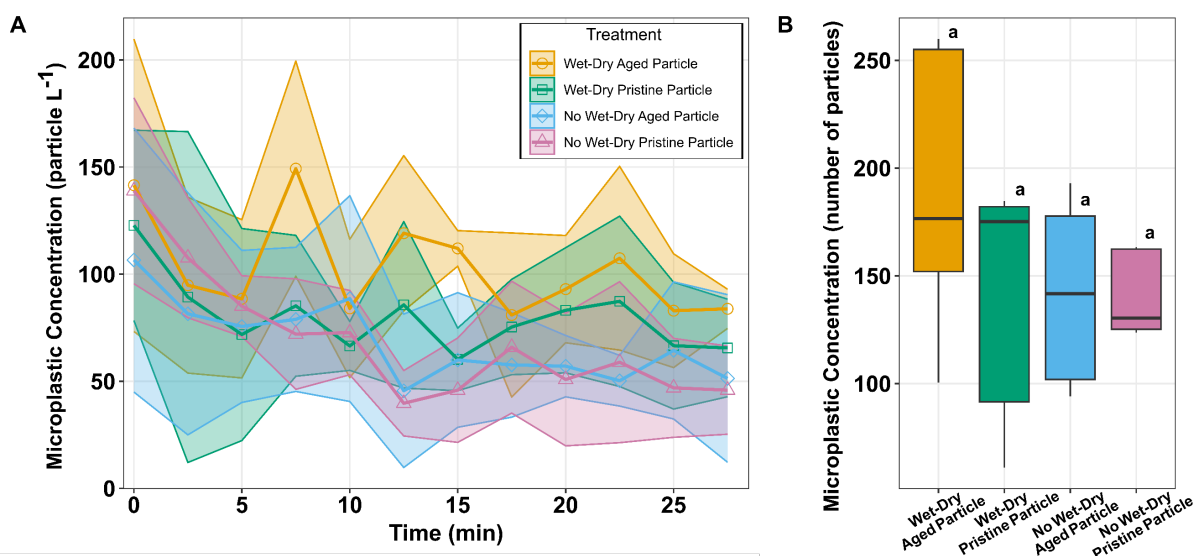


Figure 4.6. The number of microplastics (MPs) per litre of runoff throughout the rainfall simulation (A) and total number of MPs transported during the rainfall simulations (B). In panel A, lines represent the mean number of particles while the shaded regions mark \pm one standard deviation. In panel B, boxplots show the median, 1st, and 3rd quartiles; whiskers represent the minimum and maximum values (n=5). Letter on the boxplots indicate significance ($p < 0.05$).

4.4 Discussion

4.4.1 Accelerating environmental conditions for lab-based microplastics studies

In this research, we endeavoured to create environmentally relevant conditions in the laboratory to investigate MP transport. Using oxidative processes, we aimed to accelerate MP degradation to assess how aged MP compares to pristine MP transport in terms of transport via surface runoff. Additionally, we used wet-dry cycles to create interactions between MPs and soil aggregates to examine how MP aggregation with soil influences MP transport.

However, our results showed that the oxidative process employed in the research had no significant aging effects on the PS MP. The lack of aging is not likely to be error in the procedure, because the reference polymer PE went through the same process and showed significant signs of aging (Figure 4.2 and 4.3). While other research using heat-activated $K_2S_2O_8$ to artificially age MP have found significant degradation of PS (Liu *et al.*, 2019b; Sarkar *et al.*, 2021), one research study using this process did observe relatively slow degradation of PS MPs due to by-products derived from the PS which acted as plasticizers and thus inhibited degradation (Nakatani *et al.*, 2022). It has been noted that a majority of research investigating oxidative processes to artificially age plastics has been conducted on plastics free of chemical additives, which the presence of, is likely to significantly hinder the

aging of MPs (Binda *et al.*, 2024). As the PS used in this research, was manufactured as a commercial plastic product, it is likely that it contained high amounts of additives which made it more resilient to degradation.

Wet-dry cycles are commonly used in laboratory experiments to simulate aggregation as wet-dry cycles facilitate both chemical and microbial processes which induce aggregation formation in soil (Bronick and Lal, 2005). Our research found 1-3% of MPs placed in the soil were bound to soil aggregates after 4 wet-dry cycles. Others using wet-dry cycles to incorporate MPs into soil aggregates found a similar 1-2% increase in MPs bound to newly formed aggregates in sterile soil after wet-dry cycles compared to soils without wet-dry cycles (Lehmann *et al.*, 2019). Whilst the soil and water in our research was not sterile, the soil had a low organic matter content, which is a known limiting factor in soil aggregate formation (Wagner *et al.*, 2007). Other research has found that after wet-dry cycles less than 30% of MPs were bound to soil aggregates in soils with low organic matter content and that increasing organic matter content increased the number of MPs bound to soil aggregates (Zhang and Zhang, 2020).

Surveys of agricultural soils have found various amounts of MPs bound in aggregates: Yang *et al.* finding 35% and Zhang & Liu finding 72% (Yang *et al.*, 2022; Zhang and Liu, 2018). Whilst wet-dry cycles are effective to stimulate aggregation in soils, this mechanism alone cannot completely simulate aggregation processes in the environment. A combination of processes in agricultural soils including tillage, the impacts of raindrops, and soil biota mix the MPs within the soil and likely increase the aggregation of MPs into the soil (Lehmann *et al.*, 2021a; Liang *et al.*, 2021). The lack of these processes in our experiments may explain the lower proportion of MPs bound to soil aggregates compared to findings from other research in agricultural soils.

To date one piece of research has investigated the role of polymer age on MP incorporation into soil aggregates. The authors of this research found that while interaction of aging and polymer type influence the number of aggregates formed, no consistent pattern emerged regarding whether aged or pristine MPs increased or decreased aggregation (Amaya, 2023). Understanding how aged and pristine MPs interact with soil aggregates is an important area of future research, as aggregation of soil influences several other soil properties aside from erodibility such as soil structure and porosity. Field trials which incorporate drivers of

aggregation other than wet-dry cycles, including microbial activity, tillage, impacts of raindrops and soil biota should be a particular focus for future research.

4.4.2 Microplastic transport in surface runoff processes

Using photography to track the movement of fluorescent particles over the soil surface during rainfall simulations has been shown to provide rich insight into the transport processes of the particles (Chapter 2 and 3; Hardy *et al.* 2017). Images of the soil surface and changepoint analysis indicated greater decreases in the number of MPs from the soil surface in the initial stages of the rainfall simulations as compared to the latter stages of the rainfall simulation (Figure 4.4). This suggests the impact of raindrops plays an important role in transporting MPs from the soil surface prior to the commencement of surface runoff. These transport processes may include splash erosion and raindrops mixing the MPs into the near soil surface layer.

We report no significant differences between the number of MPs transported from the soil boxes via surface runoff across both soil wet-dry cycle and polymer age treatments. There are two possible reasons for why there was no significant differences in the transport of MPs via surface runoff depending on whether soils had previously been exposed to wet dry cycles. Firstly, only a small proportion (1-3%) of MPs were found to be bound in soil aggregates following wet-dry cycles. This small proportion may not have been high enough to reduce MP transport. Other research found when approximately 40-60% of MPs were held in soil aggregates there was a reduction in MPs transported in surface runoff (Rehm *et al.*, 2021). Second, in this research the MP-soil layer was 3 cm deep. It is possible that MPs bound to soil aggregates were below the erodible layer in the soil, thus had no influence on the number of MPs transported in surface runoff.

The research presented here did not find evidence of aging to the MPs as a result of oxidative treatments to the MPs, so conclusions cannot be drawn as to how aging influences MP transport in surface runoff. However, it is still likely that the degree of aging influences MP transport in surface runoff, not least because differences due to aging in transport have been shown in terms of vertical transport processes (Liu *et al.*, 2019a; Li *et al.*, 2024b). We hypothesized that aged MPs will have decreased movement as compared to pristine MPs because increased surface roughness of the aged MPs will “grip” or “snag” soil particles as it is being transported. Similarly, the decreased hydrophobicity will likely reduce the transport of aged MPs because they will be slightly less buoyant and more resilient to detachment and

transport by raindrops. We also hypothesized that aged MPs are more likely to form aggregates than pristine MPs, due to rough surfaces which act as binding points and decreased hydrophobicity increases interactions with water and soil particles, this increased aggregation subsequently reducing MP transport. As the aging process proved to be ineffective, we were unable to corroborate or refute the hypotheses. Further research is needed to test these hypotheses and fill this critical gap in MP transport and aggregation research.

4.5 Conclusion

Microplastics are transported through and from agricultural soils by surface runoff. In this research, we aimed to understand how pristine PS MPs are transported in surface runoff and bound to soil aggregates in comparison with aged PS MPs. A chemical oxidizing process using potassium persulfate produced little aging effects on the PS MP but had substantial effect on the reference polymer, PE. Therefore, we cannot draw conclusions to the hypotheses set out in this experiment regarding how aging influences MP transport in surface runoff. However, our results indicate that additives or the polymer composition itself can hinder artificial aging of MPs. Wet-dry cycles incorporated 1-3% of MPs into soil aggregates, showing potential to recreate more environmentally realistic conditions in laboratory erosion experiments. Rainfall simulations on the soils, found no significant differences in the number of MPs transported in surface runoff among pristine and aged MP nor soils which underwent wet-dry cycles. Further research is needed to understand if there are differences in aggregation and transport processes of aged and pristine MPs. This future research will be critical in understanding the mobilization and transport processes of MPs in rainfall-induced erosion.

4.6 Acknowledgements

This project has received funding from the European Union's Horizon 2020 research and innovation programme under the Marie Skłodowska-Curie grant agreement No 955334. The authors would like to express their sincere appreciation to Azahara Ramos, Clemente Trujillo, Manuel Redondo, and Francisco Mendez for their technical support.

Chapter 5. General Discussion

5.1 Summary of aims and objectives

Microplastics are being cycled throughout the globe driven by various processes. Rainfall-induced erosion is increasingly recognized as an important process transporting MPs from soils to freshwater environments, however, there remains little evidence detailing MP transport in this process.

This thesis examined the transport processes MPs are subject to during rainfall-induced erosion. This thesis aimed to (1) investigate how MP properties enhance or diminish their transport in rainfall-induced erosion and (2) explore the transport pathways MPs follow as influenced by MP properties. To meet these aims, this thesis addressed the following objectives:

1. To compare the transport pathways and rates of movement between MPs of various polymer types with a natural soil particle in a rainfall simulation (chapter 2);
2. To evaluate the transport pathways MPs of various size follow during rainfall simulations (chapter 3);
3. To investigate how the degree of MP aging effects aggregation and the transportation of MPs in a rainfall simulation (chapter 4).

The objectives were met through three data chapters. The key findings are outlined below as follows:

Chapter 2 addressed objective 1 by conducting laboratory rainfall simulations which compared the transport pathways of three MPs of various polymer types with a fluorescent sand particle in response to surface runoff and splash erosion. Using UV photography this research tracked the number of MPs on the soil surface throughout the rainfall simulation. The number of MPs transported from the surface of the soil through surface runoff, splash erosion and vertical transport into the soil was also measured.

The main findings of this chapter are as follows:

1. Fluorescent sand particles were preferentially retained in the soil at the conclusion of the experiment as compared to the MP particles which were preferentially transported outside of the soil boxes through splash erosion processes.

2. Temporal differences were found between transport of sand particles and MPs in surface runoff. Microplastics were transported in greater numbers in the first half of surface runoff then drastically decreased in the latter half of surface runoff, whereas the sand particles were transported in steady numbers in surface runoff throughout the rainfall simulation.
3. Images of the soil surface through time showed that there were drastic initial decreases in the number of particles on the soil surface. As the decrease in particles could not be explained by the number of particles transported in splash erosion and surface runoff, we concluded that the decrease in particles from the soil surface was due to raindrops mixing MPs and sand particles into the soil matrix. Microplastics had faster rates of decline from the soil surface compared to the sand particle.

Chapter 3 addressed objective 2 by conducting field-scale rainfall simulations which compared the transport pathways of MPs of varying size. Using UV photography this research tracked the number of MPs on the soil surface throughout the rainfall simulation. The number of MPs transported in surface runoff and the depth to which MPs were transported into the soil was also measured.

The main findings of this chapter are as follows:

1. Compared to soil particles, MPs were preferentially eroded from the soil. This was evidenced by a high enrichment ratio of MPs in the eroded sediments compared to the concentration of MPs in the soil.
2. Microplastics sized 53-63 μm , 125-150 μm and 425-500 μm were all discovered in soil as deep as 8 cm. The depth to which MPs were transported mirrored the depth the isotopically labelled rainwater infiltrated into the soil, illustrating the ability of infiltrating water to transport MPs of various sizes into the soil profile.
3. At the beginning of the rainfall simulations, there was a large decrease in the number of MPs on the surface of the soil. This decrease was attributed to the impact of raindrops on the soil surface as surface runoff was not being delivered from the plot at this time.

Chapter 4 addressed objective 3 by conducting laboratory rainfall simulations to test the influence of MP age and aggregation on MP transport in surface runoff. Methodologies were tested to accelerate MP aging and aggregation processes. Microplastics on the soil surface

were monitored through UV photography and the number of MPs transported in surface runoff were reported.

The main findings of this chapter are as follows:

1. Heat-activated chemical oxidizing processes produced variable rates of aging between polymers. Indicating that additives or the polymer composition itself can hinder artificial aging of MPs.
2. No differences were detected in the number of MPs transported in surface runoff between soils which were put through wet-dry cycles and soils which were not. As only 1-3% of MPs were bound to soil aggregates it was concluded that low levels of MP-soil aggregation do not reduce MP transport in surface runoff.

The aims and objectives in this thesis address several knowledge gaps in our understanding of MP transport in rainfall-induced erosion. The key findings across the entire thesis are summarized in Figure 5.1 and are discussed in detail in the sections below.

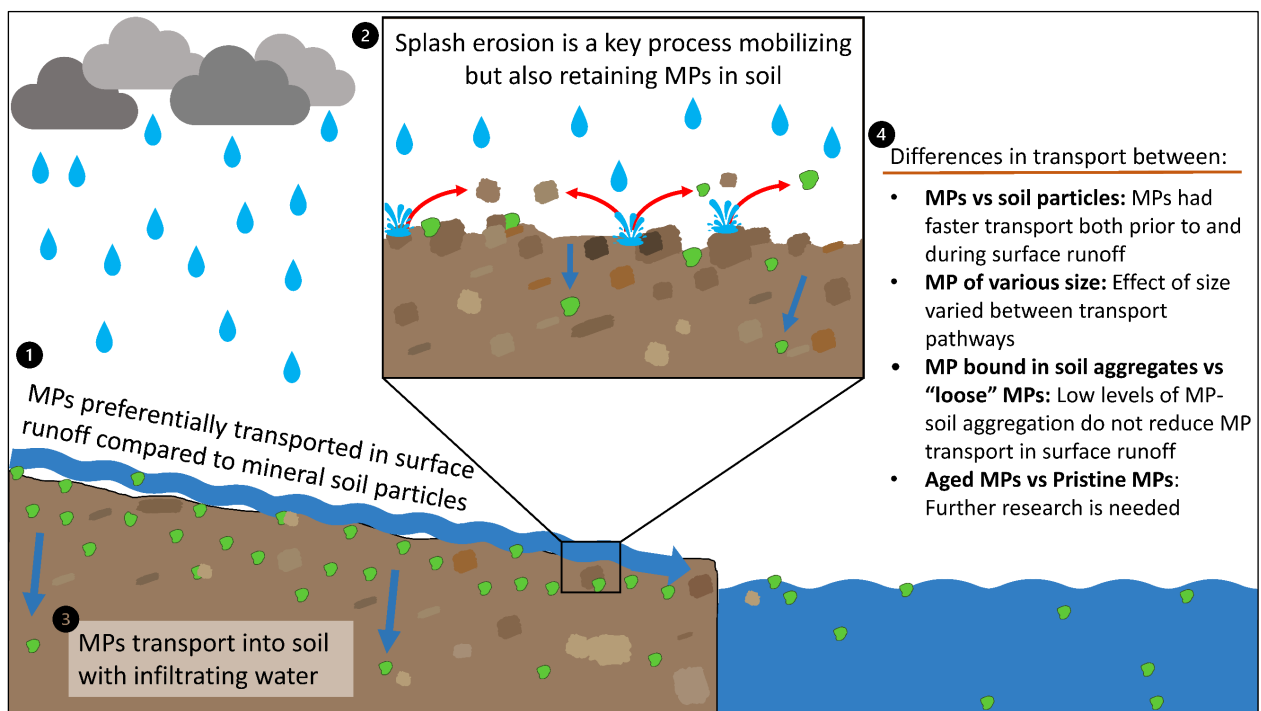


Figure 5.1. Conceptual model summarizing the key findings of this thesis. MP represents microplastic.

5.2 Microplastic properties and their influence on transport

Across this thesis, MP characteristics were shown to influence the rate and magnitude of their transport in rainfall-induced erosion. Microplastics currently represents an all-encompassing

term which includes plastics of all polymer types, morphology, degrees of aging, and sizes from 1 μm to 5 mm. This diversity creates numerous combinations of MP characteristics which to date have not been investigated. In this thesis, we focused on characteristics which distinguish MPs from natural soil particles specifically, density (chapter 2), aging or degradation processes (chapter 4). We also investigate how MP size (chapter 3) influence transport as this is thought to be a significant characteristic controlling MP transportation processes.

The relatively light density of MPs was found to be a distinguishing characteristic influencing the magnitude and rate of transport in both splash erosion and surface runoff. In chapter 2, direct comparisons between the transport of MPs with densities ranging from 0.92-1.19 g cm^{-3} and sand particles with a density of 2.65 g cm^{-3} , found MPs were transported from the soil surface more rapidly than sand particles both prior to and following the onset of surface runoff. Similar research has found that MP transport in flows of water is akin to particulate organic carbon, which have similar densities to MPs (Hoellein *et al.*, 2019; Rehm *et al.*, 2021). This research along with the research in chapter 2 show differences in density is a driving factor of MPs preferential transport in surface runoff as compared to mineral soil particles.

In chapter 2, small differences in density between MPs of the same morphology and size (PMMA = 1.19 g cm^{-3} , PS = 1.05 g cm^{-3}) showed no statistical difference between the rates of transport from the soil surfaces nor in the number of particles transported in splash erosion or surface runoff. This finding challenges the assumption that slight differences in density between MPs can make an impact on transport rates in rainfall-induced erosion (Nizzetto *et al.*, 2016a). The hydrophobic nature of MPs might also impact their buoyancy, which could reduce the influence that small differences in densities between MPs have on their movement in surface runoff and splash erosion.

In chapter 4, we endeavoured to understand the differences in transportation in surface runoff between aged MPs and pristine MPs. Aged MPs typically have increased surface roughness, alterations to polymer surface chemistry, and decreased hydrophobicity (Du *et al.*, 2023; Liu *et al.*, 2019b). These characteristics have been shown to influence the vertical transportation of MPs in soil columns but it has not been tested in surface runoff (Li *et al.*, 2024b; Liu *et al.*, 2019a). Of particular interest was how the decreased hydrophobicity may influence MP transport as hydrophobicity is a distinguishing characteristic between MPs and soil particles.

Other research investigating soil erosion has found hydrophobic soil particles to be more mobile than hydrophilic soil particles (Ahn *et al.*, 2013; Terry and Shakesby, 1993). As MPs are generally hydrophobic this could mean MPs are more influenced by surface runoff compared to soil particles which are typically hydrophilic. Due to the aging processes being ineffective on the MP polymers used in this research we were unable to corroborate our hypothesis. Together, density and hydrophobicity are distinct characteristics of MPs which could explain the differences in transport between MPs and natural soil particles.

In chapter 3, size was not statistically found to influence the number of MPs which were transported in surface runoff, between MPs sized 125-150 μm and 425-500 μm . Of the MPs that were initially inputted into the soil, 19% of MPs sized 125-150 μm and 20% for MPs sized 425-500 μm were transported in surface runoff. Other research has found substantial differences in the number of MPs transported in surface runoff of different sizes as shown in Table 5.1. Whilst research to date reports a mixed influence of particle size on MP transport in surface runoff, it seems clear that MPs <1 mm are more likely to be transported than MPs > 1mm in surface runoff.

Table 5.1 Synthesis of research along with results from this thesis showing influence of size on the transport of microplastics (MPs) in surface runoff. Coloured cells indicate the size fraction which were transported in the greatest numbers in surface runoff.

Author	Microplastic Size 1	Microplastic Size 2	Microplastic Size 3	Notes
Chapter 3	125-150 μm	425-500 μm	-	No statistical difference between the two sizes but slightly more 425-500 μm were transported in surface runoff.
Han <i>et al.</i> (2022)	250 μm	1 mm	-	Plastics sized 4 mm, 15 mm and 50 mm, were also studied but no plastics > 4 mm were transported in surface runoff.
Rehm <i>et al.</i> (2021)	53-100 μm	250-300 μm	-	No statistical difference between the two sizes but more 250-300 μm were found in surface runoff
Zhang <i>et al.</i> (2022)	< 0.3 mm	0.3-1 mm	1-5 mm	

For the vertical transport, results from chapter 3 found MPs of all sizes (53-63 μm , 125-150 μm and 425-500 μm) were detected down to 8 cm, though 425-500 μm were found in greater numbers per kg^{-1} than the other two size ranges in every soil depth layer. These results along with current research show that vertical transport of small MPs in soils in response to rainfall or irrigation don't necessarily preferentially transport further in the soil compared to MPs of a larger size (Table 5.2). This contrasts research in laboratory column experiments where, as

MP size decreases the depth MPs are transported increases (Li *et al.*, 2024a; O'Connor *et al.*, 2019; Qi *et al.*, 2022; Ranjan *et al.*, 2023). However, these studies often use sand particles, sediment or glass beads which have a homogeneous size and shape, while research in Table 5.2 was conducted in natural soils as well as having water applied to the soils as raindrops. Natural soils having a range of chemical properties, amounts of organic matter and large ranges of soil particle sizes may facilitate electrostatic interactions between small MPs and soil and thereby reduce smaller MPs from vertical transport (Lu *et al.*, 2021a, 2021b; Li *et al.*, 2020; Wu *et al.*, 2020).

Table 5.2 Synthesis of research along with results from this thesis showing influence of size on the vertical transport of microplastics (MPs) from the soil surface with the impact of raindrops. Coloured cells indicate the size fraction which were transported furthest into the soil.

Author	Microplastic Size 1	Microplastic Size 2	Microplastic Size 3	Notes
Chapter 3	53-63 μm	125-150 μm	425-500 μm	Field-scale experiment with rainfall simulation. Microplastics of all sizes were detected down to 8 cm.
Du <i>et al.</i> (2024)	0-25 μm	25-147 μm	147-250 μm	Column experiments with soil. Irrigation with raindrops was used.
Rehm <i>et al.</i> (2021)	53-100 μm	250-300 μm	-	Field-scale experiment reporting microplastics vertical migration due to natural rainfall over 1.5 years.
Zhang <i>et al.</i> (2022)	< 0.3 mm	0.3-1 mm	1-5 mm	Laboratory rainfall simulations experiments.

5.3 Dynamic understanding of microplastic transport during rainfall events

Throughout this thesis, the movement of MPs on the soil surface was tracked using UV photography, unlocking valuable insights and more holistic understanding into MP transport pathways during rainfall-induced erosion. This includes gaining insight into the rates of change for MPs on the soil surface as well as the location MPs were transported to. This information was used to understand the pathways MPs follow for example, splash erosion transporting MPs outside of soil boxes.

Comparing the number of MP particles on the soil surface with the onset of surface runoff and the number of particles transported by splash erosion provided understanding for the fate of MPs throughout the rainfall simulation. For example, in chapters 2, 3 and 4 images of the soil surface through time showed substantial disappearances of MPs prior to surface runoff. Experimental evidence in chapters 2 and 3 indicate that the decreases were not due to splash erosion processes transporting MPs outside of the soil boxes and plots but rather mixing with the soil which resulted in burial of the MPs. This thesis showed that during rainfall-induced

erosion the relatively light density of MPs did not lead to rapid transport down the soil slope in surface runoff. Instead, their movement involved a more complex process including MPs “hopping” due to splash erosion, being buried then uncovered, vertically moving through the soil by infiltration, and floating down the soil slope in surface runoff (Figure 5.2). Chapter 2 showed that sand particles also had this complex transport process but the images of the soil surface indicate that the transport was slower compared to MPs.

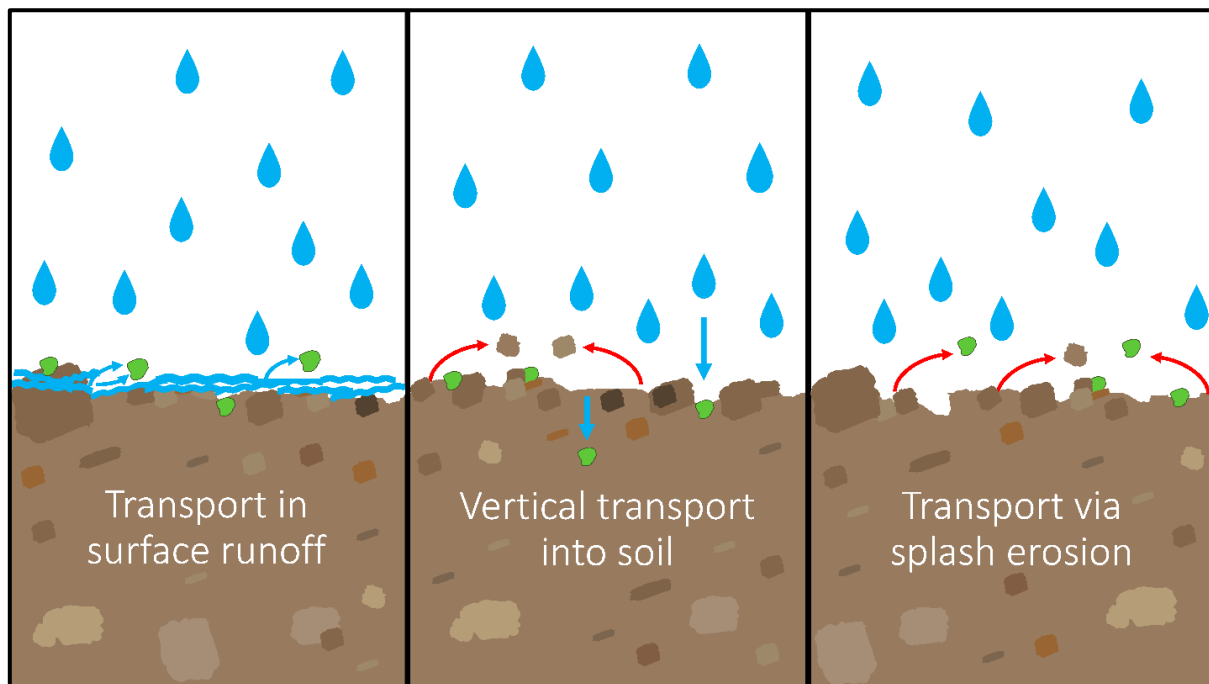


Figure 5.2. Conceptual diagram showing microplastics (green particles) the complexity of transport during a rainfall-induced erosion event. The three transport pathways are shown in detail: surface runoff, vertical transport into the soil and splash erosion.

5.4 Reducing microplastic transport from agricultural soils

This thesis showed that the transport of MPs in rainfall-induced erosion is complex. Microplastic transport during rainfall-induced erosion is not limited to surface runoff, but splash erosion and vertical transport into the soil are substantial processes governing MP movement. Therefore, while surface runoff from agricultural soils undeniably contributes MPs to aquatic ecosystems, soils also exhibit a high capacity to retain MPs as a sink (Rehm and Fiener, 2024).

Understanding MP transport is important not only to help provide accurate estimates of the magnitude of MPs transported from terrestrial to aquatic ecosystems, but also aid in devising effective strategies to mitigate this transport. The research in this thesis confirms that MPs

have different transport behaviour compared to mineral soil particle transport in rainfall-induced erosion, which poses the question: Will current soil erosion mitigation strategies also work for MPs?

There is some evidence that interventions to reduce soil erosion also reduce MP export, for example increasing vegetation density on soil (Forster *et al.*, 2023; Han *et al.*, 2022). However, Han *et al.* (2022) showed that the number of MPs transported were dependent on MP size, MP morphology, as well as vegetation type. In their research, the presence of vegetation on the soil impeded the movement of large MPs and similar to soil erosion research grassy vegetation was found to inhibit the transport of MPs in surface runoff (Han *et al.*, 2022; Martinez-Mena *et al.*, 2000).

Another mitigation strategy to reduce MP export from agricultural soils is to manage soils to foster soil aggregation. Results from chapter 4 found that when 1-3% of MPs were bound in soil aggregates there was no difference in the number of MPs transported in surface runoff compared to soil with no MPs bound to aggregates. However, previous research has found that when more than 40% of MPs are incorporated into soil aggregates smaller amounts of MPs are transported from soils in surface runoff (Rehm *et al.*, 2021). This research indicates increased levels of MPs bound to soil aggregates likely reduce MP mobility in surface runoff. Therefore practices which increase aggregation such as reduced tillage and increasing soil carbon are encouraged to reduce MP transport to freshwater ecosystems by surface runoff (Bronick and Lal, 2005; Panagea *et al.*, 2022).

5.5 Future Research

This thesis has advanced understanding of MP transport in rainfall-induced erosion events and provided experimental evidence which is severely lacking in this area of research. Throughout this thesis opportunities for future research are recommended, a summary of which are outlined below:

1. **Microplastic chemical properties influence on transport-** Chapter 2 found that MP particles were transported at faster rates from the soil surface as compared to sand, a proxy for natural soil. While density is a major factor driving these differences in transport, future research should also explore how other physio-chemical differences (e.g. hydrophobicity, plasticity) between soil particles and MPs influence transport processes.

2. **Further understanding size on microplastic transport-** Chapter 3 found that there were no preferential transport pathways between MPs sized 125-150 μm and 425-500 μm . Further research is needed to understand the influence of size in the likelihood of MP mobilization and transport in surface runoff; as well as research investigating the vertical movement of MPs in natural soils. In particular, future research should be conducted with multiple size ranges of MPs focusing on sizes less than 1 mm.
3. **Impact of microplastic age on transport in surface runoff** - In chapter 4, we hypothesized that aged MPs would be transported less than pristine MPs. Though because the aging process used in our research was ineffective, we were unable to corroborate the hypothesis. Future research should further test the hypothesis we outlined in chapter 4 to fill this critical gap in our knowledge of MP transport.

These suggested research directions explore the unique properties of MPs which differentiate their transportation from other pollutants in agricultural soils. As a particulate, insoluble contaminate MP could be inhibited in their transport by management practices which have been shown to reduce other solid pollutants such as sediment or particulate nutrients. However, their low density, hydrophobic properties, slow degradation rates, and diverse size ranges present unique challenges in limiting MP transport to aquatic ecosystems in surface runoff processes, highlighting the need for future research on these properties.

Overall, despite growing research on MPs in terrestrial environments significant knowledge gaps remain especially regarding MPs impact on soil health, as well as its transport and retention in agricultural soils. Early research suggests that soils with low or environmentally relevant concentrations, MPs have minimal effect on soil properties (Špela *et al.*, 2025; Yu *et al.*, 2023). However, at high concentrations negative impacts on soil properties have been observed (de Souza Machado *et al.*, 2018; Ingrassia *et al.*, 2022; Špela *et al.*, 2025). Extensive research has demonstrated that MPs negatively affect aquatic biota (Cole *et al.*, 2015; Palmer and Herat, 2021; Vázquez and Rahman, 2021). These risks coupled with the potential threats MPs may pose to human health (Bastyans *et al.*, 2022; Jenner *et al.*, 2022; Prata *et al.*, 2020; Yan *et al.*, 2022) should drive personal, community and governmental action to reduce plastic consumption, remediate polluted environments and develop sustainable alternatives to conventional plastics.

6. References

- Ahn, S. et al. (2013) Effects of hydrophobicity on splash erosion of model soil particles by a single water drop impact. *Earth Surface Processes and Landforms*, 38(11), 1225–1233. Wiley Online Library.
- Ainali, N.M. et al. (2021) Aging effects on low- and high-density polyethylene, polypropylene and polystyrene under UV irradiation: An insight into decomposition mechanism by Py-GC/MS for microplastic analysis. *Journal of Analytical and Applied Pyrolysis*, 158, 105207.
- Allen, R.F. (1988) The mechanics of splashing. *Journal of Colloid and Interface Science*, 124(1), 309–316.
- Allen, S. et al. (2019) Atmospheric transport and deposition of microplastics in a remote mountain catchment. *Nature Geoscience*, 12(5), 339–344.
- Álvarez-Lopezello, J. et al. (2021) Microplastic pollution in neotropical rainforest, savanna, pine plantations, and pasture soils in lowland areas of Oaxaca, Mexico: Preliminary results. *Ecological Indicators*, 121, 107084.
- Alves Sobrinho, T. et al. (2008) A portable integrated rainfall and overland flow simulator. *Soil Use and Management*, 24(2), 163–170. Wiley Online Library.
- Amaya, D.P.T. (2023) *Distribution of pristine and aged microplastics in soil aggregate fractions*. Masters Thesis. Ghent University. Available at: https://libstore.ugent.be/fulltxt/RUG01/003/151/975/RUG01-003151975_2023_0001_AC.pdf
- Andrady, A.L. et al. (2022) Oxidation and fragmentation of plastics in a changing environment; from UV-radiation to biological degradation. *Science of The Total Environment*, 851, 158022.
- Andrady, A.L. & Neal, M.A. (2009) Applications and societal benefits of plastics. *Philosophical Transactions of the Royal Society B: Biological Sciences*, 364(1526), 1977–1984. The Royal Society Publishing.
- Bank, M.S. & Hansson, S.V. (2019) The Plastic Cycle: A Novel and Holistic Paradigm for the Anthropocene. *Environmental Science & Technology*, 53(13), 7177–7179. American Chemical Society.
- Bastyans, S. et al. (2022) Micro and nano-plastics, a threat to human health? *Emerging Topics in Life Sciences*, 6(4), 411–422.
- Beczek, M. et al. (2018) Application of X-ray computed microtomography to soil craters formed by raindrop splash. *Geomorphology*, 303, 357–361.
- Beguiría, S. et al. (2015) Detachment of soil organic carbon by rainfall splash: Experimental assessment on three agricultural soils of Spain. *Geoderma*, 245–246, 21–30.
- Beltrán-Sanahuja, A. et al. (2021) Degradation of conventional and biobased plastics in soil under contrasting environmental conditions. *Science of The Total Environment*, 787, 147678.

- van den Berg, P. et al. (2020) Sewage sludge application as a vehicle for microplastics in eastern Spanish agricultural soils. *Environmental Pollution*, 261, 114198. Elsevier.
- Bergmann, M. et al. (2017) Citizen scientists reveal: Marine litter pollutes Arctic beaches and affects wild life. *Marine Pollution Bulletin*, 125(1), 535–540.
- Bergmann, M. et al. (2019) White and wonderful? Microplastics prevail in snow from the Alps to the Arctic. *Science advances*, 5(8), eaax1157. American Association for the Advancement of Science.
- Binda, G. et al. (2024) Microplastic aging processes: Environmental relevance and analytical implications. *TrAC Trends in Analytical Chemistry*, 172, 117566.
- Blake, G.R. (2008) Particle density. In: Chesworth, W. (ed.) *Encyclopedia of Soil Science*. [Online]. Dordrecht: Springer Netherlands. Available at: doi:10.1007/978-1-4020-3995-9_406
- Bläsing, M. & Amelung, W. (2018) Plastics in soil: Analytical methods and possible sources. *Science of the total environment*, 612, 422–435. Elsevier.
- Blenkinsop, S. et al. (2017) Quality-control of an hourly rainfall dataset and climatology of extremes for the UK. *International Journal of Climatology*, 37(2), 722. Wiley.
- Boumaiza, L. et al. (2023) Vadose zone water stable isotope profiles for assessing groundwater recharge: Sensitivity to seasonal soil sampling. *Journal of Hydrology*, 626, 130291.
- Bowers, C.M. & Johansen, R.J. (2002) Photographic evidence protocol: the use of digital imaging methods to rectify angular distortion and create life size reproductions of bite mark evidence. *Journal of forensic sciences*, 47(1), 178–185. ASTM International.
- Brahney, J. et al. (2020) Plastic rain in protected areas of the United States. *Science*, 368(6496), 1257–1260. American Association for the Advancement of Science.
- Brahney, J. et al. (2021) Constraining the atmospheric limb of the plastic cycle. *Proceedings of the National Academy of Sciences*, 118(16), e2020719118. Proceedings of the National Academy of Sciences.
- Brandes, E. et al. (2021) Identifying hot-spots for microplastic contamination in agricultural soils—a spatial modelling approach for Germany. *Environmental Research Letters*, 16(10), 104041. IOP Publishing.
- Braun, M. et al. (2023) Microplastic contamination of soil: Are input pathways by compost overridden by littering? *Science of The Total Environment*, 855, 158889.
- Brodowski, R. (2010) The influence of water layer depth on the loess soil detachability by rainfall. *Acta Agroph.*, 16(2), 255–261.
- Bronick, C.J. & Lal, R. (2005) Soil structure and management: a review. *Geoderma*, 124(1), 3–22.

- Büks, F. & Kaupenjohann, M. (2020) Global concentrations of microplastics in soils—a review. *Soil*, 6(2), 649–662. Copernicus GmbH.
- Bullard, J.E. et al. (2021) Preferential transport of microplastics by wind. *Atmospheric Environment*, 245, 118038.
- Caldwell, J. et al. (2021) Fluorescent plastic nanoparticles to track their interaction and fate in physiological environments. *Environmental Science: Nano*, 8(2), 502–513. Royal Society of Chemistry.
- Cao, L. et al. (2021) Occurrence, distribution and affecting factors of microplastics in agricultural soils along the lower reaches of Yangtze River, China. *Science of The Total Environment*, 794, 148694.
- Chamas, A. et al. (2020) Degradation Rates of Plastics in the Environment. *ACS Sustainable Chemistry & Engineering*, 8(9), 3494–3511. American Chemical Society.
- Chen, K. et al. (2023) Long-term aged fibrous polypropylene microplastics promotes nitrous oxide, carbon dioxide, and methane emissions from a coastal wetland soil. *Science of The Total Environment*, 896, 166332.
- Chen, Y. et al. (2020) Microplastic pollution in vegetable farmlands of suburb Wuhan, central China. *Environmental Pollution*, 257, 113449.
- Christiansen, J.E. (1942) *Irrigation by sprinkling*. [Online]. University of California Berkeley. Available at: https://brittlebooks.library.illinois.edu/brittlebooks_closed/Books2009-04/chrije0001irrspr/chrije0001irrspr.pdf
- Cole, M. et al. (2015) The Impact of Polystyrene Microplastics on Feeding, Function and Fecundity in the Marine Copepod *Calanus helgolandicus*. *Environmental Science & Technology*, 49(2), 1130–1137. American Chemical Society.
- Collins, K.S. & Gazley, M.F. (2017) Does my posterior look big in this? The effect of photographic distortion on morphometric analyses. *Paleobiology*, 43(3), 508–520. GeoScienceWorld.
- Corradini, F. et al. (2019) Evidence of microplastic accumulation in agricultural soils from sewage sludge disposal. *Science of the total environment*, 671, 411–420. Elsevier.
- Corradini, F. et al. (2021) Microplastics occurrence and frequency in soils under different land uses on a regional scale. *Science of the Total Environment*, 752, 141917. Elsevier.
- Cottom, J.W. et al. (2024) A local-to-global emissions inventory of macroplastic pollution. *Nature*, 633(8028), 101–108.
- Cramer, A. et al. (2022) Microplastic induces soil water repellency and limits capillary flow. *Vadose Zone Journal*, n/a(n/a), e20215. John Wiley & Sons, Ltd.
- Cromey, D.W. (2010) Avoiding Twisted Pixels: Ethical Guidelines for the Appropriate Use and Manipulation of Scientific Digital Images. *Science and Engineering Ethics*, 16(4), 639–667.

Crossman, J. et al. (2020) Transfer and transport of microplastics from biosolids to agricultural soils and the wider environment. *Science of the Total Environment*, 724, 138334. Elsevier.

Cusworth, S.J. et al. (2022) Sustainable production of healthy, affordable food in the UK: The pros and cons of plasticulture. *Food and Energy Security*, n/a(n/a), e404. John Wiley & Sons, Ltd.

Cusworth, S.J. et al. (2024) A nationwide assessment of microplastic abundance in agricultural soils: The influence of plastic crop covers within the United Kingdom. *PLANTS, PEOPLE, PLANET*, 6(2), 304–314. John Wiley & Sons, Ltd.

Dong, S. et al. (2021) Transport characteristics of fragmental polyethylene glycol terephthalate (PET) microplastics in porous media under various chemical conditions. *Chemosphere*, 276, 130214.

Du, A. et al. (2024) Experimental Study on the Migration and Distribution of Microplastics in Desert Farmland Soil Under Drip Irrigation. *Environmental Toxicology and Chemistry*, 43(6), 1250–1259. John Wiley & Sons, Ltd.

Du, T. et al. (2023) Aging of Nanoplastics Significantly Affects Protein Corona Composition Thus Enhancing Macrophage Uptake. *Environmental Science & Technology*, 57(8), 3206–3217. American Chemical Society.

Edwards, C.-C. et al. (2023) Microplastic ingestion perturbs the microbiome of *Aedes albopictus* (Diptera: Culicidae) and *Aedes aegypti*. *Journal of Medical Entomology*, 60(5), 884–898.

Ehlers, S.M. et al. (2020) Low-cost microplastic visualization in feeding experiments using an ultraviolet light-emitting flashlight. *Ecological Research*, 35(1), 265–273.

Ekwue, E.I. et al. (1993) Effects of incorporating two organic materials at varying levels on splash detachment of some soils from Borno state, Nigeria. *Earth Surface Processes and Landforms*, 18(5), 399–406. John Wiley & Sons, Ltd.

Ellison, W. (1948) Soil detachment by water in erosion processes. *Eos, Transactions American Geophysical Union*, 29(4), 499–502. Wiley Online Library.

Ellison, W.D. (1950) Soil Erosion by Rainstorms. *Science*, 111(2880), 245–249. American Association for the Advancement of Science.

Esders, E.M. et al. (2023) Is transport of microplastics different from mineral particles? Idealized wind tunnel studies on polyethylene microspheres. *Atmos. Chem. Phys.*, 23(24), 15835–15851. Copernicus Publications.

FAO (2021) *Assessment of agricultural plastics and their sustainability: A call for action*. 160. Rome, Italy. Available at: <https://doi.org/10.4060/cb7856en>

Fernández-Raga, M. et al. (2017) Splash erosion: A review with unanswered questions. *Earth-Science Reviews*, 171, 463–477.

- Feuilloley, P. et al. (2005) Degradation of polyethylene designed for agricultural purposes. *Journal of Polymers and the Environment*, 13(4), 349–355. Springer.
- Forster, N.A. et al. (2023) Microplastic surface retention and mobility on hiking trails. *Environmental Science and Pollution Research*, 30(16), 46368–46382.
- Geyer, R. et al. (2017) Production, use, and fate of all plastics ever made. *Science advances*, 3(7), e1700782. American Association for the Advancement of Science.
- Gonzalez, R.C. & Woods, R.E. (2008) *Digital image processing*. 3rd ed. Upper Saddle River, N.J.: Pearson/Prentice Hall.
- Guzmán, G. et al. (2010) Evaluation of magnetic iron oxides as sediment tracers in water erosion experiments. *CATENA*, 82(2), 126–133.
- Guzmán, G. et al. (2013) Sediment tracers in water erosion studies: current approaches and challenges. *Journal of Soils and Sediments*, 13(4), 816–833.
- Hadad, D. et al. (2005) Biodegradation of polyethylene by the thermophilic bacterium *Brevibacillus borstelensis*. *Journal of Applied Microbiology*, 98(5), 1093–1100.
- Han, N. et al. (2022) Horizontal transport of macro- and microplastics on soil surface by rainfall induced surface runoff as affected by vegetations. *Science of The Total Environment*, 831, 154989.
- Han, N. et al. (2023) Threshold migration conditions of (micro) plastics under the action of overland flow. *Water Research*, 242, 120253.
- Hand, W.H. et al. (2004) A study of twentieth-century extreme rainfall events in the United Kingdom with implications for forecasting. *Meteorological Applications*, 11(1), 15–31. Cambridge University Press.
- Hardy, R.A. et al. (2016) A novel fluorescent tracer for real-time tracing of clay transport over soil surfaces. *CATENA*, 141, 39–45.
- Hardy, R.A. et al. (2017) Using real time particle tracking to understand soil particle movements during rainfall events. *CATENA*, 150, 32–38. Elsevier.
- He, Z. et al. (2014) Soil erosion and pollutant transport during rainfall-runoff processes. *Water resources*, 41, 604–611. Springer.
- Heerey, L. et al. (2023) Export pathways of biosolid derived microplastics in soil systems – Findings from a temperate maritime climate. *Science of The Total Environment*, 888, 164028.
- Heinze, W.M. et al. (2021) Nanoplastic Transport in Soil via Bioturbation by *Lumbricus terrestris*. *Environmental Science & Technology*, 55(24), 16423–16433. American Chemical Society.
- Heinze, W.M. et al. (2024) Vertical distribution of microplastics in an agricultural soil after long-term treatment with sewage sludge and mineral fertiliser. *Environmental Pollution*, 356, 124343.

Hochmuth, G. (2017) 5 - Drip Irrigation. In: Orzolek, M.D. (ed.) *A Guide to the Manufacture, Performance, and Potential of Plastics in Agriculture*. [Online]. Elsevier. Available at: doi:10.1016/B978-0-08-102170-5.00005-1

Hoellein, T.J. et al. (2019) Microplastic deposition velocity in streams follows patterns for naturally occurring allochthonous particles. *Scientific Reports*, 9(1), 1–11. Nature Publishing Group.

Horton, A.A. et al. (2017) Large microplastic particles in sediments of tributaries of the River Thames, UK – Abundance, sources and methods for effective quantification. *Marine Pollution Bulletin*, 114(1), 218–226.

Horton, A.A. & Dixon, S.J. (2018) Microplastics: An introduction to environmental transport processes. *WIREs Water*, 5(2), e1268. John Wiley & Sons, Ltd.

Huang, Y. et al. (2020) Agricultural plastic mulching as a source of microplastics in the terrestrial environment. *Environmental Pollution*, 260, 114096.

Huerta Lwanga, E. et al. (2017) Incorporation of microplastics from litter into burrows of *Lumbricus terrestris*. *Environmental Pollution*, 220, 523–531.

Hurley, R.R. & Nizzetto, L. (2018) Fate and occurrence of micro (nano) plastics in soils: Knowledge gaps and possible risks. *Current Opinion in Environmental Science & Health*, 1, 6–11. Elsevier.

Ingraffia, R. et al. (2022) Polyester microplastic fibers in soil increase nitrogen loss via leaching and decrease plant biomass production and N uptake. *Environmental Research Letters*. IOP Publishing.

Jenner, L.C. et al. (2022) Detection of microplastics in human lung tissue using μ FTIR spectroscopy. *Science of The Total Environment*, 831, 154907.

Jeřábek, J. et al. (2022) Soil surface connectivity of tilled soil with wheel tracks and its development under simulated rainfall. *Journal of Hydrology*, 613, 128322.

Kasirajan, S. & Ngouajio, M. (2012) Polyethylene and biodegradable mulches for agricultural applications: a review. *Agronomy for Sustainable Development*, 32(2), 501–529.

Kavka, P. & Neumann, M. (2021) Swinging-pulse sprinkling head for rain simulators. *Hydrology*, 8(2), 74. MDPI.

Kedzierski, M. et al. (2023) Continents of plastics: An estimate of the stock of microplastics in agricultural soils. *Science of The Total Environment*, 880, 163294.

Killick, R. & Eckley, I.A. (2014) changepoint: An R Package for Changepoint Analysis. *Journal of Statistical Software*, 58(3), 1–19.

Kinnell, P.I.A. (2005) Raindrop-impact-induced erosion processes and prediction: a review. *Hydrological Processes*, 19(14), 2815–2844. John Wiley & Sons, Ltd.

- Kinnell, P.I.A. (2009) The influence of raindrop induced saltation on particle size distributions in sediment discharged by rain-impacted flow on planar surfaces. *CATENA*, 78(1), 2–11.
- Klaus, J. et al. (2024) Microplastics in vineyard soils: First insights from plastic-intensive viticulture systems. *Science of The Total Environment*, 947, 174699.
- Koch, T. et al. (2024) A review of the characteristics of rainfall simulators in soil erosion research studies. *MethodsX*, 12, 102506. Elsevier.
- Koelmans, A.A. et al. (2019) Microplastics in freshwaters and drinking water: Critical review and assessment of data quality. *Water Research*, 155, 410–422.
- Kooi, M. & Koelmans, A.A. (2019) Simplifying Microplastic via Continuous Probability Distributions for Size, Shape, and Density. *Environmental Science & Technology Letters*, 6(9), 551–557. American Chemical Society.
- Kosuth, M. et al. (2018) Anthropogenic contamination of tap water, beer, and sea salt. *PLOS ONE*, 13(4), e0194970. Public Library of Science.
- Kreuger, J. (1998) Pesticides in stream water within an agricultural catchment in southern Sweden, 1990–1996. *Science of The Total Environment*, 216(3), 227–251.
- Laburda, T. et al. (2021) SfM-MVS Photogrammetry for Splash Erosion Monitoring under Natural Rainfall. *Earth Surface Processes and Landforms*, 46(5), 1067–1082. Wiley Online Library.
- Laermans, H. et al. (2021) Tracing the horizontal transport of microplastics on rough surfaces. *Microplastics and Nanoplastics*, 1(1), 1–12. SpringerOpen.
- Lamont, W.J. (2017) 3 - Plastic Mulches for the Production of Vegetable Crops. In: Orzolek, M.D. (ed.) *A Guide to the Manufacture, Performance, and Potential of Plastics in Agriculture*. [Online]. Elsevier. Available at: doi:10.1016/B978-0-08-102170-5.00003-8
- Legout, C. et al. (2005) Splash distance and size distributions for various soils. *Geoderma*, 124(3), 279–292.
- Legu dois, S. et al. (2005) Splash projection distance for aggregated soils: theory and experiment. *Soil Science Society of America Journal*, 69(1), 30–37. Wiley Online Library.
- Lehmann, A. et al. (2019) Abiotic and Biotic Factors Influencing the Effect of Microplastic on Soil Aggregation. *SOIL SYSTEMS*, 3(1).
- Lehmann, A. et al. (2021a) Microplastics have shape- and polymer-dependent effects on soil aggregation and organic matter loss – an experimental and meta-analytical approach. *Microplastics and Nanoplastics*, 1(1), 7.
- Lehmann, M. et al. (2021b) Ejection of marine microplastics by raindrops: a computational and experimental study. *Microplastics and Nanoplastics*, 1(1), 18.
- Li, M. et al. (2020) Different surface charged plastic particles have different cotransport behaviors with kaolinite ☆particles in porous media. *Environmental Pollution*, 267, 115534.

- Li, S. et al. (2022a) Macro-and microplastic accumulation in soil after 32 years of plastic film mulching. *Environmental Pollution*, 118945. Elsevier.
- Li, T. et al. (2022b) Effects of prescribed fire on topsoil properties: a small-scale straw burning experiment. *Journal of Hydrology and Hydromechanics*, 70(4), 450–461.
- Li, W. et al. (2024a) Experimental and simulated microplastics transport in saturated natural sediments: Impact of grain size and particle size. *Journal of Hazardous Materials*, 468, 133772.
- Li, X. et al. (2024b) Aging microplastics and coupling of “microplastic-electric fields” can affect soil water-stable aggregates’ stability. *Journal of Hazardous Materials*, 469, 134048.
- Liang, Y. et al. (2021) Effects of Microplastic Fibers on Soil Aggregation and Enzyme Activities Are Organic Matter Dependent. *Frontiers in Environmental Science*, 9, 97.
- Liu, J. et al. (2019a) Aging Significantly Affects Mobility and Contaminant-Mobilizing Ability of Nanoplastics in Saturated Loamy Sand. *Environmental Science & Technology*, 53(10), 5805–5815. American Chemical Society.
- Liu, P. et al. (2019b) New Insights into the Aging Behavior of Microplastics Accelerated by Advanced Oxidation Processes. *Environmental Science & Technology*, 53(7), 3579–3588. American Chemical Society.
- Liu, Y. et al. (2021) Transport and transformation of microplastics and nanoplastics in the soil environment: A critical review. *Soil Use and Management*, 37(2), 224–242. John Wiley & Sons, Ltd.
- Lu, T. et al. (2021a) Effects of clay minerals on the transport of nanoplastics through water-saturated porous media. *Science of The Total Environment*, 796, 148982.
- Lu, T. et al. (2021b) Relevance of Iron Oxyhydroxide and Pore Water Chemistry on the Mobility of Nanoplastic Particles in Water-Saturated Porous Media Environments. *Water, Air, & Soil Pollution*, 232(5), 168.
- Lwanga, E.H. et al. (2022a) Microplastic appraisal of soil, water, ditch sediment and airborne dust: The case of agricultural systems. *Environmental Pollution*, 120513.
- Lwanga, E.H. et al. (2022b) Review of microplastic sources, transport pathways and correlations with other soil stressors: a journey from agricultural sites into the environment. *Chemical and Biological Technologies in Agriculture*, 9(1), 20.
- Maqbool, A. et al. (2023) Macro- and micro-plastics change soil physical properties: a systematic review. *Environmental Research Letters*, 18(12), 123002. IOP Publishing.
- Maqbool, A. et al. (2024) Tracing macroplastics redistribution and fragmentation by tillage translocation. *Journal of Hazardous Materials*, 477, 135318.
- Martinez-Mena, M. et al. (2000) Influence of vegetal cover on sediment particle size distribution in natural rainfall conditions in a semiarid environment. *CATENA*, 38(3), 175–190.

- McCord, C.P. (1964) Celluloid: The First American Plastic—The World’s First Commercially Successful Plastic. *Journal of Occupational and Environmental Medicine*, 6(11).
- Mitrano, D.M. et al. (2019) Synthesis of metal-doped nanoplastics and their utility to investigate fate and behaviour in complex environmental systems. *Nature Nanotechnology*, 14(4), 362–368.
- Moeck, C. et al. (2022) Microplastics and nanoplastics in agriculture—A potential source of soil and groundwater contamination? *Grundwasser*, 28, 23–35.
- Möller, J.N. et al. (2020) Finding microplastics in soils: a review of analytical methods. *Environmental science & technology*, 54(4), 2078–2090. ACS Publications.
- Morgan, R.P.C. (1977) Soil erosion in the United Kingdom: field studies in the Silsoe area, 1973-75. *Occasional Paper. National College of Agricultural Engineering (UK). no. 4.*
- Morgan, R.P.C. (2009) *Soil erosion and conservation*. John Wiley & Sons.
- Mouzai, L. & Bouhadef, M. (2003) Water drop erosivity: Effects on soil splash. *Journal of Hydraulic Research*, 41(1), 61–68. Taylor & Francis.
- Munhoz, D.R. et al. (2024) Exploring the potential of earthworm gut bacteria for plastic degradation. *Science of The Total Environment*, 927, 172175.
- Mutchler, C. et al. (1994) Laboratory and field plots for erosion research. In: Soil and Water Conservation Society Ankeny, IA. *Soil erosion research methods*. Soil and Water Conservation Society Ankeny, IA.
- Nakatani, H. et al. (2022) Degradation and fragmentation behavior of polypropylene and polystyrene in water. *Scientific Reports*, 12(1), 18501.
- Neumann, M. et al. (2022) Effect of plot size and precipitation magnitudes on the activation of soil erosion processes using simulated rainfall experiments in vineyards. *Frontiers in Environmental Science*, 10, 949774. Frontiers.
- Nizzetto, L. et al. (2016a) A theoretical assessment of microplastic transport in river catchments and their retention by soils and river sediments. *Environmental Science: Processes & Impacts*, 18(8), 1050–1059. Royal Society of Chemistry.
- Nizzetto, L. et al. (2016b) Are Agricultural Soils Dumps for Microplastics of Urban Origin? *Environmental Science & Technology*, 50(20), 10777–10779. American Chemical Society.
- Norling, M. et al. (2024) Retention efficiency for microplastic in a landscape estimated from empirically validated dynamic model predictions. *Journal of Hazardous Materials*, 464, 132993.
- Novara, A. et al. (2012) Effects of soil compaction, rain exposure and their interaction on soil carbon dioxide emission. *Earth Surface Processes and Landforms*, 37(9), 994–999. Wiley Online Library.
- Obbard, R.W. et al. (2014) Global warming releases microplastic legacy frozen in Arctic Sea ice. *Earth’s Future*, 2(6), 315–320. John Wiley & Sons, Ltd.

- O'Connor, D. et al. (2019) Microplastics undergo accelerated vertical migration in sand soil due to small size and wet-dry cycles. *Environmental Pollution*, 249, 527–534. Elsevier.
- Orzolek, M.D. (2017) 1 - Introduction. In: Orzolek, M.D. (ed.) *A Guide to the Manufacture, Performance, and Potential of Plastics in Agriculture*. [Online]. Elsevier. Available at: doi:10.1016/B978-0-08-102170-5.00001-4
- Palmer, J. & Herat, S. (2021) Ecotoxicity of Microplastic Pollutants to Marine Organisms: a Systematic Review. *Water, Air, & Soil Pollution*, 232(5), 195.
- Palmer, R. (1964) The influence of a thin water layer on waterdrop impact forces. *International Association of Scientific Hydrology Publication*.
- Panagea, I.S. et al. (2022) Impact of agricultural management on soil aggregates and associated organic carbon fractions: analysis of long-term experiments in Europe. *SOIL*, 8(2), 621–644. Copernicus Publications.
- Pereira, R. et al. (2021) *EIP-AGRI Focus Group Reducing the plastic footprint of agriculture FINAL REPORT*. European Commission. Available at: https://ec.europa.eu/eip/agriculture/sites/default/files/eip-agri_fg_plastic_footprint_final_report_2021_en.pdf
- Piehl, S. et al. (2018) Identification and quantification of macro-and microplastics on an agricultural farmland. *Scientific reports*, 8(1), 1–9. Nature Publishing Group.
- Plastics Europe (2024) *The Circular Economy for Plastics—A European Analysis*. Plastics Europe Brussels, Belgium.
- PlasticsEurope, E. (2019) Plastics—the facts 2019. An analysis of European plastics production, demand and waste data. *PlasticEurope* <https://www.plasticseurope.org/en/resources/publications/1804-plastics-facts-2019>.
- Prata, J.C. et al. (2020) Environmental exposure to microplastics: An overview on possible human health effects. *Science of The Total Environment*, 702, 134455.
- Pryce, O. (2011) *Development of environmental tracers for sediments and phosphorus*. PhD Thesis. Lancaster University (United Kingdom). Available at: <https://core.ac.uk/download/pdf/196591388.pdf>
- Qi, S. et al. (2022) Attachment and detachment of large microplastics in saturated porous media and its influencing factors. *Chemosphere*, 305, 135322.
- Quigley, E. et al. (2024) Pristine and UV-aged polyethylene microplastics' impact on gut microbiome and reproduction of earthworm *Eisenia andrei*. *European Journal of Soil Biology*, 122, 103640. Elsevier.
- R Core Team (2023) *R: A Language and Environment for Statistical Computing*. R Foundation for Statistical Computing. Available at: <https://www.R-project.org/>
- Ranjan, V.P. et al. (2023) Preliminary investigation on effects of size, polymer type, and surface behaviour on the vertical mobility of microplastics in a porous media. *Science of The Total Environment*, 864, 161148.

- Rehm, R. et al. (2021) Soil erosion as transport pathway of microplastic from agriculture soils to aquatic ecosystems. *Science of The Total Environment*, 148774. Elsevier.
- Rehm, R. & Fiener, P. (2024) Model-based analysis of erosion-induced microplastic delivery from arable land to the stream network of a mesoscale catchment. *SOIL*, 10(1), 211–230. Copernicus Publications.
- Rezaei, M. et al. (2019) Wind erosion as a driver for transport of light density microplastics. *Science of The Total Environment*, 669, 273–281. Elsevier.
- Rezaei, M. et al. (2022) Microplastics in agricultural soils from a semi-arid region and their transport by wind erosion. *Environmental Research*, 212, 113213.
- Rillig, M.C. (2012) Microplastic in terrestrial ecosystems and the soil? *Environmental Science & Technology*, 46(12). ACS Publications.
- Rillig, M.C. et al. (2017) Microplastic incorporation into soil in agroecosystems. *Frontiers in Plant Science*, 8, 1805. Frontiers.
- Ripley, H. (2023) *Maximising the effectiveness of soil erosion reducing cover crops through plant trait analysis*. [Online]. Lancaster University (United Kingdom). Available at: <https://doi.org/10.17635/lancaster/thesis/2060>
- Rodriguez, A.K. et al. (2020) Effect of UV-aging on the mechanical and fracture behavior of low density polyethylene. *Polymer Degradation and Stability*, 180, 109185.
- Sadeghi, S.H. et al. (2017) Variability of particle size distributions of upward/downward splashed materials in different rainfall intensities and slopes. *Geoderma*, 290, 100–106.
- Samandra, S. et al. (2022) Microplastic contamination of an unconfined groundwater aquifer in Victoria, Australia. *Science of The Total Environment*, 802, 149727.
- Sander, M. et al. (2019) Assessing the environmental transformation of nanoplastic through ¹³C-labelled polymers. *Nature Nanotechnology*, 14(4), 301–303.
- Sander, M. et al. (2024) Polymer Biodegradability 2.0: A Holistic View on Polymer Biodegradation in Natural and Engineered Environments. In: Künkel, A. et al. (eds.) *Synthetic Biodegradable and Biobased Polymers: Industrial Aspects and Technical Products*. [Online]. Cham: Springer International Publishing. Available at: doi:10.1007/12_2023_163
- Sarkar, A.K. et al. (2021) Engineered Polystyrene-Based Microplastics of High Environmental Relevance. *Environmental Science & Technology*, 55(15), 10491–10501. American Chemical Society.
- Scarascia-Mugnozza, G. et al. (2011) Plastic materials in European agriculture: actual use and perspectives. *Journal of Agricultural Engineering*, 42(3), 15–28.
- Schell, T. et al. (2022) Fate of microplastics in agricultural soils amended with sewage sludge: Is surface water runoff a relevant environmental pathway? *Environmental Pollution*, 293, 118520.

- Scherer, C. et al. (2020) Toxicity of microplastics and natural particles in the freshwater dipteran *Chironomus riparius*: Same same but different? *Science of The Total Environment*, 711, 134604.
- Scheurer, M. & Bigalke, M. (2018) Microplastics in Swiss Floodplain Soils. *Environmental Science & Technology*, 52(6), 3591–3598. American Chemical Society.
- Schöpfer, L. et al. (2022) Microplastics persist in an arable soil but do not affect soil microbial biomass, enzyme activities, and crop yield. *Journal of Plant Nutrition and Soil Science*. Wiley Online Library.
- Shi, J. et al. (2022) Microplastic presence significantly alters soil nitrogen transformation and decreases nitrogen bioavailability under contrasting temperatures. *Journal of Environmental Management*, 317, 115473.
- Sommer, F. et al. (2018) Tire abrasion as a major source of microplastics in the environment. *Aerosol and air quality research*, 18(8), 2014–2028. Taiwan Association for Aerosol Research.
- de Souza Machado, A.A. et al. (2018) Impacts of microplastics on the soil biophysical environment. *Environmental science & technology*, 52(17), 9656–9665. ACS Publications.
- Špela, Ž. et al. (2025) Soil water repellency of two disturbed soils contaminated with different agricultural microplastics tested under controlled laboratory conditions. *Geoderma*, 453, 117124.
- Stašek, J. et al. (2023) Using a Rainfall Simulator to Define the Effect of Soil Conservation Techniques on Soil Loss and Water Retention. *Land*, 12(2), 431. MDPI.
- Steinmetz, Z. et al. (2016) Plastic mulching in agriculture. Trading short-term agronomic benefits for long-term soil degradation? *Science of the total environment*, 550, 690–705. Elsevier.
- Strungaru, S.-A. et al. (2019) Micro- (nano) plastics in freshwater ecosystems: Abundance, toxicological impact and quantification methodology. *TrAC Trends in Analytical Chemistry*, 110, 116–128.
- Su, L. et al. (2022) Global transportation of plastics and microplastics: A critical review of pathways and influences. *Science of The Total Environment*, 831, 154884.
- Taipale, S.J. et al. (2019) Tracing the fate of microplastic carbon in the aquatic food web by compound-specific isotope analysis. *Scientific Reports*, 9(1), 19894.
- Tekman, M.B. et al. (2017) Marine litter on deep Arctic seafloor continues to increase and spreads to the North at the HAUSGARTEN observatory. *Deep Sea Research Part I: Oceanographic Research Papers*, 120, 88–99.
- Terry, J.P. & Shakesby, R.A. (1993) Soil hydrophobicity effects on rainsplash: simulated rainfall and photographic evidence. *Earth Surface Processes and Landforms*, 18(6), 519–525. Wiley Online Library.

- Thompson, R.C. et al. (2009) Our plastic age. *Philosophical Transactions of the Royal Society B: Biological Sciences*, 364(1526), 1973–1976. The Royal Society Publishing.
- Thompson, R.C. et al. (2024) Twenty years of microplastics pollution research—what have we learned? *Science*, 0(0). American Association for the Advancement of Science. [Accessed: 23 September 2024].
- Tian, X. et al. (2022) Plastic mulch film induced soil microplastic enrichment and its impact on wind-blown sand and dust. *Science of The Total Environment*, 813, 152490.
- Treilles, R. et al. (2021) Abundance, composition and fluxes of plastic debris and other macrolitter in urban runoff in a suburban catchment of Greater Paris. *Water Research*, 192, 116847.
- Ullah, R. et al. (2021) Microplastics interaction with terrestrial plants and their impacts on agriculture. *Journal of Environmental Quality*, 50(5), 1024–1041. John Wiley & Sons, Ltd.
- Umeh, O.R. et al. (2024) Groundwater systems under siege: The silent invasion of microplastics and cock-tails worldwide. *Environmental Pollution*, 356, 124305.
- Vázquez, O.A. & Rahman, M.S. (2021) An ecotoxicological approach to microplastics on terrestrial and aquatic organisms: A systematic review in assessment, monitoring and biological impact. *Environmental Toxicology and Pharmacology*, 84, 103615.
- Wagner, S. et al. (2007) Soil-aggregate formation as influenced by clay content and organic-matter amendment. *Journal of Plant Nutrition and Soil Science*, 170(1), 173–180. John Wiley & Sons, Ltd.
- Waldschläger, K. et al. (2022) Learning from natural sediments to tackle microplastics challenges: A multidisciplinary perspective. *Earth-Science Reviews*, 228, 104021.
- Waldschläger, K. & Schüttrumpf, H. (2019) Erosion Behavior of Different Microplastic Particles in Comparison to Natural Sediments. *Environmental Science & Technology*, 53(22), 13219–13227. American Chemical Society.
- Wang, J. et al. (2022a) Runoff and discharge pathways of microplastics into freshwater ecosystems: A systematic review and meta-analysis. *FACETS*, 7, 1473–1492. Canadian Science Publishing.
- Wang, X. et al. (2022b) Recent advances on the effects of microplastics on elements cycling in the environment. *Science of The Total Environment*, 849, 157884.
- Wassenaar, L.I. et al. (2008) High Resolution Pore Water $\delta^2\text{H}$ and $\delta^{18}\text{O}$ Measurements by $\text{H}_2\text{O}(\text{liquid})\text{--H}_2\text{O}(\text{vapor})$ Equilibration Laser Spectroscopy. *Environmental Science & Technology*, 42(24), 9262–9267. American Chemical Society.
- Weber, C.J. et al. (2022) Investigating the dispersal of macro- and microplastics on agricultural fields 30 years after sewage sludge application. *Scientific Reports*, 12(1), 6401.
- Weber, C.J. & Opp, C. (2020) Spatial patterns of mesoplastics and coarse microplastics in floodplain soils as resulting from land use and fluvial processes. *Environmental Pollution*, 267, 115390.

- Weithmann, N. et al. (2018) Organic fertilizer as a vehicle for the entry of microplastic into the environment. *Science Advances*, 4(4), eaap8060. American Association for the Advancement of Science.
- Wu, X. et al. (2020) Transport of polystyrene nanoplastics in natural soils: Effect of soil properties, ionic strength and cation type. *Science of The Total Environment*, 707, 136065.
- Xing, X. et al. (2021) Interactions between water flow and microplastics in silt loam and loamy sand. *SOIL SCIENCE SOCIETY OF AMERICA JOURNAL*, 85(6), 1956–1962.
- Xu, Z. et al. (2022) Distribution characteristics of plastic film residue in long-term mulched farmland soil. *Soil Ecology Letters*, 5(3), 220144.
- Yan, X. et al. (2020) Downward transport of naturally-aged light microplastics in natural loamy sand and the implication to the dissemination of antibiotic resistance genes. *Environmental Pollution*, 262, 114270.
- Yan, Z. et al. (2022) Analysis of Microplastics in Human Feces Reveals a Correlation between Fecal Microplastics and Inflammatory Bowel Disease Status. *Environmental Science & Technology*, 56(1), 414–421. American Chemical Society.
- Yang, M. et al. (2022) Effect of Dry Soil Aggregate Size on Microplastic Distribution and Its Implications for Microplastic Emissions Induced by Wind Erosion. *Environmental Science & Technology Letters*. American Chemical Society.
- Yang, S. et al. (2021) In vitro evaluation of nanoplastics using human lung epithelial cells, microarray analysis and co-culture model. *Ecotoxicology and Environmental Safety*, 226, 112837.
- Yang, X. et al. (2024) Spotlight on the vertical migration of aged microplastics in coastal waters. *Journal of Hazardous Materials*, 469, 134040.
- Yoshida, S. et al. (2016) A bacterium that degrades and assimilates poly(ethylene terephthalate). *Science*, 351(6278), 1196–1199. American Association for the Advancement of Science.
- Yu, L. et al. (2021) Distribution characteristics of microplastics in agricultural soils from the largest vegetable production base in China. *Science of The Total Environment*, 756, 143860.
- Yu, Y. et al. (2023) Minimal Impacts of Microplastics on Soil Physical Properties under Environmentally Relevant Concentrations. *Environmental Science & Technology*, 57(13), 5296–5304. American Chemical Society.
- Zhang, G.S. & Liu, Y.F. (2018) The distribution of microplastics in soil aggregate fractions in southwestern China. *Science of The Total Environment*, 642, 12–20.
- Zhang, G.S. & Zhang, F.X. (2020) Variations in aggregate-associated organic carbon and polyester microfibrils resulting from polyester microfibrils addition in a clayey soil. *Environmental Pollution*, 258, 113716.
- Zhang, S. et al. (2023) Microplastic Accumulation in Agricultural Soils with Different Mulching Histories in Xinjiang, China. *Sustainability*, 15(6).

Zhang, X. et al. (2022) Size/shape-dependent migration of microplastics in agricultural soil under simulative and natural rainfall. *Science of The Total Environment*, 815, 152507.

Zhao, R. et al. (2015) Granular impact cratering by liquid drops: Understanding raindrop imprints through an analogy to asteroid strikes. *Proceedings of the National Academy of Sciences*, 112(2), 342–347. Proceedings of the National Academy of Sciences.

Zhao, Z. et al. (2022) Irrigation-facilitated low-density polyethylene microplastic vertical transport along soil profile: An empirical model developed by column experiment. *Ecotoxicology and Environmental Safety*, 247, 114232.

Zhou, B. et al. (2020) Microplastics in agricultural soils on the coastal plain of Hangzhou Bay, east China: Multiple sources other than plastic mulching film. *Journal of Hazardous Materials*, 388, 121814.

Ziajahromi, S. et al. (2018) Environmentally relevant concentrations of polyethylene microplastics negatively impact the survival, growth and emergence of sediment-dwelling invertebrates. *Environmental Pollution*, 236, 425–431.

Zimmermann, L. et al. (2020) What are the drivers of microplastic toxicity? Comparing the toxicity of plastic chemicals and particles to *Daphnia magna*. *Environmental Pollution*, 267, 115392.

Zubris, K.A.V. & Richards, B.K. (2005) Synthetic fibers as an indicator of land application of sludge. *Environmental pollution*, 138(2), 201–211. Elsevier.

Zumstein, M.T. et al. (2018) Biodegradation of synthetic polymers in soils: Tracking carbon into CO₂ and microbial biomass. *Science Advances*, 4(7), eaas9024. American Association for the Advancement of Science.

7. Appendix 1: UV photography and image analysis to detect fluorescent particles during rainfall simulations

1.1 Overview

This appendix is a compilation of notes used to create the standard operating procedure for the UV photography and image analysis and the resulting standard operating procedure used in chapters 2, 3 and 4.

1.2 Camera Settings

A Canon EOS 850D camera was used in this research as it was capable of capturing high resolution images (24.2 million pixels). This high resolution was required as images of the relatively small MPs would be taken from a distance, to ensure the camera would not interfere with the falling raindrops from the rainfall simulators.

Prior to each experiment, camera settings were tested in the laboratory or field conditions of the experiment and settings which maximized fluorescent particle visibility were chosen. In general, the camera settings followed the same guidelines as outlined below. For the purposes of this research, the aperture value was set at or around $f/9$ so that each image would have a high depth of field. ISO values were also kept low so images would not appear grainy and thus create difficulties in particle identification. Having a relatively long exposure time of 1 second was necessary to have the fluorescent particles visible in the images but this resulted in some particles appearing streaked or blurred if the image was taken while the particle was in motion.

1.3 General Procedure for UV Photography

1. Mount camera on tripod and place in front of the soil box/plot (in the laboratory tape marks the location where the tripod should be placed.)
2. Double check that the camera is in manual shooting mode and the camera settings are correct.
3. With room lights on (or white light floodlights) turn the camera to autofocus and take an image of the illuminated soil box/plot.

- a. Carefully secure the focus ring with tape so the focus does not drift during rainfall simulations.
 - b. Once secured turn the camera back to manual focus mode.
4. Ensure that the intervalometer is correctly programmed or if using mobile device to remote capture images ensure that the camera is connected by Bluetooth.
5. Turn on UV lamp and capture image of plot before rainfall simulator is turned on.
 - a. If using the gravity-fed simulator, cover the soil box with umbrella to take the initial photo.
6. Turn on simulator or uncover soil box and begin image capture.

1.4 Image Processing and Analysis

Image analysis was mainly carried out in Image J although Adobe Photoshop was used for some image processing. The purpose of these steps is to process the images so that only the soil surface is present in the images and MPs outside or trapped on the sides of the soil box/plot are not included in the particle counting. The steps listed below are designed to accomplish this purpose. Therefore, the images that result from these processing steps should not be used for other analysis such as quantifying the distances particles travel.

1. Upload images to computer and re-label images using Bulk Rename Utility app to indicate the time image was taken and place images in a separate folder for each soil box/plot.
2. Using Adobe Photoshop's Image Processing tool, convert the RAW format images to TIFF using LZW compression. TIFF format is a preferred image format for scientific analysis as it uses compression algorithms that does not lead to data loss (Cromey, 2010).
3. Resample the images to correct for perspective so that the image can be cropped to the dimensions of the soil box/plot.
 - a. For these steps a recording action is used for batch processing. To get the correct area of interest use the image of the illuminated soil box/plot prior to the laboratory (or white light flood lights) being turned off.
 - b. Using the actions tool bar create an "action" specific for the soil box/plot and press record.

- c. Under the edit tab click Perspective Warp and place the points on each of the edges of the soil box/plot.
 - d. Once in place click the Warp button and then select Auto Warp to Vertical and Horizontal and click Confirm Warp.
 - e. Save file and ensure that image compression is LZW and layer compression is RLE.
 - f. Stop the action recording. Batch processing can now be used to make the adjustment to all the images within each soil box/plot. Ensure that the correct action for each soil box/plot is used.
4. Crop images in Image J by using the Macros tool to create an automation code for each soil box/plot.
- a. Open the image of the illuminated soil box/plot prior to the laboratory (or white light flood lights) being turned off.
 - b. Click the Plugins menu and select Macros then Record.
 - c. Select the Rectangle tool and make a rectangle of the surface of the soil. Place the rectangle just inside the boundary of the soil box/plot so that none of the edges are visible in the image.
 - d. Click the Image menu then select Crop.
 - e. In the Macro recorder window click Create and save the macro command.
 - f. The macro command can now be used to crop all the images in the soil box/plot by clicking the Process menu select Batch then Macro then open the desired macro command.

Note: When the camera was bumped or moved inadvertently the images were split into sub batches and new perspective warp and crop commands were generated. This ensured the perspective warp and cropping would capture the soil surface and not outside of the soil box/plot.

1.5 Extracting and Detecting MP Particles

The Color Thresholding tool in Image J was used to identify and count the fluorescent particles on the soil surface. Color thresholding converts images from RGB to binary images by segmenting pixels to set values. The HSB color space was used to threshold particles in the image as it is robust against changes in illumination (Gonzalez and Woods, 2008). For

each experiment thresholding values specific to each fluorescent particle were tested before use to ensure the most effective particle detection, this is described in detail in section 1.6.

1. Macros were created through the Color Threshold tool (Image Menu- Adjust- Color Threshold).
 - a. Ensure macros recorder is running with any image of the soil surface open then adjust the HSB values to the predetermined values.
 - b. Click Macro and save the Macro.
 - c. Macro can now be used to detect fluorescent particles of the same type in all the soil boxes/plots by clicking the Process menu selecting Batch then Macro then choosing the desired macro command to run.
2. An additional Macro command was created to (i) run the Watershed Separation tool to identify and separate potential adjoining particles and (ii) count the particles and save to excel spreadsheet.
 - a. Ensure Macros recorder is running with any image of the soil surface open.
 - b. In the Process menu select Binary then Watershed.
 - c. To count the particles, in the Analyze menu select Analyze particles. Ensure the Exclude on Edges option is unchecked and that Include Holes and Overlay is checked. Click okay and save macro.
 - d. Batch processing can then be used with the macro to extract the number of particles in each image. After the batch is complete save the data in excel.

Note: Additional coding can be written to combine these steps into one macro command.

1.6 Selecting Color Threshold and Evaluating Image Analysis

In order to choose the optimal threshold values and to quantify the effectiveness of the image analysis process a training image set was created. This set included a selection of random images chosen to represent the soil surface at various points of the rainfall simulation. The results from the training sets were used to develop the thresholding method.

To evaluate the thresholding method a test set was created. This set also included a selection of random images chosen to represent the soil surface at various points of the rainfall

simulation. The results from the test sets were used to report the effectiveness of the thresholding methods.

The particles in both of these image sets were manually counted and used as ground truth. Trial and error was used to find 3-5 thresholding values that appeared to detect the most particles without including background interference from the soil. Images were then run through the color threshold and watershed macros. Images were then manually counted again and were marked as true positives, false positives, and false negatives.

Performance of the image analysis was evaluated by calculating the recall, precision and f-score. Recall, precision and f-score are calculated on a scale of 0 to 1, with 1 reflecting the highest performance. Recall describes the percentage of particles detected which were correctly classified ($\text{true positive} / (\text{true positive} + \text{false negative})$). Precision describes the proportion of the positives detected that were correctly classified as particles ($\text{true positive} / (\text{true positive} + \text{false positive})$). F-score considers both the precision and the recall to measure the proportion of particles which were correctly classified in the images ($2 * ((\text{precision} * \text{recall}) / (\text{precision} + \text{recall}))$).

The thresholding values that scored the highest in the training set was then ran on the test set and the results were used to report the effectiveness of the thresholding methods

8. Appendix 2: Chapter 3- Supplemental Information

3.1 Water and soil isotope

Deuterium, ($\delta^2\text{H}$), was used to trace the extent to which rainwater infiltrated into the soil profile. An average isotope value of $229.3 \pm 1.08 \text{ ‰}$ was observed, indicating a similar isotopic signature of deuterated water across all plots (Figure S3.3a). Background soil water isotopic signatures are reported from the soil prior to rainfall simulations (Figure S3.3b). Infiltration of the labelled water was visible in the upper soil depth (0-6 cm), whereas it diminished in the deeper soil layers (8-13 cm) (Figure S3.3b), which suggested that the infiltrating water reached 8 cm depth after one hour of simulated rainfall. Relative tracer fraction of $\delta^2\text{H}$ (Figure S3.3b) showed a hyper-exponential shape in soil profiles, further supporting the isotopic mixing between infiltrated and pre-event soil water, with $\delta^2\text{H}$ value ranging from $127.0 \pm 4.18 \text{ ‰}$ (0-2 cm) to $-32.9 \pm 5.28 \text{ ‰}$ (11-13 cm). Applying a two-component mixing approach, results in the contribution of event water ranging from $62.77 \pm 1.29\%$ at 0-2 cm to $1.23 \pm 0.05\%$ at 6-8 cm (Figure S3.3c).

3.2 Laboratory splash erosion experiment

3.2.1 Rational

To isolate the mechanisms driving the surface movement of microplastics (MPs) during the rainfall simulation in the field, controlled laboratory rainfall simulations were conducted to identify the influence of splash erosion on MP transport and retention in the soil. Specifically, the following questions were investigated: (1) Was splash erosion responsible for less 125-150 μm detected on the soil surface? Was splash erosion responsible for large number of particles ($\sim 25\text{-}75\%$ loss depending on the particle and plot) disappearing from the soil surface in the first 3-5 minutes?

3.2.2 Methods

As much as possible the same set-up and conditions which were present in the field were used in the laboratory simulation. Soil was gathered from the Āisuty field site and sieved to 1.5 cm the same size as the top 1 cm of soil in the field experiment. Each splash cup was packed to a dry bulk density of 1.25 g cm^{-3} and raised to the same soil moisture as the field plots on the night of the experiment which was $\sim 14\%$ VWC. The procedure for packing the splash cups and raising the soil to the appropriate VWC level included weighing the soil for each centimeter layer in a container then applying water using a spray bottle to the soil while mixing to ensure a homogeneous application. The amount of plastic applied in the splash cups was proportionate to the amount in the field plots which equated to 1,062 MPs of each size to the 78.54 cm^3 area of each splash cup. In total, 5 splash cups were prepared.

The same pressure-fed swinging nozzle rainfall simulator set at 60 mm hr^{-1} and kinetic energy $4.14 \text{ J m}^{-2} \text{ mm}^{-1}$ was used in the laboratory (Kavka and Neumann, 2021). Similar to the field there were two simulations for each cup a 3 minute dry run and 3 minute wet run simulation with a 30 minute break between simulations. The duration of 3 minutes was chosen as this was the average time it took for the water in the splash cups to begin to pool. Thus, the dry run showed the movement of particles due to splash erosion on dry soil and the

wet runs showed the movement of the MPs when there was a film of water on the surface of the splash cup.

A 1.6 m² geotextile mat was spread under the rainfall simulator, with tape measures and targets marking a 1.0 m² area (Figure S3.1). The splash cup was placed in the centre of the mat and the mat was photographed before and after each simulation. Following each simulation, the geotextile mat was changed. Images were captured in RAW format and converted to TIFF (LZW compression) using Adobe Photoshop. MPs were manually counted in Image J.

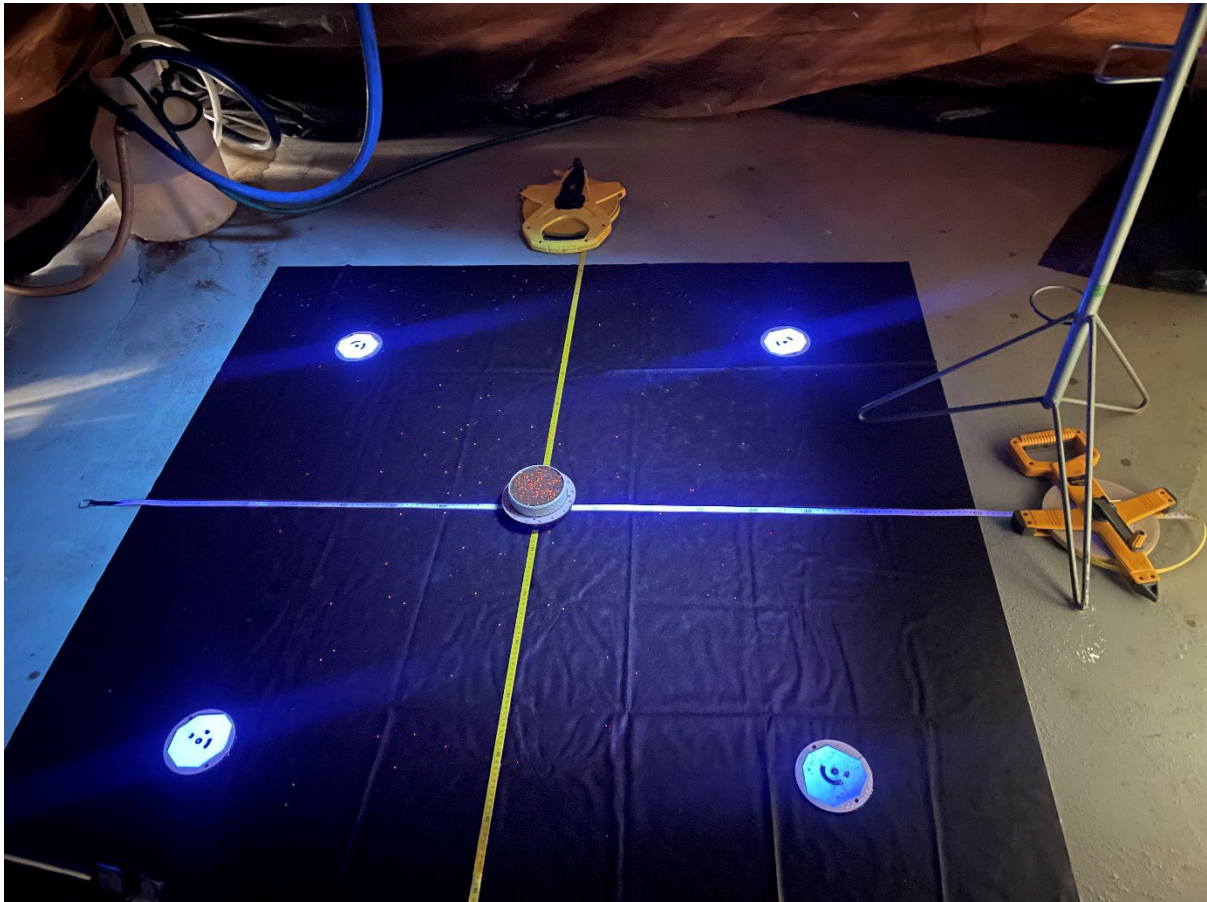


Figure S3.1. Image showing the splash cup and mat following a rainfall simulation. Photogrammetry targets mark the 1 m x 1 m area and black geotextile splash mat measures 1.6 m x 1.6 m. Red (425-500 μm) and green (125-150 μm) MPs are visible on the splash mat.

3.2.3 Results

Prior to the rainfall simulation, there were approximately 66% fewer 125-150 μm MPs on the surface of the soil as compared to the 425-500 μm MPs (Table S3.1). More 425-500 μm MPs were transported from the splash cup in both the dry and wet run simulations as compared to the 125-150 μm MPs. The number of MPs transported from the splash cup decreased during the wet run simulations. The majority of MPs transported were within 1 m of the splash cup. Overall, less than 12% of MPs sized 425-500 μm and 6% of MPs sized 125-150 μm were transported out of the splash cup to a cumulative distance of 1.6 m after 6 minutes of rainfall simulations.

Table S3.1 The mean \pm standard deviation of the number of microplastics (MPs) found in each location and timepoint during the rainfall simulations. Soil surface start refers to the number of MPs on the soil surface prior to the rainfall simulations. 1 m² mat is the number of MPs on the 1 m² mat at the conclusion of the rainfall simulations. Outer 0.6 m² mat refers to the number of MPs found a distance of 1 m to 1.6 m from the splash cup. Soil surface end refers to the number of MPs on the surface of the soil at the conclusion of the rainfall simulations.

	Dry Run		Wet Run	
	425-500 μm	125-150 μm	425-500 μm	125-150 μm
Soil Surface Start	100 \pm 18	34 \pm 8	68 \pm 26	10 \pm 4
1 m ² mat	62 \pm 9	34 \pm 13	30 \pm 19	10 \pm 7
Outer 0.6 m ² mat	13 \pm 7	10 \pm 4	11 \pm 3	5 \pm 3
Soil Surface End	70 \pm 30	11 \pm 4	42 \pm 23	4 \pm 3

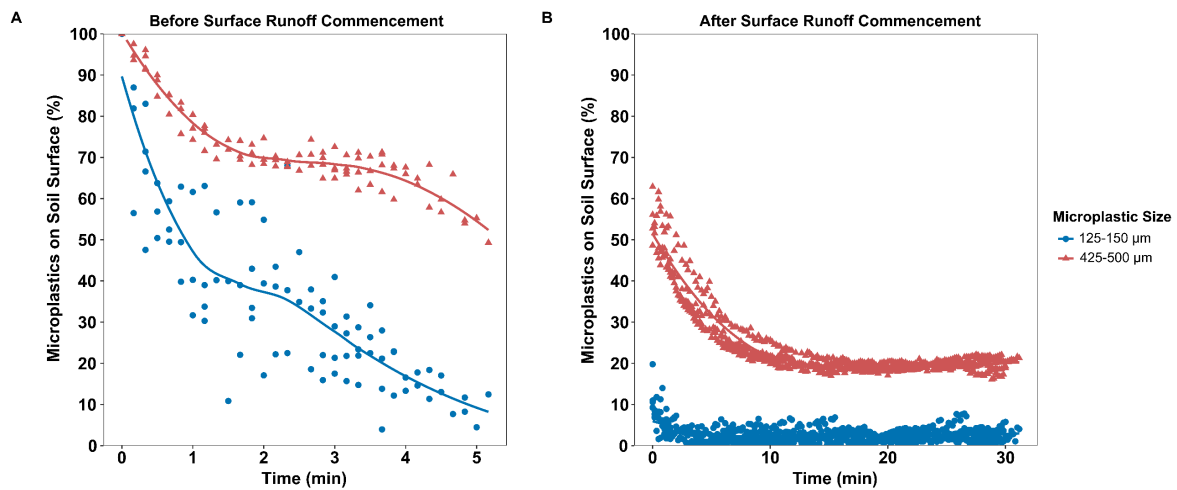


Figure S3.2. Graphs showing the percentage of microplastics (MPs) with respect to the initial number of MPs detected on the soil surface before (A) and after surface runoff (B) in the dry run simulation. Data points from each plot are represented in the graphs (n=5). The data was fitted to a locally estimated scatterplot smoothing (loess) model to showcase the trends in the data.

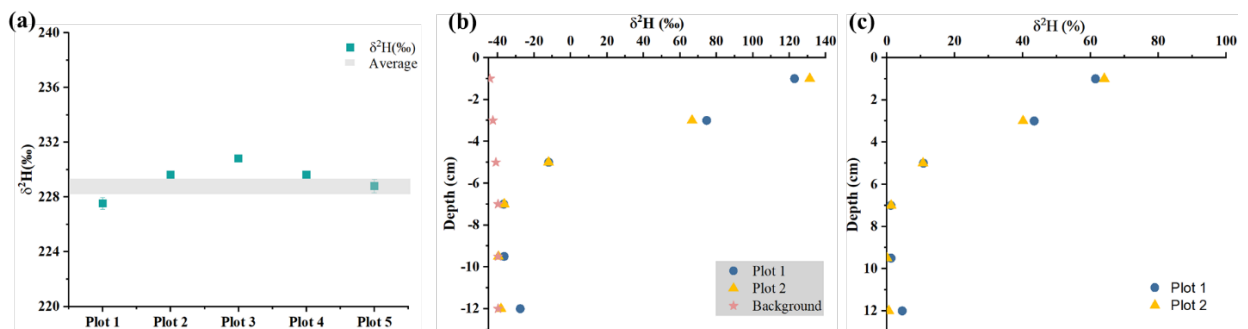


Figure S3.3. Water isotopic signature of simulated rainwater in different plots (a). Soil water isotope profiles were obtained from 2 sampling plots (b). Contribution of simulated rainwater (c).